D 38926/82

MUNOZ J.M.

IP
182

Double Payed Insert
Back

SEMICLASSICAL METHODS

IN

MOLECULAR COLLISIONS

by

JOSE M. MUNOZ, "Profesor de Fisica"

Thesis submitted to the University of Stirling

for the degree of Doctor of Philosophy

Physics Department
University of Stirling
STIRLING
Scotland

December, 1980.

ABSTRACT

Part 1

A classical path method using hyperbolic orbits and perturbation theory has been used to calculate rotational excitation cross sections for polar-ion-electron collisions. Good agreement with corresponding Coulomb-Born calculations is obtained close to threshold. The focussing effect of the Coulomb field is shown to be important for close collisions. Previous calculations including the dipole potential only are shown to underestimate substantially the $\Delta J = \pm 1$ rotational cross section particularly for weak dipoles. Calculations using the quadrupole interaction only are shown to be unreliable. Cross sections including an empirical estimate of short-range effects have been performed for HD^+, CH^+ and H_3O^+ at electron energies up to a few electron volts.

Part 2

The Strong Coupling Correspondence Principle (SCCP) method is applied to rotationally inelastic HF-HF and HCl-HCl collisions. Transitions probabilities and cross sections have been calculated for different transitions and energies. Good agreement with corresponding quantum mechanical close coupling (CC) is found only for some transitions. Comparison with other theories suggests that all theories are unreliable for adiabatic collisions. The first-order correspondence principle (FOCP) is consistently unreliable, overestimating the transition probability. The body-fixed correspondence principle (BFCP) approximation, the M-conserving correspondence principle (MCCP) and the decoupled-L-dominant correspondence principle (DLDCP) approximation are derived and applied to the molecule-molecule collision.

Comparison with SCCP shows that MCCP is the better approximation.
BFCP is good for short-range adiabatic collisions while DLDCP is
good at large impact parameters only for some transitions.

ACKNOWLEDGEMENTS

CONTENTS

INTRODUCTION

The simplest energy-transfer collision process involves rotationally inelastic scattering. The study of collision-induced rotational transitions is useful because the knowledge of these transitions is required to interpret phenomena such as ultrasonic absorption and disperson (Herzfeld and Litovitz 1959, Cottrell and McCoubrey 1961), pressure broadening of spectral lines (Birnbaum 1967, Rabitz 1974), and various transport properties in gases (Levine and Bernstein 1974). Moreover, theory of rotational transitions combined with appropriated experiments can provide us with a reliable way to determine intermolecular potentials.

We are concerned here with semiclassical studies of rotationally inelastic scattering. During the last decade, a considerable interest has been shown in the development of semiclassical methods to treat complex molecular collisions (Miller 1974, 1975; Clark et.al. 1977). The term "semiclassical" is normally applied to two classes of methods: 1) The most common is the "classical path model". Here a classical trajectory is assumed for the translational motion. Thus a time-dependent perturbation is caused on the interal degrees of freedom, which are treated quantum mechanically. In this method the Schroedinger's equation reduces to a finite set of first-order differential equations (Schiff 1955, p.196); following Dickinson (1979a) we term them time-dependent close coupling equations (TDCC). Any solution to the TDCC equations which maintain the quantum mechanical treatment of the internal degrees of freedom yields what we call a classical path method.

2)   The second class treats both the translational motion and
the internal degrees of freedom classically.   The basic idea is
to use a quantum mechanical description of the collision process and
then classical mechanics is invoked to determine all dynamical
relationships.   Thus an asymptotic solution of the Schroedinger's
equation is obtained with the help of classical solutions of Hamilton's
equations.   Between the most successful of these methods are: the
Classical-S-Matrix introduced independently by Miller,and Marcus (1970)
(extensively reviewed by Miller 1974, 1975),   and the Strong Coupling
Correspondence Principle (SCCP) of Percival and Richards (1970).
Excellent discussions of the SCCP approximation can be found in
Clark et.al. (1977), and Dickinson (1979b).

        This thesis, exemplifies the use of a classical path
approximation, and the SCCP   method in rotational inelastic
scattering.

        The first part of this work (Chapters 1-3) presents a study on
rotational excitation of polar molecular ions by slow electrons.   This
process may play an important role in the understanding of the
constituents of the interestellar medium (Somerville 1977).   The knowledge
of the collisional excitation cross sections may facilitate the
detection of new molecular ions.

        Previous work on linear ions (Boikova and Ob'edkov 1968, Chu
and Dalgarno 1974) has considered the transition as due solely to the
dipole potential, which has been treated in the Coulomb-Born approximation.
Following Faisal (1971) and Ray and Barua (1975), we use First-Order
Time-dependent Perturbation Theory (FOTDPT) with hyperbolic orbit for
the incident particle.   The FOTDPT is perhaps one of the simplest

versions of a classical path approximation as it is obtained by applying first-order perturbation theory to solve the TDCC equations.

Employing FOTDPT, we argue that, in this approach, unphysically low values are used for the transition probability for close collisions. In the absence of a detailed description of the short-ranged electronic interactions, we assume a conservative value of the transition probability in the strong coupling region. This shows that the Coulomb-Born Approximation almost certainly underestimates significantly the total rotational inelastic cross section.

For symmetric-top ions, we examine the contributions from the quadrupolar interaction and we find that the regions for which perturbation theory and the quadrupolar interaction are valid are very limited. We compare also with the work of Ray and Barua (1975) on the rotational excitation of HD^+ by electrons and positrons. They used at short range a truncated form of the long-range anisotropic interaction. Since this modification takes little account of the strong coupling occurring for electrons in close encounters their results differ little from the Coulomb-Born values.

In chapter one, we examine the FOTDPT for the dipole and quadrupole potentials using a hyperbolic classical path for the incident electron. In chapter two we derive the dipolar probability and cross section. Limiting forms for low and high velocities are derived and comparison with the Coulomb-Born results confirm the validity of the time-dependent approach. Our simple modification to the short range contribution is made in chapter three, and compared with other results. Our conclusions are presented at the end of chapter three.

The second part of this thesis (Chapter 4 - 8) presents a study of rotational excitation in collisions between two linear molecules. Information obtained from such a study can be useful to determine the intermolecular potential. Some experiments like optical flourescence (Oka 1973) and pressure broadening (Rabitz 1974) require detailed calculation of either collision cross sections or rates for their interpretation in terms of molecular potential parameters.

The quantal theory of scattering of two linear molecules has been known for a number of years (reviewed by Takayanagi 1965). However to the author knowledge only three quantal Close Coupling Calculations (CC) have been reported (Green 1975, DePristo and Alexander 1977, Alexander 1980). The major difficulty is the large number of degenerate levels which must be included for each rotational level, so that the problem becomes prohibitive whenever the number of accessible molecule rotational levels is large. This has stimulated the development and use of various approximations (Bhattacharayya et.al. 1977, Bhattacharayya and Saha 1978, Alper et.al. 1978, Alexander and DePristo 1979, Hashi et.al. 1978).

We concentrate in this work on the detailed application of the SCCP method.

The SCCP approximates the solution of the TDCC equations using a classical description of the internal degrees of freedom of the molecules. Thus classical action-angle variables are used; the rotational levels of energy are obtained by an appropriate quantization of the action variables. The change in action of the system is now determined using classical perturbation theory. The SCCP is expected to be most successful for large quantum numbers but quite good accuracy has in fact been obtained for transitions out of the ground level in H_2-He

collisions (Clark 1977).   It has been successfully applied to
rotational and rotational-vibrational excitation of molecules by atoms
(Dickinson and Richards 1974, Clark 1977), and is the basis for some
current semiclassical approximations (Dickinson and Richards 1977, 1978).

Using SCCP we calculated dipole-dipole rotationally inelastic
transition probabilities and cross sections for HF-HF and HCl-HCl
collisions.   A detailed study of the dependence of the transition
probability on the different collision parameters is presented.   A
detailed comparison with other approximations has been done.   We
examine the advantages of each method and attempt to determine ranges
of validity.   We argue that none of the current calculations has
offered a consistent quantitative description of the collision.

Subsidiary correspondence principle approximations have been
derived and applied to the molecule-molecule collision problem.
Through comparison with SCCP we attempted to determine their accuracy
and feasibility.   It is argued that a combination of these approximations
can prove to be efficient and accurate.

In chapter four we determine the parameters of the collision
and examine their dynamical relations.   The general SCCP transition
probability is examined in Chapter 5.   The first-order limit of our
approximation is derived and compared with other first-order models.

In Chapter 6 we derive the correspondence principle equations
for the dipole-dipole interaction.   The transition amplitude is obtained
in closed form.

The corresponding first-order and straight-line (SL) limits are
examined.   The numerical techniques used to evaluate transition
probabilities and cross sections are described.

Our numerical results are presented and discussed in Chapter
seven.   The correspondence principle transition probabilities are
examined in detail.   Our results are compared with other theories
and the range of validity of our approach is analysed.

In Chapter 8 we derive correspondence principle equivalents
of some of the current decoupling approximations.   The simplifications
introduced are examined and some limiting forms are studied.
Numerical results are compared against SCCP.

The investigation presented in this work is a first attempt
to use the SCCP method in the study of rotational excitation of two
linear molecules.   Work is already planned to study the scattering
of two rigid rotors, using SCCP and its subsidiary approximations
(Richards private communication).   It is intended to assess the ranges
of validity and computational convenience of these approximations.
It is intended also to include in the computer program developed here
terms of interaction potential other than the dipole-dipole term.
The eventual aim of this study is to produce a general purpose computer
program for cross sections and rates.

We use a_o, e and m for the Bohr radius, electron charge and
mass respectively and we use Ry for $me^4/2\hbar^2 \equiv 13.6eV$.

The first part of the work presented in this thesis has been
published by Dickinson and Munoz (1977).

FIRST PART

Rotational excitation of polar molecular ions by slow electrons

CHAPTER 1

BASIC THEORY

1.1   First-order time-dependent perturbation theory (FOTDPT)

1.1.1 The molecular ion rotational state.   The rotational state of
a symmetric-top molecular ion is characterised by the three quantum
numbers J, M and K.   The first two, J and M, represent the rotational
angular momentum and its Z-component in a space-fixed frame respectively,
and K is the angular momentum component directed along the symmetry
axis.   The corresponding rotational eigen functions are given by
Edmonds (1960, p66):

$$\Psi_{JKM} = [(2J+1)/8\pi^2]^{1/2} \mathcal{D}_{MK}^{(J)}(\Omega)$$ (1.1)

where $\mathcal{D}_{MK}^{(J)}$ is the matrix element of the operator of finite
rotations, and $\Omega \equiv (\alpha, \beta, \gamma)$ are the Euler angles specifying the
orientation of the ion with respect to a space-fixed frame.

1.1.2
The interaction potential and motion of the incident electron.   The
asymptotic interaction potential between the molecular ion and the
electron can be expanded in the form (Chu 1975)

$$V(r, \alpha, \gamma) = -e^2/r + \sum_{\lambda k} v_{\lambda k}(r) Y_{\lambda k}(\alpha, \gamma)$$ (1.2)

where r is the electron distance from the centre of mass of the
molecular ion, (α, γ) specify the direction of the incident
electron with respect to the molecular ion-fixed co-ordinates, and
$Y_{\lambda k}$ is the spherical harmonic (Edmonds 1960).   In symmetric-top

molecular ions with symmetry C_{3v} the term $\mathcal{V}_{\lambda k}$ vanishes unless $|k| = 3n$ ($n = 0, 1, 2, \ldots$). In this work, we are particularly interested in the first two non-vanishing terms. These are (Itikawa 1971)

$$\mathcal{V}_{10}(r) = -\left(4\pi/3\right)^{1/2} \frac{eD}{r^2} \quad ; \quad \mathcal{V}_{20}(r) = -\left(4\pi/5\right)^{1/2} \frac{eQ}{r^3} \, , \qquad (1.3)$$

where D and Q are the dipole and quadrupole moments respectively. Transforming (1.2) into the space-fixed frame (Edmonds 1960, p54) we obtain

$$V(r, \theta, \phi, \Omega) = -e^2/r + \sum_{\lambda k \nu} \mathcal{V}_{\lambda k}(r) \, \mathcal{D}^{(\lambda)}_{-\nu -k}(\Omega) \, Y_{\lambda \nu}(\theta, \phi) \, , \quad (1.4)$$

where (θ, ϕ) specify the spherical polar angles of the incident electron in the space-fixed frame.

We assume the incident electron moves on a classical trajectory determined by the spherical part of the potential (1.2). The energy E, on the trajectory, is taken to be

$$E = \frac{1}{2} m v^2 \quad , \quad v = \left(v_i \, v_f\right)^{1/2} \qquad (1.5)$$

where v_i and v_f are the initial and final speeds respectively of the electron.

1.2   The first-order transition amplitude.

The first-order transition amplitude $S(i \to f; b)$, for a transition between two states $|i\rangle \equiv |JKM\rangle$ and $|f\rangle \equiv |J'K'M'\rangle$ at impact parameter b is given by (Landau and Lifshitz 1965, p140-41)

$$S(i \to f; b) = -\frac{i}{\hbar} \int_{-\infty}^{\infty} dt \, \exp(i \omega_{if} t) \langle i \, | V[\underline{r}(t), \Omega] | f \rangle \, , \quad (1.6)$$

where $\omega_{if} = (E_i - E_f)/\hbar \equiv \Delta E/\hbar$, the electron co-ordinates have been written explicitly as functions of the time, and $E_i (E_f)$ is the initial (final) translation energy of the electron. The matrix element $<i|V|f>$, is given by

$$\langle JKM | V[\underline{r}(t), \Omega] | J'K'M' \rangle = \sum_{\lambda k \nu} [(2J'+1)(2J+1)]^{\frac{1}{2}} U_{\lambda k}(r) Y_{\lambda \nu}(\theta, \phi) \qquad (1.7)$$

$$\times (-1)^{M'-K'} \begin{pmatrix} J & J' & \lambda \\ M & -M' & \nu \end{pmatrix} \begin{pmatrix} J & J' & \lambda \\ K & -K' & -k \end{pmatrix} ,$$

where the 3-j symbol is defined by Edmonds (1960, p46).

1.2.1
The first-order probability and cross section.
The calculation of the degeneracy-averaged probability $\mathcal{P}$, for a transition from the level JK to J'K' is straightforward:

$$\mathcal{P}(JK \to J'K'; b; E) = (2J'+1) \sum_{\lambda \nu} \frac{1}{2\lambda+1} \left| \sum_{k} \begin{pmatrix} J & J' & \lambda \\ K & -K' & -k \end{pmatrix} V_{\lambda \nu}(E, b) \right|^2 \quad (1.8)$$

where $V_{\lambda \nu}$ is given by

$$V_{\lambda \nu}(E, b) = \frac{1}{\hbar} \int_{-\infty}^{\infty} dt \, \exp(i \omega_{if} t) \, U_{\lambda k}[r(t)] \, Y_{\lambda \nu}[\theta(t), \phi(t)] \quad . \quad (1.9)$$

For notational simplicity, we derive transition probabilities for upward transitions only; probabilities for downward transitions are derived using the detailed-balance relation.

The terms in the potential contributing in first-order to the transition JK → J'K' are those $U_{\lambda k}$ with (λ, k) satisfying

$$|J - J'| \leq \lambda \leq J + J' \quad , \quad K - K' = k \quad . \quad (1.10)$$

If K = K' = O, as occurs for a linear molecular ion, there is the additional condition

$$J + J' + \lambda = even \quad . \tag{1.11}$$

Since we treat the target quantum-mechanically and the projectile classically, the probability (1.8) does not satisfy the detailed-balance relation. To enforce detailed-balance, we redefine our first-order probability for initial translation energy E_i as

$$P^{FO}(JK \rightarrow J'K'; b; E_i) = (v_f/v_i) \, \mathcal{P}(JK \rightarrow J'K'; b; E) \, , \tag{1.12}$$

where E is obtained from (1.5).

The first-order cross-section σ^{FO} is

$$\sigma^{FO}(JK \rightarrow J'K'; E_i) = 2\pi \int_0^\infty P^{FO}(JK \rightarrow J'K'; b; E_i) \, b \, db \, . \tag{1.13}$$

1.3 The $V\lambda\nu$ integral

Since we consider the electron moving classically in a Coulomb potential its trajectory is a hyperbola and we choose $\theta = \pi/2$. It is convenient to treat the motion in terms of the parametric representation of the orbit given by (Landau and Lifshitz, 1960, p38)

$$r = a(\epsilon \cosh\tau - 1) \quad , \quad t = \frac{a}{v}(\epsilon \sinh\tau - \tau) \, ,$$
$$x = a(\epsilon - \cosh\tau) \quad , \quad y = a(\epsilon^2 - 1)^{1/2} \sinh\tau \, , \tag{1.14}$$

where τ , the eccentric anomaly, takes values from $-\infty$ to ∞, a is given by

$$a = e^2/2E \equiv a_o \, (R_Y/E) \, , \qquad (1.15)$$

and ϵ , the eccentricity of the hyperbola, can be written as

$$\epsilon = \left(1 + b^2/a^2 \right)^{1/2} \, . \qquad (1.16)$$

1.3.1

<u>The I$_{\lambda\nu}$ integral.</u> We take $U_{\lambda k} = C_\lambda / r^{\lambda+1}$ where C_λ is a constant, see (1.3). Proceeding as for Coulomb excitation of nuclei (Alder et al 1956) we find

$$V_{\lambda\nu}(E,b) = \left[C_\lambda Y_{\lambda\nu}(\pi/2,0)/\hbar \, v \, a^\lambda \right] I_{\lambda\nu}(\epsilon,\xi) \, , \qquad (1.17)$$

where I$_{\lambda\nu}$ is given by

$$I_{\lambda\nu}(\epsilon,\xi) = \int_{-\infty}^{\infty} \exp\left[i \xi (\epsilon \sinh\tau - \tau) \right]$$

$$\times \frac{\left[\epsilon - \cosh\tau + i(\epsilon^2-1)^{1/2} \sinh\tau \right]^\nu}{(\epsilon \cosh\tau - 1)^{\lambda+\nu}} \, d\tau \, , \qquad (1.18)$$

with ξ, the adiabaticity parameter, defined by

$$\xi = a \, \omega_{if} / v \, . \qquad (1.19)$$

The corresponding $\bar{I}_{\lambda\nu}(\epsilon,\xi)$ integral for a repulsive Coulomb

potential has been examined by Alder et al (1956).   To transform
the attractive case into the repulsive case (and vice versa) we may
use the formal substitution (Biedenharn et al 1972):

$$\tau \rightleftarrows -\tau + i\pi \, sgn(\xi) \, ,$$

which leads to the relation

$$I_{\lambda\nu}(\epsilon,\xi) = e^{\pi|\xi|} \, \overline{I}_{\lambda\nu}(\epsilon,\xi) \, . \tag{1.20}$$

1.3.2

Solution for $\lambda = 1$.   In the dipole case ($\lambda = 1$), it is easily
verified by direct integration of (1.18) that relation (1.20) is
satisfied.   The $\overline{I}_{1\pm1}(\epsilon,\xi)$ integrals have been given explicitly by
Ter-Martirosyan (1952), and we obtain for $I_{1\pm1}(\epsilon,\xi)$

$$I_{1\pm1}(\epsilon,\xi) = \pi\xi \left[\mp i \frac{(\epsilon^2-1)}{\epsilon} H^{(1)}_{i\xi}(i\xi\epsilon) + H^{(1)'}_{i\xi}(i\xi\epsilon) \right] \, , \tag{1.21}$$

where $H^{(1)}_{\nu}(Z)$ and $H^{(1)'}_{\nu}(Z)$ are the Hankel function of the first kind
and its derivative respectively (Abramowitz and Stegun 1965, p358).
For ν and Z imaginary the Hankel function $H^{(1)}_{\nu}(Z)$ is purely
imaginary, while its derivative is real.   The evaluation of the
corresponding $V_{1\pm1}$ is straightforward.

In the quadrupole case ($\lambda = 2$) the $I_{\lambda\nu}$ integral cannot be
evaluated analytically but numerically, and as we show below, relation
(1.20) breaks down.

In the next chapters the theory presented above is used to
calculate rotational cross sections for HD+, CH+ and H_3O+.   The
values of the various molecular parameters needed are collected in
table 1.1

Table 1.1   Table of molecular data used in this work.   A and B are rotational constants. (All values in atomic units)

Ion	D	Q	A	B
CH^+	0.67[a]	–	–	6.46×10^{-5}[c]
HD^+	0.34[b]	1.578[b]	–	1.02×10^{-4}[c]
H_3O^+	0.22[d]	-2.214[e]	2.85×10^{-5}[f]	5.55×10^{-5}[f]

[a]   Green (1973), unpublished work (quoted by Chu and Dalgarno 1974) based on the wave function given by Green et.al. (1972)

[b]   Ray and Barua (1975)

[c]   Herzberg (1950)

[d]   Moskowitz and Harrison (1965)

[e]   Chu (1975)

[f]   Derived by Chu (1975) from OH distance and HOH angle calculated by Moskowitz and Harrison (1965).

CHAPTER 2

EVALUATION OF THE TRANSITION PROBABILITY AND CROSS SECTION

2.1 The Dipolar probability

From the condition (1.10), the dipole term $\mathcal{U}_{10}(r)$ of the potential can produce only the transition $|\Delta J|=1$. Because of the slow decrease of $\mathcal{U}_{10}(r)$ with r it is the dominant term for distant collisions. Making use of (1.21), we obtain for P_{10}^{FO}, the probability due to the dipole potential

$$P_{10}^{FO}(JK \to J'K; b; E_i) = \frac{1}{3}(\pi\xi a_0/a)^2 (D/ea_0)^2 \, G(J,J',K)(R_y/E_i)$$

$$\times \left\{ -\frac{(\epsilon^2-1)}{\epsilon^2}\left[H_{i\xi}^{(1)'}(i\xi\epsilon)\right]^2 + \left[H_{i\xi}^{(1)}(i\xi\epsilon)\right]^2 \right\}, \quad (2.1)$$

where $G(J, J', K)$ is given by

$$G(J,J',K) = (2J'+1)\begin{pmatrix} J & J' & 1 \\ K & -K & 0 \end{pmatrix}^2 . \quad (2.2)$$

We consider the probability (2.1) for b=0 (ϵ = 1), where the probability takes its maximum value. Then

$$P_{10}^{FO}(JK \to J'K; 0; E_i) = \frac{1}{3}(\pi\xi a_0/a)^2 (D/ea_0)^2 \, G(J,J',K)$$

$$\times (R_y/E_i)\left[H_{i\xi}^{(1)'}(i\xi)\right]^2 . \quad (2.3)$$

There are two natural energy regions: $\xi \gg 1$ and $\xi \ll 1$. The transition between these two regions occurs at energy $\bar{E}$ where

$\xi = 1$, i.e.

$$\overline{E}/R_Y = \left(\Delta E / 2 R_Y\right)^{2/3} .$$

2.1.1
The low-energy limit.   For small energies ($\xi \gg 1$), we have (Landau and Lifshitz 1971, p185)

$$H_{i\xi}^{(1)}(i\xi) \cong \left(1/\pi\sqrt{3}\right)\left(6/\xi\right)^{2/3} \Gamma(2/3) , \qquad (2.4)$$

and the probability (2.3) in this limit is

$$P_{10}^{FO}(JK \to J'K; 0; E_i) \cong C(v_f/v_i)(D/ea_0)^2 G(J,J',K)$$
$$\times \left(\Delta E/2 R_Y\right)^{2/3} , \quad E_i \ll \overline{E} , \qquad (2.5)$$

where $C = \left(\frac{4}{3}\right)^{2/3} |\Gamma(2/3)|^2 = 2.221$.

For all realistic systems the probability in this limit is much less than 1.

2.1.2
The high energy limit.   For high energies ($\xi \ll 1$), we have (Landau and Lifshitz 1971, p185)

$$H_{i\xi}^{(1)'}(i\xi) \cong H_{0}^{(1)'}(i\xi) \cong 2/\pi\xi , \qquad (2.6)$$

which, when substituted in (2.3), yields

$$P_{10}^{FO}(JK \to J'K; 0; E_i) \cong \frac{1}{3}\left(2D/ea_0\right)^2 G(J,J',K) E_i/R_Y, \quad E_i \gg \overline{E} , \qquad (2.7)$$

using $E_i \simeq E$ at high energies.

The energy E_c at which the sum of the upward and downward transition probabilities at impact parameter b=0 is equal to one, in the high energy limit (2.7) of first-order perturbation theory, is

$$E_c / R_Y = 3(ea_o/2D)^2 / g(J,K) ,$$

(2.8)

where

$$g(J,K) = 1 - K^2/J(J+1) .$$

Clearly for systems with $D \leq 1e\,a_o = 2.54$ Debye and $\Delta E < 0.1$ eV, $E_c \gg \bar{E}$. As will be shown below, for head-on collisions the breakdown of the assumption of a dipole potential is more significant than the non-conservation of flux.

We note that in the time-dependent perturbation theory approximation used in this work, departures from unitarity become increasingly important as the energy increases - the reverse of the situation for neutrals (Dickinson and Richards 1975). The difference is caused by the strong acceleration of the electron by the attractive Coulomb field.

2.2   The dipolar cross section

Substituting (2.1) in (1.13), we obtain for the cross section (Landau and Lifshitz 1971, p184)

$$\sigma_{10}^{FO}(JK \to J'K ; E_i) = (2\pi^3 \xi\, a_o^2/3)(D/ea_o)^2 G(J,J',K)$$
$$\times (R_Y/E_i) \left[i\, H_{i\xi}^{(1)}(i\xi)\, H_{i\xi}^{(1)\prime}(i\xi) \right] .$$

(2.9)

2.2.1

The low energy limit.   The low-energy behaviour ($E \ll \bar{E}; \xi \gg 1$) is

obtained from (2.9) using (2.4) and the relation (Landau and

Lifshitz 1971, p185)

$$H_{i\xi}^{(1)}(i\xi) \cong -(i/\pi\sqrt{3})(6/\xi)^{1/3}\,\Gamma(1/3) \quad , \qquad (2.10)$$

yielding

$$\sigma_{10}^{th}(JK \to J'K; E_i) \cong (8\pi^2 a_0^2/3\sqrt{3})(D/ea_0)^2$$
$$\times\, G(J,J';K)\,(R_y/E_i) \quad , \quad E_i \ll \bar{E}\,. \quad (2.11)$$

This is identical with the threshold dipolar cross section in the

Coulomb-Born approximation (Chu 1975).

2.2.2

The high energy limit.   For high energies ($E \gg \bar{E}; \xi \ll 1$) we have

(Landau and Lifshitz 1971, p185)

$$i\,H_{i\xi}^{(1)}(i\xi) \cong i\,H_0^{(1)}(i\xi) \cong (2/\pi)\ln(1.1229/\xi)\,. \quad (2.12)$$

Using (2.6) and (2.12) in (2.9) we obtain for the high-energy

cross section

$$\sigma^{H}(JK \to J'K; E_i) = \tfrac{1}{3}\pi a_0^2\,(2D/ea_0)^2\,G(J,J';K)$$
$$\times\,(R_y/E_i)\,\ln[5.04\,E^3/\Delta E^2\,R_y] \quad , \quad E_i \gg \bar{E}\,, \quad (2.13)$$

recovering the usual Bethe limit for an optically allowed transition.

This high energy limit of the cross section does not appear to have

been derived previously.   All the above equations hold for linear polar ions when K=0.

2.2.3
Numerical results.   To evaluate the Hankel functions used in (2.1) and (2.9) we use the method of Goldstein and Thaler (1959) to compute the Bessel functions $J_\nu(Z)$ and $Y_\nu(Z)$.   The calculation of the Hankel function is then straightforward (Abramowitz and Stegun 1965, pp 385 and 361).

In table 2.1 we compare our results for CH^+ with the Coulomb-Born results of Chu and Dalgarno (1974) for the $0 \rightarrow 1$ transition. In the energy range (0.0035,2.04) eV, the agreement is within 4%.   For energies less than 0.007 eV Bessel functions of large imaginary argument and order ($\xi \succ \sim 4\ 5$) are required and the routine employed suffered from rounding errors.   The low-energy limit (2.11) agrees within 10% with the full result (2.9) for $E_i \leqslant \bar{E}/2$, while the high-energy limit (2.13) agrees within 15% for $E_i \geqslant 6\bar{E}$.   For this transition $\bar{E} = 0.0348$ eV.   Thus the low-energy approximation (2.11) gives acceptable accuracy in the region where our direct method of evaluating the Bessel functions suffered numerical difficulties.   Overall, the agreement between the time-dependent and the time-independent approximations is very satisfactory.

2.3   The quadrupolar contribution

To calculate the quadrupolar contribution ($|\Delta J| = 1$ and $|\Delta J| = 2$) the $I_{2\nu}$ integral (1.18) was evaluated numerically.   For small velocities (large ξ) and large ϵ , it is difficult to obtain accurate values because of the fast oscillation of the integrand. We have used a modified Simpson's rule and tested our method by comparing the results with: (1) the tabulated values of Alder et al (1956) for the corresponding $\bar{I}_{2\nu}$ integral for a repulsive potential,

(2) the analytical result for $I_{1\nu}$ and (3) the analytical expressions
for $I_{2\nu}$ in the case of a sudden collision ($\xi = 0$), given by
Biedenharn et al (1972)

$$I_{2\pm2}(\epsilon, 0) = \bar{I}_{2\pm2}(\epsilon, 0) \quad , \quad (2.14a)$$

$$I_{20}(\epsilon, 0) = \bar{I}_{20}(\epsilon, 0) + 2\pi/(\epsilon^2-1)^{3/2}, \quad (2.14b)$$

where $\bar{I}_{2\nu}(\epsilon, 0)$ has been given by Alder et al (1956). Equation
(2.14b) clearly shows that relation (1.20) breaks down for the
quadrupole case.

In figure 2.1, we show the quadrupolar first-order probability
P_{20}^{FO} as a function of the impact parameter for collisions with H_3O^+
and HD^+. The probabilities do not satisfy unitarity, for small
impact parameters. Since P_{20}^{FO} diverges strongly as b tends to
zero, the quadrupole contribution to the cross section will be
discussed below after we have considered a short-range cut-off.
No such cut-off was necessary for the dipole potential since P_{10}^{FO}
was finite for head-on collisions.

Table 2.1 : Comparison of the 0→1 rotational-excitation cross sections of CH^+ by electron impact.

E_i (eV)	$\sigma(0\to1)$ ($\mathring{A}^2$) Equation (2.9)	Coulomb-Born[b]	E_i (eV)	$\sigma(0\to1)$ ($\mathring{A}^2$) Equation (2.9)	Coulomb-Born[b]
0.00351	7403[a]	7409	0.20	235	229
0.007	3826	3835	0.31	174	173
0.010	2728	2619	0.40	145	142
0.017	1669	1675	0.50	124	121
0.028	1072	1071	0.61	108	105
0.045	719	709	0.75	93	91
0.072	496	491	1.01	75	73
0.10	387	370	2.04	44	43

a From (2.11)

b Chu and Dalgarno (1974)

CAPTION TO FIGURE 2.1

First order quadrupolar probabilities P_{20}^{FO} as a function of the impact parameter.

A: P_{20}^{FO} $(6,6 \rightarrow 7,6;\ E_i = 1eV)$ for H_3O^+;

B: P_{20}^{FO} $(0 \rightarrow 2;\ E_i = 1eV)$ for HD^+;

C: as B except $E_i = 0.1eV$;

D: as B except $E_i = 0.06eV$.

Figure 2.1
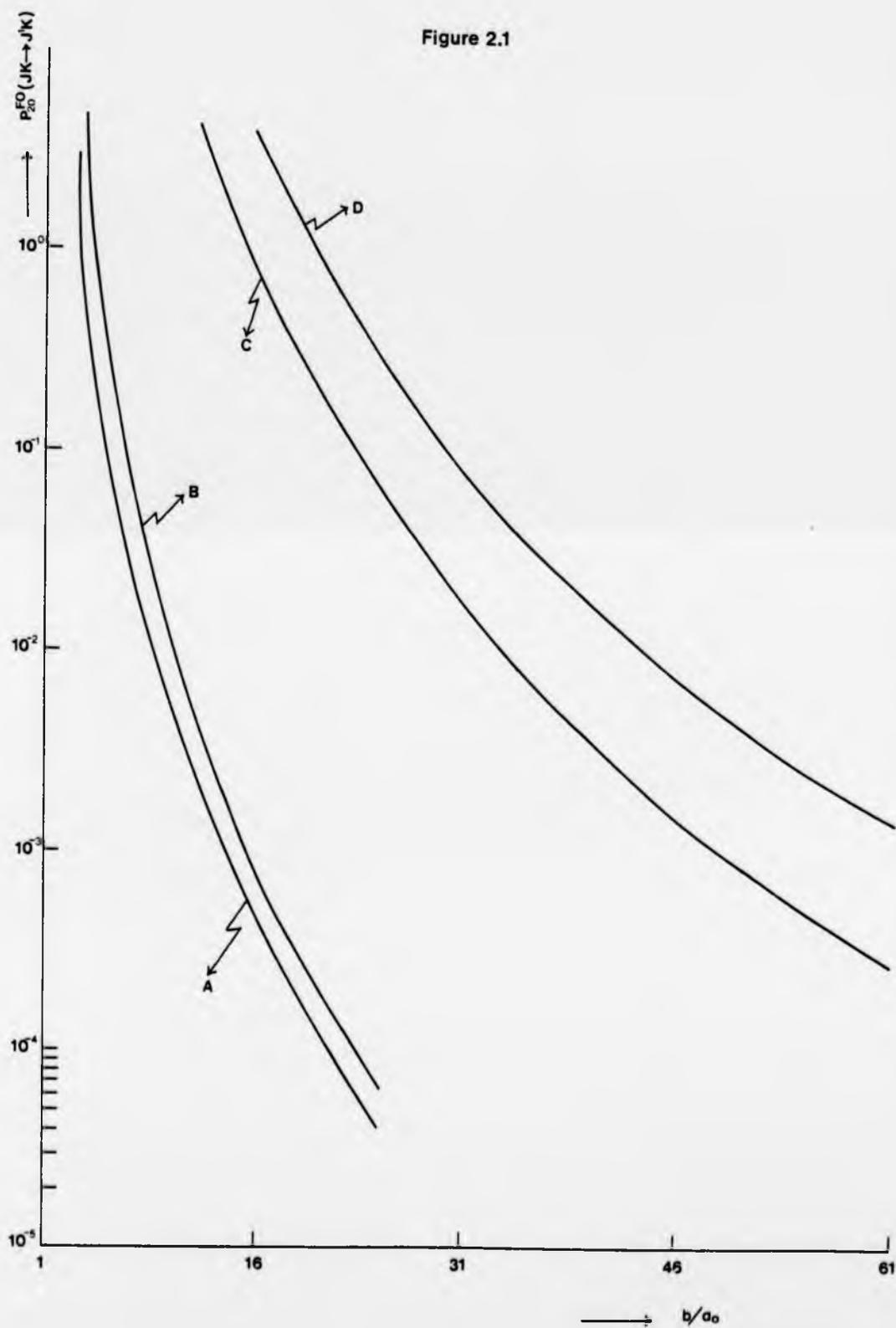
CHAPTER 3

THE SHORT RANGE MODIFICATIONS

3.1   The short range contribution

The theory presented above may become invalid at small impact parameters for the following reasons:

(i)   the incident electron must have an orbital angular momentum of at least $s\hbar$ to excite the molecular ion by an amount $\Delta J = s$;

(ii)   the interaction potential (1.2) is not valid for small r;

(iii)   the transition probability for an anisotropic term with $\lambda \geqslant 2$ is greater than unity for small impact parameters.

To allow for (i) we define

$$b_1 = s\hbar / m\sigma \tag{3.1}$$

and we assume a probability (Dickinson and Richards 1975)

$$P(JK \rightarrow J + sK; b; E_i) = 0, \quad b < b_1. \tag{3.2}$$

To correct for (ii) it is necessary to estimate the region where the potential (1.2) is reliable.   We suppose that this is for electron-molecular-ion separations larger than the charge-cloud size, r_c , of the molecular ion.   Thus we define b_2 as the impact parameter at which the Coulomb field focuses the incident electron to the edge of the charge cloud r_c

$$b_2 = \left(r_c^2 + e^2 r_c / E \right)^{1/2}. \tag{3.3}$$

when the incident electron penetrates the core region, $r < r_c$, it has considerable kinetic energy from the Coulomb field and can easily excite the high rotational levels of the ion, so becoming captured temporarily.   Subsequent collisions will then occur.   While our knowledge of the details of this process is limited, we consider it likely and it certainly should not be excluded until detailed

calculations with a realistic short-range potential have been made. To give a plausible estimate of the likely contribution from this mechanism, we assume a short-range probability

$$P(JK \to J'K; b; E_i) = \begin{cases} \dfrac{v_f}{v_i} \eta \dfrac{b}{b_m} & , \quad b_1 \leq b \leq b_m , \\[3mm] \dfrac{v_f}{v_i} \eta \dfrac{b_2 - b}{b_2 - b_m} & , \quad b_m \leq b \leq b_2 , \end{cases} \quad (3.4)$$

where η is a parameter. This form has been adopted so that the probability first increases due to the stronger collisions occurring as b decreases to b_m. There we assume that the unitarity requirement causes P to decrease in the strong-coupling regions $b_1 < b < b_m$. A similar model for the strong-coupling probability in electron-polar-molecule collisions (Dickinson and Richards 1975) yielded cross sections in good agreement with those obtained using close-coupling calculations. Strictly, $P(b_2) = P^{FO}(b_2)$ would preserve continuity but $P^{FO}(b_2)$ is generally small so such a modification makes negligible difference to the cross sections. The existence of strong rotational coupling in the interaction of slow electrons with H_2^+ is shown by the mixing observed by Herzberg (1970) between two Rydberg series of H_2 terminating on the J=0 and J=2 levels of the ground vibrational state of H_2^+. Fano (1970) has argued that this situation should be general in electron-molecular-ion-collisions. Thus we can write the cross section σ^T as

$$\sigma^T(JK \to J'K; E_i) = \sigma^{sh}(JK \to J'K; E_i) + \sigma^L(JK \to J'K; E_i) , \quad (3.5a)$$

where

$$\sigma^{sh}(JK \to J'K; E_i) = 2\pi \int_0^{b_2} P(JK \to J'K; b; E_i) \, b \, db , \quad (3.5b)$$

and

$$\sigma^L(JK \to J'K; E_i) = 2\pi \int_{b_2}^{\infty} P^{F0}(JK \to J'K; b; E_i) \, b \, db. \qquad (3.5c)$$

For simplicity we take

$$b_m = (b_1 + b_2)/2 \qquad (3.6)$$

obtaining for σ^{sh}

$$\sigma^{sh}(JK \to J'K; E_i) = (v_f/6v_i) \, \eta \pi \left[b_2(3b_2 + b_1) - 8b_1^3/(b_1 + b_2) \right] \quad (3.7)$$

For the dipole case σ^L can be obtained by a minor modification to (2.9) :

$$\sigma_{10}^L(JK \to J'K; E_i) = (2\pi^3 \xi a_0^2/3)(D/e a_0)^2 \, G(J, J', K)$$

$$\times (Ry/E_i) \left[i \epsilon_2 \, H_{i\xi}^{(1)}(i\xi\epsilon_2) \, H_{i\xi}^{(1)'}(i\xi\epsilon_2) \right], \qquad (3.8)$$

where ϵ_2 is obtained from b_2 using (1.16).

We have estimated the charge-cloud size, r_c, as twice the equilibrium internuclear distance, R_e, in diatomic ions, and twice the OH distance in the H_3O^+ ion.   We have taken $\eta = 0.2$, which should give a conservative estimate of the short-range contribution.

3.2   Results and discussion for dipole interaction

The effect of the short-range modification is shown for CH^+ in figure 3.1   The increase in the cross section falls smoothly from about 30% at threshold to 10% at 2eV.

An interesting comparison may be made with the results of Ray and Barua (1975) for rotational excitation of HD^+ by electron impact.

They have used time-dependent perturbation theory with the long-range potential given by (1.2) and (1.3) with an additional polarisability term. Their short-range potential is given by

$$V(r,\chi) = -(e^2/r_o) - (e\,D/r_o^2)\,P_1(\cos\chi)$$
$$- (e\,Q/r_o^3 + \alpha' e^2/r_o^4)\,P_2(\cos\chi)\,, \quad r < r_o\,, \quad (3.9)$$

where α' is the non-spherical part of the polarisability and r_o is a cut-off parameter. They assume $r_o = 2a_o$.

In figure 3.2, we present a comparison for the $0\rightarrow1$ transition between our results from (2.9), their results, and our modified result (3.5a) for the dipolar contribution. The agreement between their results and FOTDPT at low energies shows that the modified potential (3.9) yields small probabilities for close collisions. Since they use a straight-line trajectory inside the core, comparison with the case of neutral molecules suggests that this straight-line part will lead to higher probabilities, thus enhancing the cross section, as shown in figure 3.2. At higher energies, the effect of the straight-line trajectory is less marked and their use of a weaker short-range interaction (3.9) leads to smaller cross sections. Again, the effect of the modified probability (3.4) is to increase the cross section above the pure dipole value, in this case more than doubling the cross section at threshold.

Since $\sigma_{10}^{\perp}(JK\rightarrow J'K;Ei)$ depends mainly on the value of the dipole moment, for small dipole moments, such as HD^+, the short-range cross section σ^{sh} becomes relatively more important. This is illustrated in table 3.1, where we compare the dipolar σ^{sh} and $\sigma_{10}^{\perp}$ for H_3O^+ ($D = 0.22\ ea_o$).

3.3   Results and discussion for quadrupolar interactions

As discussed in section 2.3, there is a singularity at b=0 in the quadrupolar transition probability.   To avoid this, we have obtained cross sections for the quadrupole interaction using (3.1) and (3.2) for close encounters and FOTDPT otherwise.   The integration over impact parameter has been done using Simpson's rule.   Almost all the contribution comes from small impact parameters and the effective upper limit of the integral is always less than $130\,a_0$, while for the dipole case this limit was about $10^3\,a_0$.

Comparison with the quadrupolar Coulomb-Born results of Chu (1975) for the $(5,2 \to 6,2)$ transition in H_3O+ (an example with an intermediate K value) shows differences of less than 5% for $0.1\,eV < E_i < 1.4eV$.   This suggests that our cut-off procedure is reasonable.   Since the transition probabilities at the cut-off increased from 1.45 to 1.61 as the energy increased, it appears unlikely that the Coulomb-Born approximation satisfies unitarity for close collisions even at electron energies of several electron volts.

The arguments presented above for the effect of Coulomb focusing for close collisions should be equally valid for the quadrupolar interaction.   Thus the use of the quadrupole interaction for these collisions is unreliable.   Since any cross section derived using approximations similar to (3.3) and (3.4) would be dominated by the assumed short-range contribution, we have not thought it worthwhile to make such a calculation.   However, any cross section derived using a first-order perturbation theory and the quadrupole interaction is likely to exceed the true cross section considerably.

3.4   Conclusions

For electron-polar-molecular-ion collisions, we have used an impact-parameter method to investigate the reliability of the usual approximation of combining the Coulomb-Born approximation with the dipole and quadrupole anisotropic potentials.   We find that for a dipole potential, this method underestimates the cross section, particularly for weak dipoles.   A modified expression for the cross section has been presented.   By contrast, for collisions of electrons with neutral polar molecules, the use of the Born approximation and the dipole potential is more reliable, overestimating the cross section for large dipole moments (Dickinson and Richards 1975).   In collisions where the long-range interaction is the quadrupole, the full short-range interaction must be included to obtain reliable results.

Clearly there is a need for an accurate calculation including the detailed electronic structure of the target, similar to those already performed for electron scattering by H_2, N_2 and CO (Temkin 1976).

Table 3.1: Rotational-excitation cross section of H_3O^+ by electron

impact for the $(5,0 \rightarrow 6,0)$ transition.

E_i (eV)	$\sigma (5,0 \rightarrow 6,0)$ $(\overset{\circ}{A}{}^2)$	
	Equation (3.7)	Equation (3.8)
0.1	89	19
0.2	45	10.4
0.4	23	6
0.6	16	4.4
0.8	12	3.6
1.0	10	3
1.2	8.4	2.6
1.4	7.4	2.3
1.6	6.6	2.1
1.8	6	1.9

CAPTIONS TO FIGURES 3.1 - 3.2

Figure 3.1: Graph of $E_i \sigma(0 \rightarrow 1)$ for CH^+ plotted against energy. Curve A shows the pure dipole potential result, equation (2.27) and curve B shows the modified results (3.5a)

Figure 3.2: Graph of $E_i \sigma(0 \rightarrow 1)$ for HD^+ plotted against energy. Curve A shows the pure dipole results (2.27), curve B shows the results of Ray and Barua (1975) and curve C shows the modified results (3.5a).

Figure 3.1
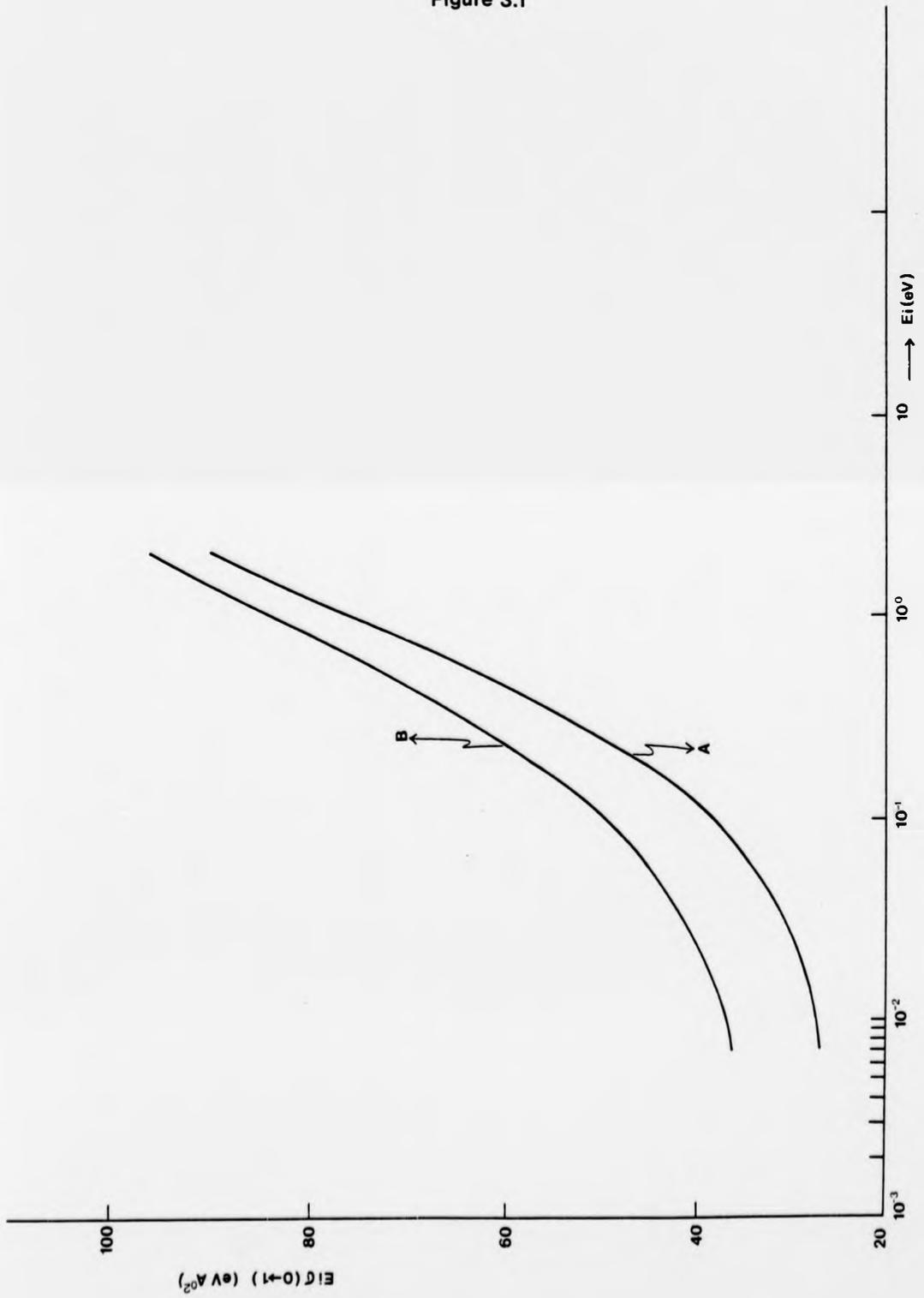
Figure 3·2
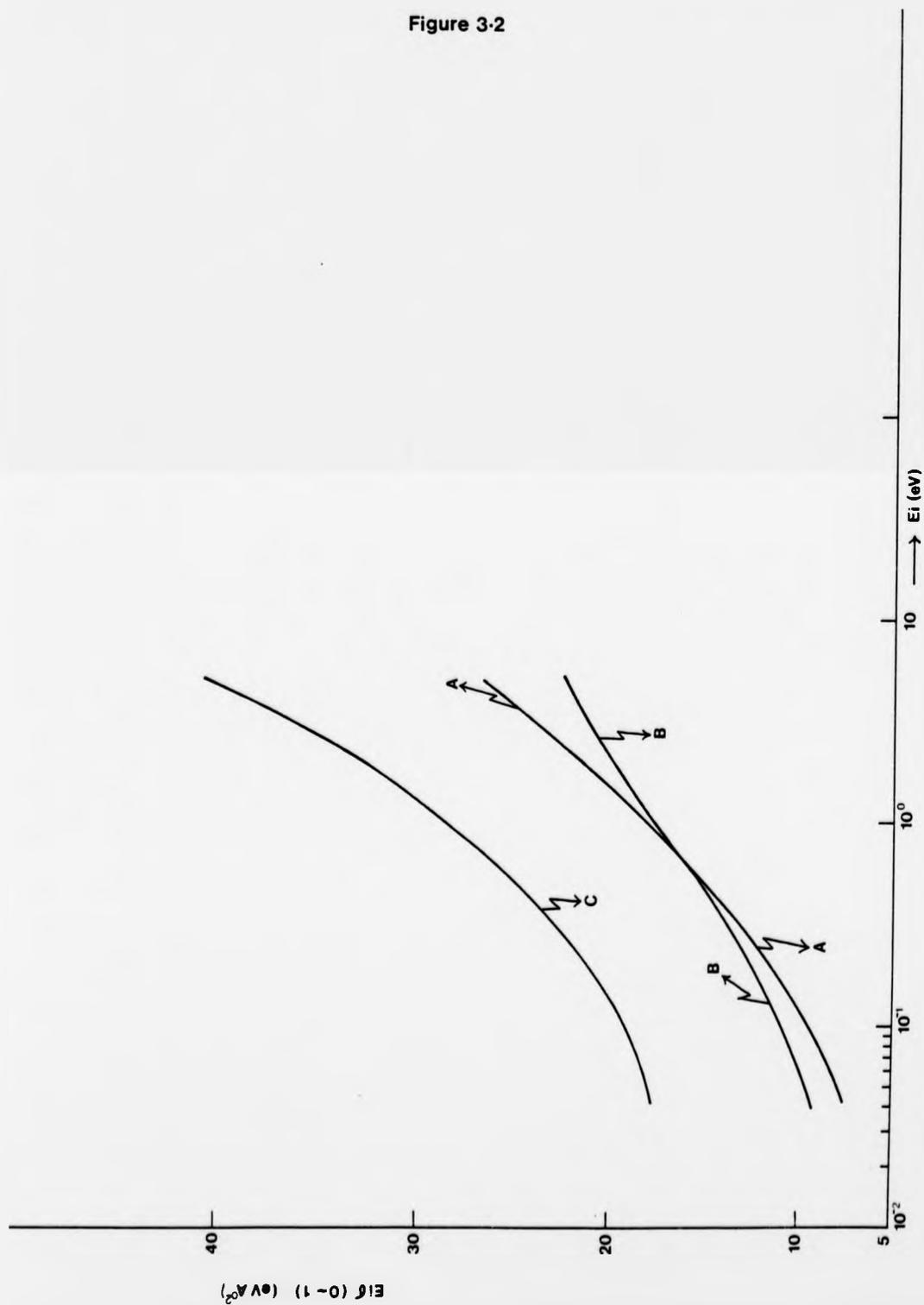
SECOND PART

Rotationally inelastic scattering of two linear

molecules

CHAPTER 4

DYNAMICS OF THE COLLISION

4.1   The Strong-Coupling Correspondence Principle (SCCP)

Consider a collision whose classical model is described in terms of the action-angle variables (Landau and Lifshitz 1960, p157). $\underline{T} \equiv (T_1, T_2, \ldots, T_n)$ and $\underline{\theta} \equiv (\theta_1, \theta_2, \ldots, \theta_n)$ respectively.   The SCCP transition amplitude $S(\underline{n}, \underline{n}')$ between two states $\underline{n} \equiv (n_1, n_2, \ldots, n_n)$ and $\underline{n}' \equiv (n_1', n_2', \ldots, n_n')$ is given by Clark et.al. (1977):

$$S(\underline{n}, \underline{n}') = \left(\tfrac{1}{2\pi}\right)^N \int_0^{2\pi} d\underline{\theta} \; \exp\left\{ i \left[\underline{\theta} \cdot (\underline{n} - \underline{n}') - A(\underline{\theta}) \right] \right\} \quad , \quad (4.1)$$

where $A(\theta)$ is $(1/\hbar)$ times the first term of the classical perturbation expansion of the change of the action of the system, given by

$$A(\underline{\theta}) = \frac{1}{\hbar} \int_{-\infty}^{\infty} dt \; V^c\left(\underline{T}, \underline{\theta} + \underline{w}^c t ; t \right) \quad , \tag{4.2}$$

with $\underline{w}^c = (w_1^c, w_2^c, \ldots, w_n^c)$ the fundamental frequency vector of the system, and $V^c(\underline{T}, \underline{\theta} + \underline{w}^c t ; t)$ the interaction potential between the partners of the collision.   To obtain approximately the quantal energy levels the system is quantized using the Bohr-Sommerfeld quantisation rule.

When the potential is weak we can approximate

$$\exp\left[-i A(\underline{\theta}) \right] \simeq 1 - i A(\underline{\theta}) \quad , \tag{4.3}$$

obtaining

$$S^{FO}(\underline{n} - \underline{n}') = -i \left(\tfrac{1}{2\pi}\right)^N \int_0^{2\pi} d\underline{\theta} \; A(\underline{\theta}) \exp\left\{ i \left[\underline{\theta} \cdot (\underline{n} - \underline{n}') \right] \right\} , \tag{4.4}$$

which is the first-order correspondence principle (FOCP) (Percival and Richards 1970).   In the next section, we describe the parameters of the collision between two linear molecules as required by the SCCP to obtain the rotationally inelastic transition amplitude.

4.2   Description of the collision

        The process we study is that of two linear molecules
(1 and 2 respectively), in initial quantum states given by the
action variables $\underline{T}_1$ and $\underline{T}_2$, which collide and change their quantum
state to $\underline{T}_1'$ and $\underline{T}_2'$ respectively.   The usual rigid-rotor model is
assumed, and the action variables T_i (i=1,2) describe the rotational
motion of isolated rotors.

        The configuration of the system is classically described
relative to an inertial coordinate system OXYZ and we consider the
relative motion of the two rotors as indicated in figure 4.1.
Following Dickinson and Richards (1974) we take a coordinate system
$O_i \xi_i \eta_i \zeta_i$ fixed to the i-th rotor as shown in figure 4.2.   The
rotational angular momentum vector, $\underline{J}_i$, is taken perpendicular to
the $O_i \xi_i \eta_i$ plane and the molecular axis is along the $O_i \eta_i$ axis so
that the polar angles of the rotor in the $O_i \xi_i \eta_i \zeta_i$ system are

$$\Theta_i = \pi/2 \quad , \quad \phi_i = \pi/2 \quad ,$$

The Euler angles $\alpha_i, \beta_i, \gamma_i$ (Edmonds 1960,p7) describe the
orientation of the i-th rotor in the OXYZ frame as follows:

- α_i is the azimuthal angle of the rotational angular momentum
        vector $\underline{J}_i$, of the rotor in the OXY plane

- β_i is the angle between $\underline{J}_i$ and the quantization axis OZ.

- γ_i is the angle of rotation of the rotor given by

$$\gamma_i = W_i \tau \quad , \quad W_i = J_i / I_i \quad , \tag{4.5}$$

where τ is a time, W_i is the frequency of rotation of the rotor,
$J_i = |\underline{J}_i|$, and I_i the rotor's moment of inertia.   Then the action-
angle variables which describe the rotational motion of our system
are

<u>Action variables</u>   <u>Angle variables</u>

$$\underline{T}_1 = \begin{cases} J_1 = \text{rotational angular} \\ \quad\quad\text{momentum of the molecule 1} \\ \\ J_1 \cos \beta_1 = \text{Z-component of } \underline{J}_1, \end{cases}$$

$$\theta_1 = w_1 t + \gamma_1$$
$$\alpha_1,$$

$$\underline{T}_2 = \begin{cases} J_2 = \text{rotational angular momentum} \\ \quad\quad\text{of the molecule 2,} \\ \\ J_2 \cos \beta_2 = \text{Z-component of } \underline{J}_2, \end{cases}$$

$$\theta_2 = w_2 t + \gamma_2$$
$$\alpha_2,$$

The J_i are quantized as (Dickinson and Richards 1974)

$$J_i = \hbar \left(j_i + \tfrac{1}{2} \right) , \tag{4.6}$$

where j_i are the rotational quantum numbers. The frequency of rotation is then

$$w_i = \hbar \left(j_i + \tfrac{1}{2} \right) / I_i . \tag{4.7}$$

4.3   The interaction potential

For two molecules in a Σ electronic state the long-range electrostatic potential is expressed, in a space-fixed system, by an expansion in a triple series of spherical harmonics as follows (Gray 1968)

$$V(\underline{R}, \Omega_1, \Omega_2) = \sum_{\lambda_1, \lambda_2 = 0} \sum_{\mu_1 = -\lambda_1}^{\lambda_1} \sum_{\mu_2 = -\lambda_2}^{\lambda_2} \left[C_{\lambda_1 \lambda_2}(R) \right.$$
$$\left. \times \left(\lambda_1 \mu_1 \, \lambda_2 \mu_2 / \lambda_1 \lambda_2 \, \lambda_{12} \mu_{12} \right) \, Y_\lambda(\Omega_1, \Omega_2, \Omega) \right] , \tag{4.8}$$

with

$$Y_\lambda(\Omega_1, \Omega_2, \Omega) = Y_{\lambda_1 \mu_1}(\Omega_1) \, Y_{\lambda_2 \mu_2}(\Omega_2) \, Y_{\lambda_{12} \mu_{12}}^*(\Omega) ,$$
$$\lambda_{12} = \lambda_1 + \lambda_2 , \tag{4.9}$$

and

$$C_{\lambda_1 \lambda_2}(R) = \frac{4\pi}{(2\lambda_{12}+1)} (-1)^{\lambda_2} \left[\frac{4\pi (2\lambda_{12}+1)!}{(2\lambda_1+1)!(2\lambda_2+1)!} \right]^{1/2} \frac{Q_{\lambda_1} Q_{\lambda_2}}{R^{\lambda_{12}+1}} \qquad (4.10)$$

where $\underline{R} = (R, \Omega)$ is the vector joining the centre of masses G_1 and G_2 of the molecules, $\Omega = (\bar{\theta}, \gamma)$ is the orientations of $\underline{R}, \Omega_i = (\bar{\theta}_i, \gamma_i)$ is the orientation of the i-th rotor, $(\lambda_1 \mu_1 \lambda_2 \mu_2 / \lambda_1 \lambda_2 \lambda_{12} \mu_{12})$ is a Clebsch-Gordan coefficient (Edmonds 1960,p.37), and the restriction $\lambda_{12} = \lambda_1 + \lambda_2$ means that (4.8) is valid when the two molecular charge clouds do not overlap significantly. The Q_{λ_i} are the scalar magnitudes of the multipole moments of order λ_i for an axially symmetric charge distribution, and are given by

$$Q_{\lambda_i} = \sum_{\text{all charges}} e \; r^{\lambda_i} P_{\lambda_i}(\cos \bar{\theta}_i) \quad .$$

Physically $V(\underline{R}, \Omega_1, \Omega_2)$ is symmetric under a coordinate inversion $\underline{R}_1, \underline{R}_2, \underline{R} \rightarrow -\underline{R}_1, -\underline{R}_2, -\underline{R}, \underline{R}_i$ being the internuclear vector of the i-th molecule. For two identical molecules $V(\underline{R}, \Omega_1, \Omega_2)$ is symmetric with respect to a coordinate interchange $\underline{R}_1, \underline{R}_2 R \rightarrow \underline{R}_2, \underline{R}_1, -\underline{R}$.

The short-range potential can also be expressed by an expansion in a triple series of spherical harmonics (Bhattacharyya et.al., 1977) and then the whole interaction potential is obtained from (4.8) on just replacing $C_{\lambda, \lambda_2}(R)$ by

$$\bar{C}_{\lambda, \lambda_2}(R) = C_{\lambda, \lambda_2}(R) + C_{\lambda, \lambda_2}^{SR}(R) \quad ,$$

where $C_{\lambda, \lambda_2}^{SR}(R)$ is the short-range contribution.

Since $O_i \xi_i \eta_i \zeta_i$ is obtained from OXYZ by the rotation $(\theta_i, \beta_i, \alpha_i)$ in the notation of Wolf (1969), we expand the spherical harmonics in (4.8) as (Wolf 1969, eq.8)

$$Y_{\lambda_i \mu_i}(\bar{\theta}_i, \gamma_i) = \sum_{\nu_i = -\lambda_i}^{\lambda_i} Y_{\lambda_i \nu_i}(\pi/2, \pi/2) \; D_{\nu_i \mu_i}^{(\lambda_i)}(\theta_i, \beta_i, \alpha_i) \quad , \qquad (4.11)$$

where the orientation of the i-th rotor in the $O_i \xi_i \eta_i \zeta_i$ system has been written explicitly, and $D_{\nu_i \mu_i}^{(\lambda_i)}$ is the matrix element

of a finite rotation (Edmonds 1960, p55).   Replacing (4.11) in
(4.8) we obtain the potential in terms of the action-angle variables
and relative coordinates as

$$
V(\underline{R}, \bar{\Omega}_i) = \sum_{\lambda_1, \lambda_2 = 0} \bar{C}_{\lambda_1 \lambda_2}(R) \sum_{\mu_1, \nu_1 = -\lambda_1}^{\lambda_1} \sum_{\mu_2, \nu_2 = -\lambda_2}^{\lambda_2} (\lambda_1 \mu_1 \lambda_2 \mu_2 / \lambda_1 \lambda_2 \lambda_{12} \mu_{12})
$$

$$
\times \; Y_{\lambda_1 \nu_1}(\pi/2, \pi/2) \, D^{(\lambda_1)}_{\nu_1 \mu_1}(\bar{\Omega}_1) \, Y_{\lambda_2 \nu_2}(\pi/2, \pi/2) \, D^{(\lambda_2)}_{\nu_2 \mu_2}(\bar{\Omega}_2) \, Y^{*}_{\lambda_{12} \mu_{12}}(\Omega) \; , \quad (4.12)
$$

where $\Omega_i = (\theta_i, \beta_i, \alpha_i)$.

We present calculations on HF-HF and HCl-HCl collisions.
To compare with previous alternative approximations (DePristo and
Alexander 1977, Bhattacharyya et.al. 1977 respectively) we use the
same potential surfaces as these authors:

HF-HF intermolecular potential

This potential is Alexander and DePristo's fit (1976) to
the "ab initio" points of Yarkony et.al. (1974).   In this work only
the first two terms corresponding to the spherically symmetric part
$\bar{C}_{oo}(R)$, and the first anisotropic interaction $\bar{C}_{11}(R)$ are retained.
They are given by (De Pristo and Alexander 1977)

$$
\bar{C}_{oo} = 1.067 \times 10^9 \exp(-2R) - 7.871 \times 10^6 \exp(-1.1R), \quad\quad (4.13a)
$$

$$
\bar{C}_{11} = -1.714 \times 10^5 \exp(-R) - 1.574 \times 10^4 \exp(-0.475R) - \frac{1.831 \times 10^6}{R^3} \quad (4.13b)
$$

where the energy has been expressed in cm^{-1} and the distance in a_o.
The third term in (4.13b) corresponds to the asymptotic dipole-dipole
form $C_{11}(R)$, obtained from (4.10) using a dipole moment value D=1.82 Debye.

HCl-HCl intermolecular potential

This potential was determined by Bhattacharyya et.al. (1977). The $C_{\lambda_1 \lambda_2}^{SR}$ (R) terms were obtained assuming a repulsive central force acting between different pairs of atoms in the molecules (Takayanagi 1954). The long-range spherically symmetric part $\bar{C}_{oo}$(R) was assumed to be

$$C_{oo}(R) = -\frac{C_{disp}^{(6)}}{R^6} - \frac{2\alpha D^2}{R^6} - \frac{3\alpha Q^2}{R^8} \quad , \tag{4.14}$$

where the first two terms correspond to the dipole-dipole dispersion and induction interactions respectively, and the third to the dipole-quadrupole interaction (Hirschfelder et.al. 1966); α is the average polarizability, D and Q the dipole and quadrupole moments respectively, and $C_{disp}^{(6)}$ is given approximately by (Hirschfelder et.al. 1966)

$$C_{disp}^{(6)} = \frac{3}{2} \left(2 \alpha^3 \right)^{1/2}$$

Only the first two terms of (4.14) are used in this work.

Again only the first two terms $\bar{C}_{oo}$(R) and $\bar{C}_{11}$(R) of the potential are retained. Using the same units as for HF-HF they can be written as

$$\bar{C}_{oo}(R) = (6.108 \times 10^6 - 5.259 \times 10^6/R)\exp(-2.06R)$$
$$+ (5.571 \times 10^7 - 4.396 \times 10^7/R)\exp(-1.99R)$$
$$+ (5.202 \times 10^7 - 2.964 \times 10^5/R)\exp(-1.92R) - \frac{3.6315 \times 10^7}{R^6} \tag{4.15a}$$

$$\bar{C}_{11}(R) = -(8.8105 \times 10^7 + 4.277 \times 10^7/R)\exp(-2.06R)$$
$$+ (4.043 \times 10^7 + 2.032 \times 10^7/R)\exp(-1.99R)$$
$$- (4.628 \times 10^6 + 2.410 \times 10^6/R)\exp(-1.92R) - \frac{6.8196 \times 10^5}{R^3} \tag{4.15b}$$

where the exponentials in both equations correspond to the short-range overlap interaction. The fourth term in (4.15b) corresponds to the asymptotic dipole-dipole term C_{11}(R) for a dipole moment value D=1.11 Debye.

4.4   The relative motion

As seen in sections 4.1 and 4.2 the SCCP considers the
dynamics of the system described by classical mechanics.   We assume
that the relative motion is on a classical trajectory determined by
the spherical part of the potential $\bar{C}_{oo}(R)$.   The energy $\bar{E}$, on the
trayectory, is taken to be

$$\bar{E} = \frac{1}{2} \mu v^2 \quad , \quad v^2 = \frac{v_i + v_f}{2} \tag{4.16}$$

where μ is the reduced mass of the system, and v_i (v_f) is the
initial (final) relative speed.   Then the relative motion is on a
plane.   We show below that a suitable choice of axis relative to
this plane can lead to further useful approximations in the calculation.

CAPTIONS TO FIGURES 4.1 - 4.2

Figure 4.1: Inertial coordinate system OXYZ where the relative motion
of the rotors is described. G_1 and G_2 are the centre
of mass of rotor 1 and rotor 2, respectively, $\underline{r}_1$ and
$\underline{r}_2$ are their corresponding position vectors, and $\underline{R}$ is
the relative position vector.

Figure 4.2: Euler angles α_i, β_i and γ_i as used in this work.
AB is the i-th rotor and O_i its centre of mass. The
system $O_i\,\xi_i\,\eta_i\,\zeta_i$ rotates fixed to the rotor respect
to the inertial system O_iXYZ. The angles given the
orientation of the rotor in $O_i\,\xi_i\,\eta_i\,\zeta_i$ are $\Theta_i = \Phi_i = 90°$.

Figure 4.1

Figure 4.2
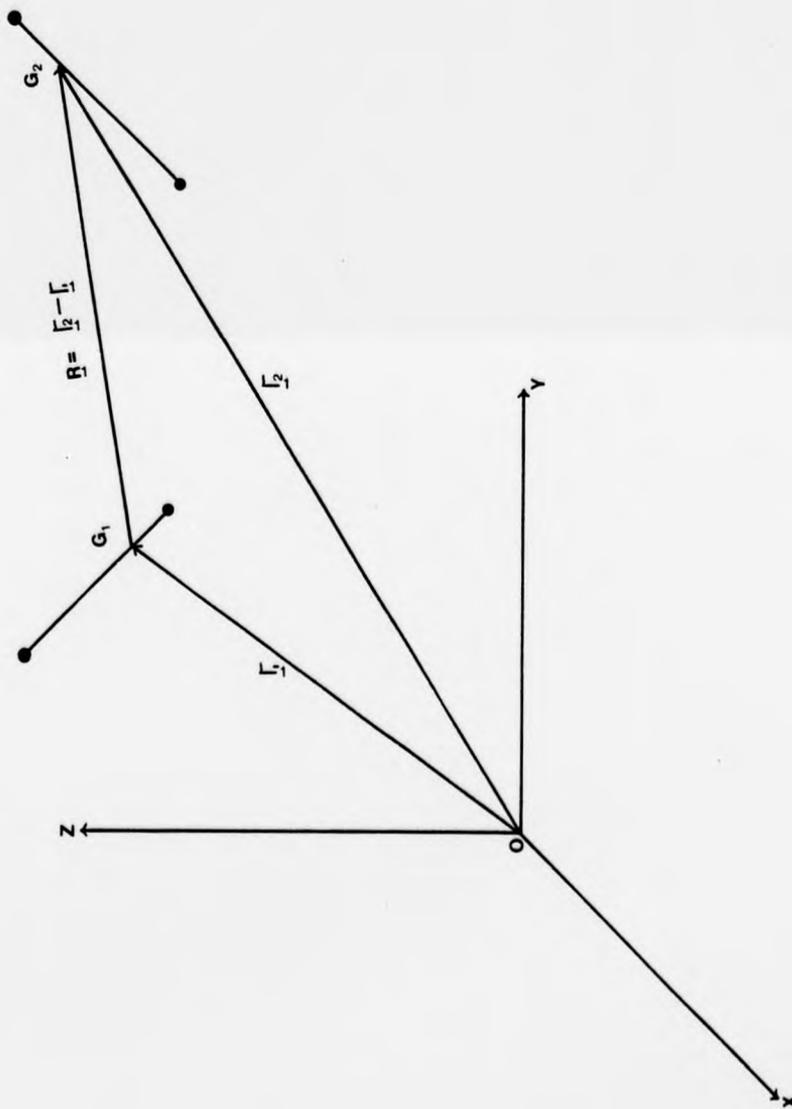
CHAPTER 5

GENERAL PROPERTIES OF THE TRANSITION PROBABILITY

5.1   The transition probability

In terms of the variables defined in sections 4.1 and 4.2 the transition amplitude $S(j_1 m_1 j_2 m_2, j_1' m_1' j_2' m_2')$, between two rotational states $|j_1 m_1 j_2 m_2\rangle$ and $|j_1' m_1' j_2' m_2'\rangle$ is

$$S(j_1 m_1 j_2 m_2, j_1' m_1' j_2' m_2') = \left(\frac{1}{2\pi}\right)^4 \int_0^{2\pi} d\gamma_1 d\gamma_2 d\alpha_1 d\alpha_2 \; \exp\left[i\left\{\Delta j_1 \gamma_1 + \Delta j_2 \gamma_2 \right.\right.$$
$$\left.\left. + \Delta m_1 \alpha_1 + \Delta m_2 \alpha_2 - A(\bar{\Omega}_1, \bar{\Omega}_2)\right\}\right], \qquad (5.1)$$

where $\Delta j_i = j_i - j_i'$ and $\Delta m_i = m_i - m_i'$ are the changes in the rotational quantum number and the proyection quantum numbers of the molecule respectively.   In this case the energy levels of the target and incident molecule are degenerate and we are concerned, in this work, in calculating the transition probability between levels (j_1, j_2) rather than states.   We therefore require the degeneracy-averaged probability $\mathcal{P}(j_1 j_2 \to j_1' j_2'; \bar{E})$ given by

$$\mathcal{P}(j_1 j_2 \to j_1' j_2'; \bar{E}) = \frac{1}{(2j_1+1)(2j_2+1)} \sum_{m_1, m_2} \sum_{m_1', m_2'} \left| S(j_1 m_1 j_2 m_2, j_1' m_1' j_2' m_2') \right|^2. \quad (5.2)$$

Replacing the sum (5.2) by a sum over $m_1, m_2, \Delta m_1$ and Δm_2, and using the relations (Clark et.al. 1977)

$$\sum_{\Delta m = -\infty}^{\infty} e^{i\Delta m \theta} = 2\pi \delta(\theta) \;,\; \sum_{m=-j}^{j} \cong \left(j+\tfrac{1}{2}\right)\int_{-1}^{1} d(\cos\beta) \;, \qquad (5.3)$$

we obtain

$$\mathcal{P}(j_1 j_2 \to j_1' j_2'; \bar{E}) = \frac{1}{16\pi^2} \int_0^{2\pi} d\alpha_1 \int_0^{2\pi} d\alpha_2 \int_{-1}^{1} d(\cos\beta_1) \int_{-1}^{1} d(\cos\beta_2) \left| S(j_1 j_2, j_1' j_2') \right|^2, \qquad (5.4)$$

where

$$S(j_1 j_2, j_1' j_2') = \frac{1}{4\pi^2} \int_0^{2\pi}\int_0^{2\pi} d\gamma_1 d\gamma_2 \; \exp\left[i\left\{\Delta j_1 \gamma_1 + \Delta j_2 \gamma_2 - A(\bar{\Omega}_1, \bar{\Omega}_2)\right\}\right]. \qquad (5.5)$$

The sums over degenerate states have been replaced by two integrals over a microcanonical ensemble of target and projectile molecules.

5.2   The change of the action

Substituting the potential (4.12) into (4.2) we obtain

$$A(\bar{\Omega}_1, \bar{\Omega}_2) = \sum_{\lambda_1 \lambda_2} \frac{1}{\hbar} \int_{-\infty}^{\infty} dt\, \bar{C}_{\lambda_1 \lambda_2}[R(t)] \sum_{\mu_1, \lambda_1' = -\lambda_1}^{\lambda_1} \sum_{\mu_2, \lambda_2' = -\lambda_2}^{\lambda_2} C_{\mu_1 \mu_2}^{\lambda_1 \lambda_2} M_{\nu_1 \mu_1}^{\lambda_1} M_{\nu_2 \mu_2}^{\lambda_2} \tag{5.6}$$

where

$$C_{\mu_1 \mu_2}^{\lambda_1 \lambda_2} = \left(\lambda_1 \mu_1 \lambda_2 \mu_2 / \lambda_1 \lambda_2 \lambda_{12} \mu_{12}\right) Y_{\lambda_{12} \mu_{12}}^{*}[\bar{\theta}(t), \varphi(t)], \tag{5.7}$$

$$M_{\nu_i \mu_i}^{\lambda_i} = Y_{\lambda_i \nu_i}(\pi/2, 0) \mathcal{D}_{\nu_i \mu_i}^{(\lambda_i)}(\gamma_i + W_i t + \pi/2, \beta_i, \alpha_i), \tag{5.8}$$

and the relative coordinates have been written explicitly as functions of time.   We consider the plane of the trajectory as the OXY plane, and take the incident velocity V_i in the direction of the OY axis. With this choice (5.6) becomes

$$A(\bar{\Omega}_1, \bar{\Omega}_2) = \sum_{\lambda_1, \lambda_2} \sum_{\mu_1, \nu_1} \sum_{\mu_2, \nu_2} N_{\lambda_{12} \mu_{12}} N_{\lambda_1 \nu_1} N_{\lambda_2 \nu_2} \left(\lambda_1 \mu_1 \lambda_2 \mu_2 / \lambda_1 \lambda_2 \lambda_{12} \mu_{12}\right)$$
$$\times \mathcal{D}_{\nu_1 \mu_1}^{(\lambda_1)}(\gamma_1 + \pi/2, \beta_1, \alpha_1)\, \mathcal{D}_{\nu_2 \mu_2}^{(\lambda_2)}(\gamma_2 + \pi/2, \beta_2, \alpha_2)\, U_{\nu_1 \nu_2 \mu_1 \mu_2}^{(\lambda_{12})}(\bar{E}, b), \tag{5.9}$$

where

$$U_{\nu_1 \nu_2 \mu_1 \mu_2}^{(\lambda_{12})}(\bar{E}, b) = \frac{1}{\hbar} \int_{-\infty}^{\infty} dt\, \bar{C}_{\lambda_1 \lambda_2}(R)\, \exp i\left[(\nu_1 W_1 + \nu_2 W_2) t - (\mu_1 + \mu_2)\varphi\right], \tag{5.10}$$

$\bar{E}$ is given by (4.16), b is the impact parameter and $N_{\lambda \nu} = Y_{\lambda \nu}(\pi/2, 0)$. Following Dickinson and Richards (1974) we define

$$\varphi'(t) = \varphi(t) + \mathcal{X}/2, \tag{5.11}$$

where $\mathcal{X}$ is the deflection angle.   Taking t=o at the classical distance of closest approach r_0, we have that $\varphi'(-t) = -\varphi'(t)$, and since $R(t) = R(-t)$ the integral (5.10) can be written as

$$U_{\nu_1 \nu_2 \mu_1 \mu_2}^{(\lambda_{12})}(\bar{E}, b) = e^{i(\mu_1 + \mu_2)\mathcal{X}/2} V_{\nu_1 \nu_2 \mu_1 \mu_2}^{(\lambda_{12})}(\bar{E}, b), \tag{5.12}$$

where

$$V^{(\lambda_{12})}_{\nu_1\nu_2\mu_1\mu_2}(\bar{E},b) = \frac{2}{\hbar}\int_0^\infty dt\, \bar{C}_{\lambda_1\lambda_2}(R)\cos\left[(\nu_1 w_1 + \nu_2 w_2)t - (\mu_1+\mu_2)\varphi\right]. \qquad (5.13)$$

The motion of both rotors is contained in the $W_i t$ terms. Each $(\bar{E},b)$ determine a function $\underline{R}(t)=\left[R(t),\varphi(t)\right]$ which describes the relative motion in the field $\bar{C}_{oo}(R)$. In this way the dynamical factors, which are contained in the $V^{(\lambda_{12})}_{\nu_1\nu_2\mu_1\mu_2}$ integrals, have been separated from the orientation dependent factors of the rotors, which are contained in the $\mathcal{D}^{(\lambda)}_{\nu\mu}$ functions. This simplification is due to the use of classical perturbation theory in evaluating $A(\bar{\Omega}_1,\bar{\Omega}_2)$, and it is independent of the form of $\bar{C}_{oo}(R)$ (Clark et.al. 1977).

Substituting (5.12) in (5.9) we obtain

$$A(\bar{\Omega}_1,\bar{\Omega}_2) = \sum_{\lambda_1\lambda_2}\sum_{\mu_1\,\nu_1=-\lambda_1}^{\lambda_1}\sum_{\mu_2\,\nu_2=-\lambda_2}^{\lambda_2} N_{\lambda_{12}\mu_{12}}N_{\lambda_1\nu_1}N_{\lambda_2\nu_2}(\lambda_1\mu_1\lambda_2\mu_2/\lambda_1\lambda_2\lambda_{12}\mu_{12})$$
$$\times\; \mathcal{D}^{(\lambda_1)}_{\nu_1\mu_1}(\gamma_1,\beta_1,\alpha_1)\,\mathcal{D}^{(\lambda_2)}_{\nu_2\mu_2}(\gamma_2,\beta_2,\alpha_2)\, V^{(\lambda_{12})}_{\nu_1\nu_2\mu_1\mu_2}(\bar{E},b), \qquad (5.14)$$

where we have made the transformations (Dickinson and Richards 1974) $\gamma_i^o + \pi/2 \longrightarrow \gamma_i$, $\alpha_i + \pi/2 \to \alpha_i$, for only the average over these variables is required in evaluating (5.4). The classical changes Δj_i^c and Δm_i^c are obtained from (5.14) using (Clark et.al. 1977).

$$\Delta j_i^c = -\frac{\partial A}{\partial \gamma_i} \quad , \quad \Delta m_i^c = -\frac{\partial A}{\partial \alpha_i} \qquad (5.15)$$

where $m_i^c = J_i\cos\beta_i$.

It is important, as we will see below, to point out that with our choice of the plane of the classical trajectory we have

$$\Delta l \equiv l - l' = -\Delta m_1^c - \Delta m_2^c \quad , \qquad (5.16)$$

where ℓ is the orbital angular momentum quantum number of the system.

5.3   The real form of the change of the action

To evaluate (5.1) it proves convenient to express $A(\bar{\Omega}_1,\bar{\Omega}_2)$ in real form.   Using the symmetry properties of the Clebsch–Gordan coefficients, the spherical harmonics and the rotation matrices we find that

$$C^{\lambda_1,\lambda_2}_{-\mu_1-\mu_2} M^{\lambda_1}_{-\nu_1,-\mu_1} M^{\lambda_2}_{-\nu_2\mu_2} = \left(C^{\lambda_1,\lambda_2}_{\mu_1,\mu_2} M^{\lambda_1}_{\nu_1,\mu_1} M^{\lambda_2}_{\nu_2\mu_2} \right)^* \tag{5.17}$$

so that the sums over μ_i, ν_i in (5.6) are written in the form

$$\sum_{\mu_1\,\nu_1=-\lambda_1}^{\lambda_1} \sum_{\mu_2\,\nu_2=-\lambda_2}^{\lambda_2} C^{\lambda_1,\lambda_2}_{\mu_1,\mu_2} M^{\lambda_1}_{\nu_1,\mu_1} M^{\lambda_2}_{\nu_2\mu_2} =$$

$$2\,\mathrm{Re} \sum_{\mu_1\,\nu_1=0}^{\lambda_1} \sum_{\mu_2\,\nu_2=0}^{\lambda_2} \Bigg[C^{\lambda_1,\lambda_2}_{\mu_1\mu_2} \Big\{ B_{\mu_1\nu_1\mu_2\nu_2} M^{\lambda_1}_{\nu_1\mu_1} M^{\lambda_2}_{\nu_2\mu_2} + B_{\mu_1\mu_2\nu_2} M^{\lambda_2}_{-\nu_1\mu_1} M^{\lambda_2}_{\nu_2\mu_2}$$

$$+ B_{\nu_1} M^{\lambda_1}_{\nu_1\mu_1} M^{\lambda_2}_{-\nu_2\mu_2} + M^{\lambda_1}_{-\nu_1\mu_1} M^{\lambda_2}_{-\nu_2\mu_2} \Big\} + C^{\lambda_1,\lambda_2}_{\mu_1-\mu_2} \Big\{ B_{\nu_1\mu_2\nu_2} M^{\lambda_1}_{-\nu_1\mu_1} M^{\lambda_2}_{-\nu_2-\mu_2}$$

$$+ B_{\mu_2\nu_2} M^{\lambda_1}_{\nu_1\mu_1} M^{\lambda_2}_{-\nu_2-\mu_2} + B_{\mu_1\nu_1} M^{\lambda_1}_{\nu_1\mu_1} M^{\lambda_2}_{\nu_2-\mu_2} + B_{\mu_1} M^{\lambda_1}_{-\nu_1\mu_1} M^{\lambda_2}_{\nu_2-\mu_2} \Big\} \Bigg], \tag{5.18}$$

where

$$B_{\mu_1\nu_1\mu_2\nu_2} = 1 - \delta_{o\mu_1} - \delta_{o\nu_1} - \delta_{o\mu_2} - \delta_{o\nu_2} + \delta_{o\mu_1}\delta_{o\nu_1} + \delta_{o\mu_1}\delta_{o\mu_2} + \delta_{o\mu_1}\delta_{o\nu_2}$$
$$+ \delta_{o\nu_1}\delta_{o\mu_2} + \delta_{o\nu_1}\delta_{o\nu_2} + \delta_{o\mu_2}\delta_{o\nu_2} - \delta_{o\mu_1}\delta_{o\nu_1}\delta_{o\mu_2} - \delta_{o\mu_1}\delta_{o\nu_1}\delta_{o\nu_2}$$
$$- \delta_{o\mu_1}\delta_{o\mu_2}\delta_{o\nu_2} - \delta_{o\nu_1}\delta_{o\mu_2}\delta_{o\nu_2} + \tfrac{1}{2}\delta_{o\mu_1}\delta_{o\nu_1}\delta_{o\mu_2}\delta_{o\nu_2} \; ,$$

$$B_{\mu_1\mu_2\nu_2} = 1 - \delta_{o\mu_1} - \delta_{o\mu_2} - \delta_{o\nu_2} + \delta_{o\mu_1}\delta_{o\mu_2} + \delta_{o\mu_1}\delta_{o\nu_2} \; ,$$

$$B_{\nu_1\mu_2\nu_2} = 1 - \delta_{o\nu_1} - \delta_{o\mu_2} - \delta_{o\nu_2} + \delta_{o\nu_1}\delta_{o\mu_2} + \delta_{o\nu_1}\delta_{o\nu_2} + \delta_{o\mu_2}\delta_{o\nu_2} \; ,$$

$$B_{\mu_2\nu_2} = 1 - \delta_{o\mu_2} - \delta_{o\nu_2} \; , \qquad B_{\mu_1\nu_1} = 1 - \delta_{o\mu_1} - \delta_{o\nu_1} + \delta_{o\mu_1}\delta_{o\nu_1} \; ,$$

$$B_{\nu_1} = 1 - \delta_{o\nu_1} \; , \qquad B_{\mu_1} = 1 - \delta_{o\mu_1} \; .$$

substituting (5.18) in (5.6) we obtain

$$A(\bar{\Omega}_1, \bar{\Omega}_2) = 2 \sum_{\lambda_1, \lambda_2} \sum_{\mu_1, \nu_1=0}^{\lambda_1} \sum_{\mu_2, \nu_2=0}^{\lambda_2} \Big[N_{\lambda_1\nu_1} N_{\lambda_2\nu_2} \, \mathrm{Re} \Big\{ C_{\mu_1\mu_2}^{\lambda_1\lambda_2}$$

$$\times \Big(B_{\mu_1\nu_1\mu_2\nu_2} \mathcal{D}_{\nu_1\mu_1}^{(\lambda_1)} \mathcal{D}_{-\nu_2\mu_2}^{(\lambda_2)} \mathcal{V}_{\nu_1\nu_2\mu_1\mu_2}^{(\lambda_{12})} + (-1)^{\nu_1} B_{\mu_1\mu_2\nu_2} \mathcal{D}_{-\nu_1\mu_1}^{(\lambda_1)} \mathcal{D}_{\nu_2\mu_2}^{(\lambda_2)} \mathcal{V}_{-\nu_1\nu_2\mu_1\mu_2}^{(\lambda_{12})}$$

$$+ (-1)^{\nu_2} B_{\nu_1} \mathcal{D}_{\nu_1\mu_1}^{(\lambda_1)} \mathcal{D}_{-\nu_2\mu_2}^{(\lambda_2)} \mathcal{V}_{\nu_1-\nu_2\mu_1\mu_2}^{(\lambda_{12})} + (-1)^{\nu_1+\nu_2} \mathcal{D}_{-\nu_1\mu_1}^{(\lambda_1)} \mathcal{D}_{-\nu_2\mu_2}^{(\lambda_2)} \mathcal{V}_{-\nu_1-\nu_2\mu_1\mu_2}^{(\lambda_{12})} \Big)$$

$$+ C_{\mu_1-\mu_2}^{\lambda_1\lambda_2} \Big((-1)^{\nu_1+\nu_2} B_{\nu_1\mu_2\nu_2} \mathcal{D}_{-\nu_1\mu_1}^{(\lambda_1)} \mathcal{D}_{-\nu_2-\mu_2}^{(\lambda_2)} \mathcal{V}_{-\nu_1-\nu_2\mu_1-\mu_2}^{(\lambda_{12})}$$

$$+ (-1)^{\nu_2} B_{\mu_2\nu_2} \mathcal{D}_{\nu_1\mu_1}^{(\lambda_1)} \mathcal{D}_{-\nu_2-\mu_2}^{(\lambda_2)} \mathcal{V}_{\nu_1-\nu_2\mu_1-\mu_2}^{(\lambda_{12})} + B_{\mu_1\nu_1} \mathcal{D}_{\nu_1\mu_1}^{(\lambda_1)} \mathcal{D}_{\nu_2-\mu_2}^{(\lambda_2)} \mathcal{V}_{\nu_1\nu_2\mu_1-\mu_2}^{(\lambda_{12})}$$

$$+ (-1)^{\nu_1} B_{\mu_1} \mathcal{D}_{-\nu_1\mu_1}^{(\lambda_1)} \mathcal{D}_{\nu_2-\mu_2}^{(\lambda_2)} \mathcal{V}_{-\nu_1\nu_2\mu_1-\mu_2}^{(\lambda_{12})} \Big) \Big\} \Big] , \tag{5.19}$$

where $\mathcal{D}_{\nu_i\mu_i}^{(\lambda_i)} \equiv \mathcal{D}_{\nu_i\mu_i}^{(\lambda_i)}(\gamma_i + \pi/2, \beta_i, \alpha_i)$ and $\mathcal{V}_{\nu_1\nu_2\mu_1\mu_2}^{(\lambda_{12})}$
is given by (5.10). Choosing again the OXY plaine as the plane
of the trajectory we can write the change of the action in real
form as

$$A(\bar{\Omega}_1, \bar{\Omega}_2) = 2 \sum_{\lambda_1, \lambda_2} \sum_{\mu_1, \nu_1=0}^{\lambda_1} \sum_{\mu_2, \nu_2=0}^{\lambda_2} \Big[N_{\lambda_1\nu_1} N_{\lambda_2\nu_2} \Big\{ C_{\mu_1\mu_2}^{\lambda_1\lambda_2}$$

$$\times \Big(B_{\mu_1\nu_1\mu_2\nu_2} \, d_{\nu_1\mu_1}^{(\lambda_1)}(\beta_1) \, d_{\nu_2\mu_2}^{(\lambda_2)}(\beta_2) \, V_{\nu_1\nu_2\mu_1\mu_2}^{(\lambda_{12})} \cos(\nu_1\gamma_1 + \nu_2\gamma_2 + \mu_1\alpha_1 + \mu_2\alpha_2)$$

$$+ (-1)^{\nu_1} B_{\mu_1\mu_2\nu_2} \, d_{-\nu_1\mu_1}^{(\lambda_1)}(\beta_1) \, d_{\nu_2\mu_2}^{(\lambda_2)}(\beta_2) \, V_{-\nu_1\nu_2\mu_1\mu_2}^{(\lambda_{12})} \cos(-\nu_1\gamma_1 + \nu_2\gamma_2 + \mu_1\alpha_1 + \mu_2\alpha_2)$$

$$+ (-1)^{\nu_2} B_{\nu_1} \, d_{\nu_1\mu_1}^{(\lambda_1)}(\beta_1) \, d_{-\nu_2\mu_2}^{(\lambda_2)}(\beta_2) \, V_{\nu_1-\nu_2\mu_1\mu_2}^{(\lambda_{12})} \cos(\nu_1\gamma_1 - \nu_2\gamma_2 + \mu_1\alpha_1 + \mu_2\alpha_2)$$

$$+ (-1)^{\nu_1+\nu_2} d_{-\nu_1\mu_1}^{(\lambda_1)}(\beta_1) \, d_{-\nu_2\mu_2}^{(\lambda_2)}(\beta_2) \, V_{-\nu_1-\nu_2\mu_1\mu_2}^{(\lambda_{12})} \cos(-\nu_1\gamma_1 - \nu_2\gamma_2 + \mu_1\alpha_1 + \mu_2\alpha_2) \Big)$$

$$+ C_{\mu_1-\mu_2}^{\lambda_1\lambda_2} \Big((-1)^{\nu_1+\nu_2} B_{\nu_1\mu_2\nu_2} \, d_{-\nu_1\mu_1}^{(\lambda_1)}(\beta_1) \, d_{-\nu_2-\mu_2}^{(\lambda_2)}(\beta_2) \, V_{-\nu_1-\nu_2\mu_1\mu_2}^{(\lambda_{12})} \cos(-\nu_1\gamma_1 - \nu_2\gamma_2 + \mu_1\alpha_1 + \mu_2\alpha_2)$$

$$+$$

$$+ (-1)^{\nu_2} B_{\mu_2 \nu_2} d^{(\lambda_1)}_{\nu_1 \mu_1}(\beta_1) d^{(\lambda_2)}_{-\nu_2-\mu_2}(\beta_2) V^{(\lambda_{12})}_{\nu_1-\nu_2\mu_1-\mu_2} \cos(\nu_1\gamma_1 - \nu_2\gamma_2 + \mu_1\alpha_1 - \mu_2\alpha_2)$$

$$+ B_{\mu_1\nu_1} d^{(\lambda_1)}_{\nu_1\mu_1}(\beta_1) d^{(\lambda_2)}_{\nu_2-\mu_2}(\beta_2) V^{(\lambda_{12})}_{\nu_1\nu_2\mu_1-\mu_2} \cos(\nu_1\gamma_1 + \nu_2\gamma_2 + \mu_1\alpha_1 - \mu_2\alpha_2)$$

$$+ (-1)^{\nu_1} B_{\mu_1}{}_{-\nu_1\mu_1} d^{(\lambda_1)}_{-\nu_1\mu_1}(\beta_1) d^{(\lambda_2)}_{\nu_2-\mu_2}(\beta_2) V^{(\lambda_{12})}_{-\nu_1\nu_2\mu_1-\mu_2} \cos(-\nu_1\gamma_1 + \nu_2\gamma_2 + \mu_1\alpha_1 - \mu_2\alpha_2) \Big)\Big]\Big], \quad (5.20)$$

where the rotation matrix $d^{(\lambda_i)}_{\nu_i\mu_i}(\beta_i)$ is defined by Edmonds (1960, p55) and $V^{(\lambda_{12})}_{\nu_1\nu_2\mu_1\mu_2}$ is given by (5.13). The general analysis cannot be taken further. We have now to determine $A(\bar\Omega_1, \bar\Omega_2)$ for particular interactions $\bar C_{\lambda_1\lambda_2}(R)$, and then evaluate the transition amplitude (5.5). We concentrate in this work on the dipole-dipole interaction ($\lambda_1 = \lambda_2 = 1$), and we shall show in the next chapter that in this case we can express (5.5) analytically.

5.4 The detailed-balance relation

To evaluate the transition amplitude (5.5) we have to employ a suitable frequency W_i of the i-th rotor. Following Dickinson and Richards (1974) we define W_i as the arithmetic mean of the initial and final values, $W_i(j_i)$ and $W_i(j'_i)$ respectively. With this definition we have

$$W_i = \hbar \left[j_i + (\Delta j_i + 1)/2 \right] / I_i . \qquad (5.21)$$

Using the translational energy given by (4.16) and the above rotor frequency the probability (5.4) is the same for both forward and backward transitions, and we have to correct it in order to obtain a probability satisfying the detailed-balance relation

$$E_i(2j_1 + 1)(2j_2 + 1) P_{(j_1 j_2 \to j'_1 j'_2; b; E)} = E_f(2j'_1 + 1)(2j'_2 + 1) P_{(j'_1 j'_2 \to j_1 j_2; b; E)}, \quad (5.22)$$

where E is the total energy and $E_i(E_f)$ is the initial (final) translational energy. We define the corrected probability as

$$P(j_1 j_2 \to j_1' j_2'; b; E) = (E_i/E_f)^{1/2} \, \mathcal{C}(j_1 j_2 j_1' j_2') \, \mathcal{P}(j_1 j_2 \to j_1' j_2'; \bar{E}) \quad,$$

(5.23)

where

$$\mathcal{C}(j_1 j_2 j_1' j_2') = \left[\frac{(2j_1'+1)(2j_2'+1)}{(2j_1+1)(2j_2+1)}\right]^{1/2}$$

(5.24)

For large (j_1, j_2) and $\Delta j_i \ll j_i$ (i=1,2) the correction (5.24) is approximately 1. The cross section $\sigma(j_1 j_2 \to j_1' j_2'; E)$ is obtained integrating (5.23) over all impact parameters

$$\sigma(j_1 j_2 \to j_1' j_2') = 2\pi \int_0^\infty P(j_1 j_2 \to j_1' j_2'; b; E) \, b \, db \quad.$$

(5.25)

5.5 The first-order transition probability

We have seen in section 5.3 that to evaluate the transition amplitude (5.5) we have to consider particular interactions. In evaluating the FOCP however we can obtain a closed form for the transition amplitude and probability for the general potential.

We require the degeneracy-averaged FOCP transition probability

$$P^{FO}(j_1 j_2 \to j_1' j_2'; b; E) = (E_i/E_f)^{1/2} \, \mathcal{C}(j_1 j_2 j_1' j_2') \, \frac{1}{16\pi^2} \int_0^{2\pi} d\alpha_1 \int_0^{2\pi} d\alpha_2 \int_{-1}^{1} d(\cos\beta_1)$$

$$\cdot \int_{-1}^{1} d(\cos\beta_2) \, |\bar{S}^{FO}(j_1 j_2, j_1' j_2')|^2 \quad,$$

(5.26)

where $\bar{S}^{FO}(j_1 j_2, j_1' j_2')$ is given by

$$\bar{S}^{FO}(j_1 j_2, j_1' j_2') = -i \left(\frac{1}{2\pi}\right)^2 \int_0^{2\pi}\int_0^{2\pi} d\gamma_1 \, d\gamma_2 \, A(\bar{\Omega}_1, \bar{\Omega}_2) \exp[i(s_1\gamma_1 + s_2\gamma_2)] \,,$$

(5.27)

where we have put $s_i = \Delta j_i$. Substituting (5.14) in (5.27) we obtain

$$\bar{S}^{FO}(j_1 j_2, j_1' j_2') = -i \sum_{\lambda_1 \lambda_2} \sum_{\mu_1 = -\lambda_1}^{\lambda_1} \sum_{\mu_2 = -\lambda_2}^{\lambda_2} (\lambda_1 \mu_1 \lambda_2 \mu_2 / \lambda_1 \lambda_2 \lambda_{12} \mu_{12}) N_{\lambda_1 s_1} N_{\lambda_2 s_2} N_{\lambda_{12} \mu_{12}}$$

$$\cdot \mathcal{D}_{s_1 \mu_1}^{(\lambda_1)}(0, \beta_1, \alpha_1) \, \mathcal{D}_{s_2 \mu_2}^{(\lambda_2)}(0, \beta_2, \alpha_2) \, V_{s_1 s_2 \mu_1 \mu_2}^{(\lambda_{12})}(\bar{E}, b) \,,$$

(5.28)

The calculation of $P^{FO}(j_1 j_2 \rightarrow j_1' j_2'; b; E)$ yields

$$P^{FO}(j_1 j_2 \rightarrow j_1' j_2'; b; E) = (E_i / E_f)^{1/2} \, \mathcal{C}(j_1 j_2 j_1' j_2') \sum_{\lambda_1, \lambda_2} \frac{N_{\lambda_1 s_1}^2 \, N_{\lambda_2 s_2}^2}{(2\lambda_1+1)(2\lambda_2+1)}$$

$$\sum_{\mu_1 \mu_2} \left| (\lambda_1 \mu_1 \lambda_2 \mu_2 / \lambda_1 \lambda_2 \lambda_{12} \mu_{12}) \, N_{\lambda_{12} \mu_{12}} \, V_{s_1 s_2 \mu_1 \mu_2}^{(\lambda_{12})}(\bar{E}, b) \right|^2 . \tag{5.29}$$

5.6 Comparison of the FOCP with other first-order models

It is interesting for the understanding of the main features of the FOCP to compare (5.29) with other similar models. Consider first the first-order time-dependent perturbation theory (FOTDPT).

The FOTDPT formulae for the transition probability has been derived previously in the literature (Cross and Gordon 1966, Rabitz and Gordon 1970). Considering the relative motion as a linear trajectory contained in the OXZ plane they obtained a general expression for the probability in terms of modified Bessel functions, $K_\lambda(Z)$ (Abramowitz and Stegun 1965, p374). To compare with our FOCP we rederived the FOTDPT equations considering the classical trajectory on the OXY plane and determined by the $\bar{C}_{oo}(R)$ potential.

For the FOTDPT transitions amplitude $S^{FOTD}(i \rightarrow f)$ between states $|i\rangle = |j_1 m_1 j_2 m_2\rangle$ and $|f\rangle = |j_1' m_1' j_2' m_2'\rangle$ we obtained

$$S^{FOTD}(i \rightarrow f) = -\frac{i}{4\pi} \left[(2j_1'+1)(2j_2'+1)(2j_1+1)(2j_2+1) \right]^{1/2} \sum_{\lambda_1, \lambda_2} \left[(2\lambda_1+1)(2\lambda_2+1) \right]^{1/2}$$

$$\times \begin{pmatrix} j_1 & j_1' & \lambda_1 \\ 0 & 0 & 0 \end{pmatrix} \begin{pmatrix} j_2 & j_2' & \lambda_2 \\ 0 & 0 & 0 \end{pmatrix} \sum \sum (\lambda_1 \mu_1 \lambda_2 \mu_2 / \lambda_1 \lambda_2 \lambda_{12} \mu_{12})$$

$$N_{\lambda_{12} \mu_{12}} (-1)^{-m_1' - m_2} \begin{pmatrix} j_1 & j_1' & \lambda_1 \\ m_1 & -m_1' & \mu_1 \end{pmatrix} \begin{pmatrix} j_2 & j_2' & \lambda_2 \\ m_2 & -m_2' & \mu_2 \end{pmatrix} V_{\lambda_{12} \mu_1 \mu_2}(\bar{E}, b) , \tag{5.30}$$

where $\begin{pmatrix} : & : & : \end{pmatrix}$ is a 3-j symbol (Edmonds 1960, p46), $V_{\lambda_{12} \mu_1 \mu_2}(\bar{E}, b)$ is

given by

$$V_{\lambda_{12}\mu_1\mu_2}(\bar{E},b) = \frac{1}{\hbar}\int_{-\infty}^{\infty} \bar{C}_{\lambda,\lambda_2}[R(t)] \; e^{i[W_{if}t - (\mu_1+\mu_2)\hat{P}(t)]} dt \quad , \tag{5.31}$$

with

$$W_{if} = \frac{1}{\hbar}\left(E_{j_1'} - E_{j_1} + E_{j_2'} - E_{j_2}\right) = \Delta E_j/\hbar \quad , \tag{5.32}$$

where Ej_i is the rotational energy of the i-th rotor. The degeneracy averaged transition probability is

$$P^{FOTD}(j_1 j_2 \to j_1' j_2' ; b) = \frac{1}{16\pi^2}\sum_{\lambda,\lambda_2}(2j_1'+1)(2j_2'+1)\begin{pmatrix} j_1 & j_1' & \lambda \\ 0 & 0 & 0 \end{pmatrix}^2\begin{pmatrix} j_2 & j_2' & \lambda \\ 0 & 0 & 0 \end{pmatrix}^2$$

$$\sum_{\mu_1,\mu_2}\left|(\lambda_1\mu_1\,\lambda_2\mu_2/\lambda_1\lambda_2\lambda_{12}\mu_{12})\,N_{\lambda_{12}\mu_{12}}\,V_{\lambda_{12}\mu_1\mu_2}(\bar{E},b)\right|^2 \quad , \tag{5.33}$$

which is similar to (5.29). Using the quantal relation for the rotational energy $E_j = Bj(j+1)$, in (5.32) we have that for any transition $s_1 + s_2$

$$W_{if} = s_1 W_1 + s_2 W_2 \quad , \tag{5.34}$$

where W_i (i=1,2) is given by (5.21);
then $V_{\lambda_{12}\mu_1\mu_2}(\bar{E},b) = V_{s_1 s_2 \mu_1 \mu_2}^{(\lambda_{12})}(\bar{E},b)$. Using the expansion (Dickinson and Richards 1974)

$$(2j'+1)\begin{pmatrix} j & j' & \lambda \\ 0 & 0 & 0 \end{pmatrix}^2 = \frac{4\pi}{2\lambda+1}\,N_{\lambda s}^2\left[1 - \frac{s}{(2j+1)} - \frac{\lambda(\lambda+1)-2s^2}{2(2j+1)^2} + \cdots\right], \tag{5.35}$$

and assuming that j_i and j_i' are large compared with λ_i we obtain

$$P^{FOTD}(j_1 j_2 \to j_1' j_2' ; b) = \sum_{\lambda,\lambda_2}\frac{N_{\lambda_1 s_1}^2\,N_{\lambda_2 s_2}}{(2\lambda_1+1)(2\lambda_2+1)}\sum_{\mu_1,\mu_2}\left|(\lambda_1\mu_1\,\lambda_2\mu_2/\lambda_1\lambda_2\lambda_{12}\mu_{12})\,N_{\lambda_{12}\mu_{12}}\,V_{s_1 s_2 \mu_1 \mu_2}^{(\lambda_{12})}\right|^2,$$

$$\tag{5.36}$$

which, except for the term $(E_i/E_f)^{1/2} \mathcal{C} (j_1 j_2 \, j_1' j_2')$, is identical with (5.29). For a linear trajectory the $V_{\mu J_2 \mu_1 \mu_2}^{(\lambda_{12})}$ integrals can be expressed in terms of modified Bessel functions recovering the usual Rabitz and Gordon result (1970). It has been shown (Cross and Gordon 1966) that, for the dipole-dipole interaction, the straight-line (SL) trajectory limit of FOTDPT at relative initial translational energy $E_i \gg \Delta E_j$ gives the same cross section as the time-independent first-order Born approximation (BA).

Another first-order limit which has been applied to the problem studied here is the distorted-wave Born approximation (DWBA). Davison (1962) has derived the DWBA expression for the rotational inelastic cross-section and used it for H_2-H_2 collisions. Following Miller and Smith (1978) we can write the semiclassical DWBA transition amplitude, $S^{DW}(\underline{n}, \underline{n}')$ between two states $\underline{n} \equiv (n_1, n_2, \ldots, n_n)$ and $\underline{n}' \equiv (n_1', n_2', \ldots, n_n')$ as

$$S^{DW}(\underline{n}, \underline{n}') = \frac{e^{i(\phi + \phi')}}{(2\pi)^N} \int_0^{2\pi} d\underline{\theta} \; e^{i[\underline{\theta} \cdot (\underline{n} - \underline{n}')]} \left[1 - A(\theta) \right], \qquad (5.37)$$

where

$$\phi = \frac{\pi}{4} + \lim_{R \to \infty} \left(-kR + \int_{R_0}^{R} dR' \left[2\mu \{ E - V_0(R) \} \right]^{1/2} \right), \qquad (5.38)$$

with k the wave number corresponding to a translational energy $E = \hbar^2 k^2 / 2\mu$, μ is the reduced mass of the system and $V_0(R)$ the spherical potential. Apart from the phases ϕ (ϕ'), (5.37) is identical to (4.4) and when applied to rotor-rotor collision it yields (5.29).

In general the first-order models do not satisfy unitarity for close collisions, and for small impact parameters some kind of unitarization is required. Our numerical results, presented in Chapter 7, show that with the interactions of interest here the SCCP converges into the FOCP only at very small values of the probability.

5.7 General remarks

The accuracy of the model presented here is dependent on the validity of classical perturbation theory (CPT) to describe the coupling between the rotors and the relative motion. We have not attempted here to investigate the validity of CPT, as we expect that the general conclusions of Cohen and Marcus (1970) for atom-rotor collisions are valid for rotor-rotor collision. Thus the change of the action $A(\bar{\Omega}_1, \bar{\Omega}_2)$ as given by (5.20) is expected to be valid within 10%, tending to be better for large incident energies, large rotational energies, and for rotors with large moment of inertia. A higher accuracy can be expected for the probabilities (5.23) and (5.29) and the cross section (5.25) as they are averages over the orientation and impact parameter respectively; it has been argued by Dickinson and Richards (1976) and Clark et.al. (1977) that CPT could be more accurate in predicting averaged quantities rather than individual orbits.

Central to CPT are the trajectory integrals $V_{\nu_1 \nu_2 \mu_1 \mu_2}^{(\lambda_{12})}$ defined by (5.12). Since for a given orientation of the system they determine the value of the change of the action $A(\bar{\Omega}_1, \bar{\Omega}_2)$, their absolute value can be considered as a measure of the strength of the collision. It is interesting at this point to introduce the relation (Dickinson and Richards 1974)

$$\left| \int_0^\infty dR\, W_{\ell'}(k')\, \bar{C}_{\lambda_1 \lambda_2}(R)\, W_{\ell}(k) \right| \cong \frac{\hbar\, (k k')^{1/2}}{4\mu}$$

$$\left| \int_{-\infty}^\infty dt\, \bar{C}_{\lambda_1 \lambda_2}[R(t)]\, e^{i[(s_1 W_1 + s_2 W_2)t - (\mu_1 + \mu_2)\varphi(t)]} \right| ,$$

$$(5.39)$$

where $W_\ell(k)$ is the wave function for a particle of orbital angular momentum $\hbar\ell$ and wave number k in the potential $\bar{C}_{oo}(R)$, and $\{R(t), \mathcal{P}(t)\}$ is the classical orbit followed by the particle in the same potential. The prime (') indicates final state.

From (5.39) and (5.29) we can see that the only $V_{\nu_1 \nu_2 \mu_1 \mu_2}^{(\lambda_{12})}$ integrals appearing in the FOCP result are those associated with a net change in the rotational energy of the molecules $\Delta E_j = \hbar(s_1 w_1 + s_2 w_2)$, equal in absolute value to the translational-rotational (T-R) energy transfer $\Delta E = E_f - E_i$, during the collision. This is equivalent to the first-order quantal description where the only matrix element determining the transition between two states, is the one coupling those states.

We point out one difference between the FOCP and the SCCP. In the latter the $V_{\nu_1 \nu_2 \mu_1 \mu_2}^{(\lambda_{12})}$ integrals appearing in the change of the action (5.20) do not necessarily correspond to $\Delta E_j = \Delta E$. Although complex we interpret this as the way in which the SCCP considers the effect of the transitions between intermediates channels, and then $\nu_i = \Delta j_i$, $\mu_i = \Delta m_i$ would indicate the way in which these transitions are most likely to occur. So, the $V_{\nu_1 \nu_2 \mu_1 \mu_2}^{(\lambda_{12})}$ integrals contain information about the form in which the couplings between intermediate levels take place. This will be clearly seen in Chapter 8, where we present the correspondence principle version of some quantal decoupling schemes; in all the cases the decoupling takes the form of the conditions on the $V_{\nu_1 \nu_2 \mu_1 \mu_2}^{(\lambda_{12})}$'s.

The value of the $V_{\nu_1 \nu_2 \mu_1 \mu_2}^{(\lambda_{12})}$ integrals depends on the four parameters, $\bar{E}$, λ_{12}, b, and $W = \nu_1 W_1 + \nu_2 W_2$. To give the effects of the variation of these parameters is not simple as there are no analytic approximations uniform in all the four parameters. Dickinson and Richards (1976, 1977, 1978) have

extensively studied these trajectory integrals, and from these works
we can summarize the general properties:

A)   In general the value of $V_{\nu_1 \nu_2 \mu_1 \mu_2}^{(\lambda_{12})}$ depends strongly on the
value of the potential $\bar{C}_{\lambda_1 \lambda_2}(R)$ at the distance of closest approach
r_0. So, as a function of the impact parameter it varies slowly
for $b \leq R_m$, where R_m is the position of the minimum, of $\bar{C}_{oo}(R)$; for
larger values of b it converges rapidly to zero.   If there is
orbiting   and b_0 is the impact parameter at which this
orbiting occurs, the absolute value of $V_{\nu_1 \nu_2 \mu_1 \mu_2}^{(\lambda_{12})}$ falls sharply
when b becomes larger than b_0.   This is because   the only R's
classically accessible are those larger than or equal to the largest
of the three turning points occuring at these b's.

B)   The absolute value of $V_{\nu_1 \nu_2 \mu_1 \mu_2}^{(\lambda_{12})}$ is a decreasing function of
the frequency $W = \nu_1 W_1 + \nu_2 W_2$.   So, for a given $\bar{E}$ and b, the largest
$\left| V_{\nu_1 \nu_2 \mu_1 \mu_2}^{(\lambda_{12})} \right|$ is associated with a resonant transition
($\Delta E_j = 0, W_i \neq 0, i = 1,2$).   For this resonant integral the integrand
is dominated by $\bar{C}_{\lambda_1 \lambda_2}(R)$ since $\cos\left[(\mu_1 + \mu_2)\gamma^p\right]$ is relatively slowly
varying;   for $W \neq 0$ but small the behaviour is similar to the W=0 case.
When W is large the oscillations of the cosine term are dominant and
for large impact parameters the integral converges rapidly to zero.

C)   The $V_{\nu_1 \nu_2 \mu_1 \mu_2}^{(\lambda_{12})}$ integral is a slowly varying function of $\bar{E}$.

It will be shown in Chapter 7 that the behaviour of the transition
probability $P(j_1 j_2 \rightarrow j_1' j_2'; b, E)$ is largely determined by the above
properties of the $V_{\nu_1 \nu_2 \mu_1 \mu_2}^{(\lambda_{12})}$ integrals.

CHAPTER 6

THE CORRESPONDENCE PRINCIPLE EQUATIONS FOR THE
DIPOLE-DIPOLE INTERACTION

6.1   The dipole-dipole change of the action

Consider the dipole-dipole interaction ($\lambda_1 = \lambda_2 = 1$) as the only anisotropic term of the potential (4.12).   In this case (5.14) becomes

$$A(\bar{\Omega}_1, \bar{\Omega}_2) = \sum_{\mu_1, \nu_1 = -1}^{1} \sum_{\mu_2, \nu_2 = -1}^{1} N_{2\mu_{12}} N_{1\nu_1} N_{1\nu_2} \left(1\mu_1 1\mu_2 / 112 \mu_{12} \right)$$

$$\mathcal{D}_{\nu_1 \mu_1}^{(1)}(\bar{\Omega}_1) \, \mathcal{D}_{\nu_2 \mu_2}^{(1)}(\bar{\Omega}_2) \, V_{\nu_1 \nu_2 \mu_1 \mu_2}^{(2)}(\bar{E}, b) \quad , \tag{6.1}$$

and its real form is

$$A(\bar{\Omega}_1, \bar{\Omega}_2) = \frac{6}{32\pi} \left(\frac{15}{2\pi} \right)^{1/2} \left[-\sin\beta_1 \sin\beta_2 \left\{ \frac{V_{1100}^{(2)}}{3} \cos(\gamma_1^* + \gamma_2^*) + \frac{V_{1-100}^{(2)}}{3} \cos(\gamma_2^* - \gamma_1^*) \right\} \right.$$

$$+ \cos(\gamma_1 + \gamma_2) \cos(\alpha_1 + \alpha_2) \left\{ V_{1111}^{(2)} \cos^2(\beta_1/2) \cos^2(\beta_2/2) + V_{11-1-1}^{(2)} \sin^2(\beta_1/2) \sin^2(\beta_2/2) \right\}$$

$$- \sin(\gamma_1 + \gamma_2) \sin(\alpha_1 + \alpha_2) \left\{ V_{1111}^{(2)} \cos^2(\beta_1/2) \cos^2(\beta_2/2) - V_{11-1-1}^{(2)} \sin^2(\beta_1/2) \sin^2(\beta_2/2) \right\}$$

$$- \cos(\gamma_1^* + \gamma_2^*) \cos(\alpha_1 + \alpha_2) \left\{ V_{1-1-1-1}^{(2)} \sin^2(\beta_1/2) \cos^2(\beta_2/2) + V_{1-111}^{(2)} \cos^2(\beta_1/2) \sin^2(\beta_2/2) \right\}$$

$$+ \sin(\gamma_2^* - \gamma_1^*) \sin(\alpha_1 + \alpha_2) \left\{ V_{1-1-1-1}^{(2)} \sin^2(\beta_1/2) \cos^2(\beta_2/2) - V_{1-11}^{(2)} \cos^2(\beta_1/2) \sin^2(\beta_2/2) \right\}$$

$$- \frac{1}{3} \cos(\gamma_1^* + \gamma_2^*) \cos(\alpha_1 - \alpha_2) \left\{ V_{111-1}^{(2)} \cos^2(\beta_1/2) \sin^2(\beta_2/2) + V_{11-11}^{(2)} \sin^2(\beta_1/2) \cos^2(\beta_2/2) \right\}$$

$$+ \frac{1}{3} \sin(\gamma_1 + \gamma_2^*) \sin(\alpha_1 - \alpha_2) \left\{ V_{111-1}^{(2)} \cos^2(\beta_1/2) \sin^2(\beta_2/2) - V_{11-11}^{(2)} \sin^2(\beta_1/2) \cos^2(\beta_2/2) \right\}$$

$$+ \frac{1}{3} \cos(\gamma_2^* - \gamma_1) \cos(\alpha_1 - \alpha_2) \left\{ V_{1-11-1}^{(2)} \cos^2(\beta_1/2) \cos^2(\beta_2/2) + V_{1-1-11}^{(2)} \sin^2(\beta_1/2) \sin^2(\beta_2/2) \right\}$$

$$\left. + \frac{1}{3} \sin(\gamma_2^* - \gamma_1) \sin(\alpha_1 - \alpha_2) \left\{ V_{1-11-1}^{(2)} \cos^2(\beta_1/2) \cos^2(\beta_2/2) - V_{1-1-11}^{(2)} \sin^2(\beta_1/2) \sin^2(\beta_2/2) \right\} \right] . \tag{6.2}$$

We notice that the $V^{(2)}_{\nu_1 \nu_2 \, \mu_1 \mu_2}$ integrals appearing in $A(\bar{\Omega}_1, \bar{\Omega}_2)$ have $|\nu_i| = 1$ and $|\mu_i| = 0, 1$. As discussed in section (5.7) this would correspond to intermediate transitions with $|\Delta j_i| = 1$ and $|\Delta m_i| = 0, 1$, i.e. dipole-dipole first-order transitions. So, CPT predicts that the coupling between two given states occur through successive first-order couplings between intermediate channels.

It proves convenient in evaluating the transitions amplitude $S(j_1 j_2, j_1' j_2')$ to express $A(\bar{\Omega}_1, \bar{\Omega}_2)$ in terms of the variables

$$\gamma_+ = \gamma_1 + \gamma_2 \qquad ; \qquad \gamma_- = \gamma_2 - \gamma_1 \quad ,$$

$$\alpha_+ = \alpha_1 + \alpha_2 \qquad ; \qquad \alpha_- = \alpha_1 - \alpha_2 \quad . \tag{6.3}$$

Using the relation

$$V^{(2)}_{\nu_1 \nu_2 \, \pm 1 \, \mp 1} = V^{(2)}_{\nu_1 \nu_2 \, 0 0} = V^{(2)}_{-\nu_1 -\nu_2 \, 0 0} \quad , \tag{6.4}$$

the change of the action is written as

$$A(\bar{\Omega}_i^+, \bar{\Omega}_i^-) = \frac{6}{32\pi} \left(\frac{15}{2\pi} \right)^{1/2} \left[-\frac{1}{3} \sin\beta_1 \sin\beta_2 \left\{ V_{1100} \cos\gamma_+ + V_{1-100} \cos\gamma_- \right\} \right.$$

$$+ \cos\gamma_+ \cos\alpha_+ \left\{ V_{1111} \cos^2(\beta_1/2) \cos^2(\beta_2/2) + V_{11-1-1} \sin^2(\beta_1/2) \sin^2(\beta_2/2) \right\}$$

$$- \sin\gamma_+ \sin\alpha_+ \left\{ V_{1111} \cos^2(\beta_1/2) \cos^2(\beta_2/2) - V_{11-1-1} \sin^2(\beta_1/2) \sin^2(\beta_2/2) \right\}$$

$$- \cos\gamma_- \cos\alpha_+ \left\{ V_{1-1-1-1} \sin^2(\beta_1/2) \cos^2(\beta_2/2) + V_{1-111} \cos^2(\beta_1/2) \sin^2(\beta_2/2) \right\}$$

$$+ \sin\gamma_- \sin\alpha_+ \left\{ V_{1-1-1-1} \sin^2(\beta_1/2) \cos^2(\beta_2/2) - V_{1-111} \cos^2(\beta_1/2) \sin^2(\beta_2/2) \right\}$$

$$- \frac{1}{3} \cos\gamma_+ \cos\alpha_- V_{1100} \left\{ \cos^2(\beta_1/2) \sin^2(\beta_2/2) + \sin^2(\beta_1/2) \cos^2(\beta_2/2) \right\}$$

$$+ \frac{1}{3} \sin\gamma_+ \sin\alpha_- V_{1100} \left\{ \cos^2(\beta_1/2) \sin^2(\beta_2/2) - \sin^2(\beta_1/2) \cos^2(\beta_2/2) \right\}$$

$$+ \frac{1}{3} \cos \gamma_- \cos \alpha_- \, V_{1\text{-}100} \left\{ \cos^2(\beta_1/2) \cos^2(\beta_2/2) + \sin^2(\beta_1/2) \sin^2(\beta_2/2) \right\}$$

$$+ \frac{1}{3} \sin \gamma_- \sin \alpha_- \, V_{1\text{-}100} \left\{ \cos^2(\beta_1/2) \cos^2(\beta_2/2) - \sin^2(\beta_1/2) \sin^2(\beta_2/2) \right\} \Bigg] ,$$

$$(6.5)$$

reducing the number of $V_{\nu_1 \nu_2 \mu_1 \mu_2}^{(2)}$ to six, and where we have put $\bar{\Omega}+_i = (\gamma_+, \beta_i, \alpha_+)$, $\bar{\Omega}-_i = (\gamma_-, \beta_i, \alpha_-)$. Here, and henceforth we drop the superscript 2.

6.2   The transition amplitude

In eq. (6.5) we define

$$R \cos \epsilon = \cos \alpha_+ \left\{ V_{1111} \cos^2(\beta_1/2) \cos^2(\beta_2/2) + V_{11\text{-}1\text{-}1} \sin^2(\beta_1/2) \sin^2(\beta_2/2) \right\} ,$$

$$R \sin \epsilon = \sin \alpha_+ \left\{ V_{1111} \cos^2(\beta_1/2) \cos^2(\beta_2/2) - V_{11\text{-}1\text{-}1} \sin^2(\beta_1/2) \sin^2(\beta_2/2) \right\} ,$$

$$R' \cos \epsilon' = \cos \alpha_+ \left\{ V_{1\text{-}1\text{-}1\text{-}1} \sin^2(\beta_1/2) \cos^2(\beta_2/2) + V_{1\text{-}111} \cos^2(\beta_1/2) \sin^2(\beta_2/2) \right\} ,$$

$$R' \sin \epsilon' = \sin \alpha_+ \left\{ V_{1\text{-}1\text{-}1\text{-}1} \sin^2(\beta_1/2) \cos^2(\beta_2/2) - V_{1\text{-}111} \cos^2(\beta_1/2) \sin^2(\beta_2/2) \right\} , \quad (6.6)$$

$$P \cos \varphi = \frac{1}{3} V_{1100} \left\{ \cos^2(\beta_1/2) \sin^2(\beta_2/2) \cos \alpha_- + \sin^2(\beta_1/2) \cos^2(\beta_2/2) \cos \alpha_- + \sin \beta_1 \sin \beta_2 \right\} ,$$

$$P \sin \varphi = \frac{1}{3} V_{1100} \sin \alpha_- \left\{ \cos^2(\beta_1/2) \sin^2(\beta_2/2) - \sin^2(\beta_1/2) \cos^2(\beta_2/2) \right\} ,$$

$$P' \cos \varphi' = \frac{1}{3} V_{1\text{-}100} \left\{ \cos^2(\beta_1/2) \cos^2(\beta_2/2) \cos \alpha_- + \sin^2(\beta_1/2) \sin^2(\beta_2/2) \cos \alpha_- - \sin \beta_1 \sin \beta_2 \right\} ,$$

$$P' \sin \varphi' = \frac{1}{3} V_{1\text{-}100} \sin \alpha_- \left\{ \cos^2(\beta_1/2) \cos^2(\beta_2/2) - \sin^2(\beta_1/2) \sin^2(\beta_2/2) \right\} ,$$

in term of which the change of the action $A(\bar{\Omega}+_i, \bar{\Omega}-_i)$ is expressed as

$$A(\bar{\Omega}_i^+, \bar{\Omega}_i^-) = R_+ \sin(\gamma_+ + \delta_+) + R_- \sin(\gamma_- + \delta_-) \;, \tag{6.7}$$

where

$$R_+ = \frac{6}{32\pi}\left(\frac{15}{2\pi}\right)^{1/2}\left\{(R\cos\epsilon - P\cos\beta)^2 + (P\sin\beta - R\sin\epsilon)^2\right\}^{1/2}, \tag{6.8a}$$

$$R_- = \frac{6}{32\pi}\left(\frac{15}{2\pi}\right)^{1/2}\left\{(P'\cos\beta' - R'\cos\epsilon')^2 + (R'\sin\epsilon' + P\cos\beta')^2\right\}^{1/2}, \tag{6.8b}$$

$$\delta_+ = \tan^{-1}\left\{\frac{R\cos\epsilon - P\cos\beta}{P\sin\beta - R\sin\epsilon}\right\}, \tag{6.8c}$$

$$\delta_- = \tan^{-1}\left\{\frac{P'\cos\beta' - R'\cos\epsilon'}{R'\sin\epsilon + P'\sin\beta'}\right\} . \tag{6.8d}$$

Replacing (6.7) in (5.5) and changing the integration variables to γ_+ and γ_- we obtain for the transition amplitude

$$S(j_1 j_2, j_1' j_2') = \frac{1}{4\pi^2}\int_0^{2\pi} d\gamma_+ \exp i\left\{n_+\gamma_+ - R_+\sin(\gamma_+ + \delta_+)\right\}$$
$$\times \int_0^{2\pi} d\gamma_- \exp i\left\{n_-\gamma_- - R_-\sin(\gamma_- + \delta_-)\right\} \;, \tag{6.9}$$

where

$$n_+ = \frac{s_1 + s_2}{2} \quad , \quad n_- = \frac{s_2 - s_1}{2} \quad . \tag{6.10}$$

For $n_+(n_-)$ half integral we have $S(j_1 j_2, j_1' j_2')=0$. For $n_+(n_-)$ integer we use the integral representation of the Bessel function (Abramowitz and Stegun 1965, p.360) obtaining

$$S(j_1 j_2, j_1' j_2') = e^{-i(n_+\delta_+ + n_-\delta_-)} J_{n_+}(R_+) J_{n_-}(R_-) . \tag{6.11}$$

Because of the integer condition for (6.10) we have the selection rules:

if s_1 odd, then s_2 odd, (6.11a)

if s_1 even, then s_2 even or zero or vice versa.

These selection rules are the same as those in the quantum treatment of this problem. It is interesting to note that the above selection rules are independent of whether or not the colliding molecules are identical.

The transition probability is

$$P(j_1 j_2 \to j_1' j_2'; b; E) = (E_i / E_f)^{1/2} \, \mathcal{C}(j_1 j_2 j_1' j_2') \frac{1}{16 \pi^2} \int_0^{2\pi} d\alpha_1 \int_0^{2\pi} d\alpha_2$$

$$\int_{-1}^1 d(\cos\beta_1) \int_{-1}^1 d(\cos\beta_2) \, J_{n_+}^2(R_+) \, J_{n_-}^2(R_-) \,, \qquad (6.12)$$

where the average on the α's and β's must be performed numerically. We can see that the phases δ_+ and δ_- play no role in determining the probability. In contrast to the atom-homonuclear rotor case (Dickinson and Richards 1974) the integrand in (6.12) has no symmetry property which permits us to simplify the four-dimensional integral; nevertheless its complexity is substantially reduced for $\beta_i = 0$ or π, in which case $|S(j_1 j_2, j_1' j_2')|^2$ is independent of α_i. This is because for $\beta_i = 0$ or π the angular momentum vector of the ith rotor is perpendicular to the OXY plane (see section 4.2).

For a given orientation of the rotors the variations of R_+ and R_- depend only on the variations of the $V_{\nu_1 \nu_2 \mu_1 \mu_2}$ integrals. It is interesting to note that the frequencies W, in the $V_{\nu_1 \nu_2 \mu_1 \mu_2}$'s determining R_+ and R_- are $W_+ = W_1 + W_2$ and $W_- = W_1 - W_2$ respectively. As seen in section (5.7) $V_{\nu_1 \nu_2 \mu_1 \mu_2}$ decreases as W increases, and then we have that in general, for a given $\bar{E}$ and b, $R_+ < R_-$. This

difference in the values of R_+ and R_- explains some features of the first-order allowed transitions which will be discussed in the next section.

6.3   The first-order result

From (5.29) we obtain for the dipole-dipole FOCP probability

$$P^{FO}(j_1 j_2 \to j_1' j_2'; b; E) = (E_i/E_f)^{1/2} \, \mathcal{C}(j_1 j_2 j_1' j_2') \frac{1}{9} N_{1S_1}^2 N_{1S_2}^2$$

$$\sum_{\mu_1 \mu_2} |(1\mu_1, 1\mu_2 / 1 1 2 \mu_{12}) N_{2\mu_{12}} V_{S_1 S_2 \mu_1 \mu_2}|^2 , \qquad (6.13)$$

where the N_{1S_i} give the selection rule $|S_1| = |S_2| = 1$.   Expanding the sum in μ's we obtain

$$P^{FO}(j_1 j_2 \to j_1' j_2'; b; E) = (E_i/E_f)^{1/2} \, \mathcal{C}(j_1 j_2 j_1' j_2') \frac{5}{1024 \, \pi^3}$$

$$\left\{ \frac{3}{2} \left(V_{S_1 S_2 11}\right)^2 + \left(V_{S_1 S_2 00}\right)^2 + \frac{3}{2} \left(V_{S_1 S_2 -1-1}\right)^2 \right\} , \qquad (6.14)$$

which is proportional to the FOTDPT result, the proportionality constant K, being

$$K = \left\{ \frac{1}{[j_1][j_2][j_1'][j_2']} \right\}^{1/2} \frac{\begin{pmatrix} j_1' & j_1 & 1 \\ 0 & 0 & 0 \end{pmatrix}^{-2} \begin{pmatrix} j_2' & j_2 & 1 \\ 0 & 0 & 0 \end{pmatrix}^{-2}}{4} \left(\frac{E_i}{E_f}\right)^{1/2}$$

with $[j_i] = (2j_i + 1)$.

6.3.1   The straight-line limit

Among the semi-classical models, the straight-line (SL) has been the most widely used approximation to the relative motion (Cross and Gordon 1966, Rabitz and Gordon 1970a, 1970b, Mehrotra and

Boggs 1975, Hashi et.al., 1978, are some examples in dipole-dipole collision).   We present here the results of the SL approximation for the dipole-dipole FOCP as an example where the probability and the cross-section can be expressed analytically, providing a better understanding of some features of the long-range collisions.

For $W = \nu_1 W_1 + \nu_2 W_2 \neq 0$ the $V_{\lambda_1 \nu_2 \mu_1 \mu_2}$ integrals can be expressed as (Dickinson and Richards 1977).

$$V_{\nu_1 \nu_2 00} = \frac{2CW}{\hbar v^2 b} K_1(z) \; , \tag{6.15a}$$

$$V_{\nu_1 \nu_2 \pm 1 \pm 1} = \frac{CW^2}{\hbar v^3} \left[\frac{4}{3} K_2(z) - \frac{2}{z} K_1(z) \pm \frac{4}{3} K_1(z) \right], \tag{6.15b}$$

where $C = (4\pi/5)(40\pi/3)^{1/2} D_1 D_2$, D_i is the dipole moment of the i-th rotor, $K_\nu(Z)$ is a modified Bessel function (Abramowitz and Stegun 1965, p.374), v is the relative speed, and $Z = Wb/v$ is a measure of the adiabaticity of the collision; for $Z \ll 1$ the collision is sudden, while for $Z \gg 1$ it is adiabatic.   Replacing (6.15) in (6.14) and using recurrence relations for the $K_\nu(Z)$ functions (Abramowitz and Stegun 1965, p.376) we obtain for the SL limit of the FOCP probability P_{SL}^{FO}

$$P_{SL}^{FO}(j_1 j_2 \rightarrow j_1' j_2'; b; E) = (E_i/E_f)^{1/2} \, \mathcal{C}(j_1 j_2 j_1' j_2') \frac{2}{9} \left(D_1/ea_0 \right)^2 \left(D_2/ea_0 \right)^2$$

$$\cdot \frac{(ea_0 W)^4}{\hbar^2 v^6} \left\{ K_0^2(z) + K_1^2(z) - \frac{1}{z} K_1(z) K_1'(z) \right\} , \tag{6.16}$$

where

$$K_\nu'(z) = \frac{d}{dz} \left\{ K_\nu(z) \right\} .$$

For a resonant transition ($\Delta E_j \equiv \hbar W = 0, W_i \neq 0, i=1,2$) the $V_{\nu_1 \nu_2 \mu_1 \mu_2}$ integrals are

$$V_{0000} = \frac{2 C}{\hbar \upsilon b^2} \quad , \tag{6.17a}$$

$$V_{0011} = \frac{2}{3} \frac{C}{\hbar \upsilon b^2} \quad , \tag{6.17b}$$

where we have put $V_{\nu_1 \nu_2 \mu_1 \mu_2} = V_{00 \mu_1 \mu_2}$ for the resonant integrals. For the SL limit of the resonant FOCP probability P_{SLR}^{FO} we obtain

$$P_{SLR}^{FO}(j_1 j_2 \rightarrow j_2' j_1' ; b ; E) = \frac{2}{9} \left(D/ea_0\right)^4 \frac{e^4}{\hbar^2 \upsilon^2} \left(\frac{a_0}{b}\right)^4, \quad |j_1 - j_2| = 1, \tag{6.18}$$

where we put $D_1 = D_2 = D$, since a resonant transition occur in a collision between identical molecules.

For small values of the impact parameter the FOCP probability does not satisfy unitarity and modifications to enforce it are necessary. Hence a cut-off b^* is defined so that for $b > b^*$ the first-order model is valid (see section 3.1). Once b^* is defined the contribution to the cross-section from the long-range region $b > b^*$ is calculated using (3.5c), where b_2 is replaced by b^*. For the general case of the probability (6.14), the integral over impact parameters must be performed numerically. However, for the SL limit the integration is analytic, and we obtain for the non-resonant long-range FOCP cross section σ_{SL}^{FO}

$$\sigma_{SL}^{FO}(j_1 j_2 \rightarrow j_1' j_2' ; E) = (E_i / E_f)^{1/2} \, \mathcal{C}(j_1 j_2 j_1' j_2') \, \frac{4\pi}{9} \left(D_1/ea_0\right)^2 \left(D_2/ea_0\right)^2 \tag{6.19}$$

$$\left(\frac{e^2 a_0 W}{\hbar \upsilon^2}\right)^2 a_0^2 \left\{ z^* K_0(z^*) K_1(z^*) + \frac{K_1(z^*)}{2} \right\} \quad , \qquad z^* = \frac{W b^*}{\upsilon} \neq 0,$$

and for the resonant cross-section σ_{SLR}^{FO}

$$\sigma_{SLR}^{FO}(j_1 j_2 \rightarrow j_2 j_1 ; E) = \frac{2}{9} \pi \left(D/ea_0\right)^4 \left(\frac{e^2 a_0}{\hbar \upsilon b^*}\right)^2 a_0^2 \quad . \tag{6.20}$$

We use b* so that $P(b^*)=P^{FO}(b^*)$, where $P(b)$ is given by (6.12)

6.3.2. Convergence of the SCCP to the first-order result

Our numerical results presented in the next chapter, show that the SCCP converges into the FOCP at very low values of the probability. This slow convergence can be understood through the occurrence of the two different frequencies, W_+ and W_-, in the $V_{\nu_1\nu_2\mu_1\mu_2}$ integrals, which produce the inequality $R_+ < R_-$, for any $\bar{E}$ and b. To see the physics implicit in this inequality we consider here two cases where $|R_+ - R_-|$ becomes large. In what follows we consider a collision between two identical molecules, and a range of impact parameters for which the dominant term of the anisotropic potential is the asymptotic term $C_{11}(R)$, given by (4.10), so that R_+ and R_- are monotonic decreasing functions of b.

A)   The $(j,j) \rightarrow (j\pm1, j\pm1)$ transition. In this case we have for the integrand of (6.12)

$$\left| S(jj, j\pm1\ j\pm1) \right|^2 = J_1^2(R_+)\, J_0^2(R_-) \tag{6.21}$$

Since $W_1 = W_2$ the $V_{\nu_1\nu_2\mu_1\mu_2}$ integrals determining R_- are resonant, and so R_- decreases with b more slowly than R_+. Then there exists a large impact parameter $\bar{b} < b^*$, for which R_+ becomes small enough to make the small argument limit for $J_1(R_+)$ valid (Abramowitz and Stegun 1965, p.360), while R_- is still large. In this case we can write (6.21) as

$$\left| S(jj, j\pm1\ j\pm1) \right|^2 = \frac{1}{4} R_+^2\, J_0^2(R_-), \quad \bar{b} \leqslant b < b^*. \tag{6.22}$$

It is easy to show that the FOCP transition probability for this transition can be obtained from (6.22) by applying the small argument limit to $J_0(R_-)$ $(\lim_{R \to 0} J_0(R_-)=1)$, and performing the average over the $\alpha's$ and $\beta's$. Since the actual limit is reached at b=b*, usually much larger than $\bar{b}$, the value of the FOCP probability is too large in the region $\bar{b}$ <b<b* since $|J_0(x)| \leq 1$. Clearly this overestimation arises because by making $J_0(R_-)=1$ we are neglecting the resonant integrals $V_{00\mu_1\mu_2}$, which may be significant even at very large impact parameters.

B)   The resonant $(j_1,j_2) \to (j_2,j_1)$ transition, $|j_1-j_2|=1$. In this case we have

$$| S(j_1 j_2 , j_2 j_1) |^2 = J_0^2(R_+) \, J_1^2(R_-) \, . \tag{6.23}$$

Again the $V_{\nu_1 \nu_2 \mu_1 \mu_2}$ integrals determining R_- are resonant, and in the region $\bar{b}$ <b<b* (6.23) becomes

$$| S(j_1 j_2 , j_2 j_1) |^2 = J_1^2(R_-) \, . \tag{6.24}$$

In contrast to (A) in this region the transition is determined only by the resonant integrals $V_{00\mu_1\mu_2}$. This is equivalent to the quantal description where at large impact parameters the matrix elements corresponding to non-resonant channels become negligible (Bhattacharyya et.al. 1977).

As in (A) to obtain the FOCP probability for this transition, we apply the small argument limit to $J_1(R_-)$ in (6.24), yielding

$$| S(j_1 j_2 , j_2 j_1) |^2 = \frac{1}{4} R_-^2 \, , \tag{6.25}$$

and then we perform the average over orientations. As before in

the region $\bar{b} < b < b^*$ the value of the FOCP probability is overestimated.
From comparison between (6.24) and (6.25) it is clear that the
overestimation is because in this region $|R_-| > 2|J_1(R_-)|$, which indicates
that the resonant trajectory integrals, $V_{00\mu_1,\mu_2}$, are significant
at large impact parameters.

It is clear that for the transitions discussed above the
resonant trajectory integrals are dominant in determining the transition
amplitude, $S(j_1 j_2, j_1' j_2')$, in the region $\bar{b} < b < b^*$. This dominance
indicates that the SCCP treats the collisions as being sudden. In
Chapter 7 (section 7.2) we present a numerical study of the adiabaticity
parameter, $Z = Wb/\mathcal{U}$, which shows that, for the energies and transitions
studied in this work HCl-HCl and HF-HF collisions are adiabatic rather than
sudden. This suggests that the slow convergence of the SCCP to the
FOCP is due to the adiabatic nature of the collision. It is
interesting to notice that large values of the $V_{00\mu_1,\mu_2}$'s indicates
a large dipole-dipole coupling potential. Clearly the FOCP should
be more accurate, in the region $\bar{b} < b < b^*$, for non-adiabatic collisions
between molecules with a small anisotropy in the potential surface.

Although the two transitions discussed above are just special
cases of the transitions $(j_1, j_2) \rightarrow (j_1 \pm 1, j_2 \pm 1)$ and $(j_1, j_2) \rightarrow (j_1 \pm 1, j_2 \mp 1)$
respectively the conclusions are expected to be general for every
first-order allowed transitions with $W_- \ll W_+$, provided they are not
both sufficiently small for the sudden approximation to be valid.

6.4   Numerical Techniques

To calculate the cross-section at a given energy we have to
evaluate the integral (5.25) of the transitions probability
$P(j_1 j_2 \rightarrow j_1' j_2'; b; E)$ over impact parameters, where the probability itself
is the four-dimensional integral (6.12) of the modulus squared of
the transition amplitude $S(j_1 j_2; j_1' j_2')$. The transition amplitude

is obtained evaluating (6.11) for each R_+ and R_- which, for each value of b, require the evaluation of the $V_{\nu_1 \nu_2 \mu_1 \mu_2}$.

6.4.1   Evaluation of the $V_{\nu_1 \nu_2 \mu_1 \mu_2}$.

The integrals $V_{\nu_1 \nu_2 \mu_1 \mu_2}$ depend on the classical trajectory followed by the incident molecule relative to the target.   As seen in section 4.4 this is determined by the spherical part of the potential $\bar{C}_{oo}(R)$.   Taking the well depth of the potential E, and its position R_m as units of energy and length respectively we write the reduced variables as

$$\tilde{r} = R/R_m \qquad , \quad \tilde{b} = b/R_m \qquad , \quad \tilde{E} = \bar{E}/\varepsilon ,$$

$$\tilde{C}_{oo} = \bar{C}_{oo}/\varepsilon \qquad , \quad \tilde{t} = 2\varepsilon t/\hbar \, B_z^{1/2} , \quad B_z = 2\mu\varepsilon R_m^2/\hbar^2 , \tag{6.26}$$

in term of which the classical equations of motion are

$$\frac{d\tilde{r}}{d\tilde{t}} = \left\{ \tilde{E} - \frac{\tilde{E}\,\tilde{b}^2}{\tilde{r}^2} - \tilde{C}_{oo}(\tilde{r}) \right\}^{1/2} , \qquad \tilde{r}(0) = \tilde{r}_0 , \tag{6.27a}$$

$$\frac{d\varphi}{d\tilde{t}} = \frac{d\varphi'}{d\tilde{t}} = \frac{\tilde{b}\,\tilde{E}^{1/2}}{\tilde{r}^2} \qquad , \quad \varphi'(0) = 0 . \tag{6.27b}$$

where the reduced distance of closest approach $\tilde{r}_0$, is the largest root of the right-hand side of (6.27a).   The integration of equations (6.27) is carried out using an algorithm of fourth-order predictor-corrector type based on the Adams-Bashforth predictor and Adams-Moulton corrector (Hamming 1962, p.194;   Crane and Klopfenstein 1965).   To start the procedure the routine employed requires that $\lim_{\tilde{t} \to 0} (d\tilde{r}/d\tilde{t}) \neq 0$ This is obtained using the substitution $\tilde{s} = (\tilde{r} - \tilde{r}_0)^{1/2}$ (A.P. Clark, private communication), so that $\lim_{\tilde{t} \to 0} (d\tilde{s}/d\tilde{t}) \neq 0$.

The $V_{\nu_1 \nu_2 \mu_1 \mu_2}$ are integrated using Clenshaw-Curtis quadrature with reliable error estimates (O'Hara and Smith 1968). The routine was checked by comparing the results at large impact parameters with those given by the SL limit (6.15). The agreement was within the expected accuracy.

To evaluate the modified Bessel functions in (6.15) we use polynomial approximations for K_0 and K_1 (Abramowitz and Stegun 1965, p.379), and then K_2 is obtained using recurrence relation (above reference, p.376).

6.4.2 Evaluation of the transition amplitude

Given the $V_{\nu_1 \nu_2 \mu_1 \mu_2}$ the calculation of R_+ and R_- for specified values of α_i and β_i is straightforward.

To evaluate the Bessel functions of the first kind $J_\nu(x)$, we use polynomial approximations for J_0 and J_1 (Abramowitz and Stegun 1965, pp.369 and 370), and then other orders are obtained using either recurrence relations or ascending series (above reference, pp.361 and 360 respectively) depending on $|X|$ being larger or smaller than $|\nu|$ respectively.

6.4.3 Evaluation of the transition probability

The rapid evaluation of cross-sections using SCCP depends strongly on the efficient evaluation of the integral (6.12). Accordingly, most of the effort in the implementation of the computing program has been spent in doing this integration. We found that Clenshaw-Curtis quadratures reconcile speed and accuracy.

The integration over α's is carried out first making full use of the simplification for $\beta_i = 0$ or π (see section 6.2). The integration over β's is performed on the variable $\cos \beta_i$ which gave

a smoother integrand.   Typically the number of points in each integrand gradually decreases from 33 in the inner integral to 5 or 9 in the outer, to give results accurate to 1%.   The accuracy of the integration was checked by doing the FOCP calculation numerically and comparing with the closed form results (6.13) for the full curved trajectory, and (6.16) for the SL approximation.

6.4.4   Evaluation of the cross-section

The evaluation of the integral (5.25) is performed using, again, Clenshaw-Curtis quadratures.   The upper limit of the integration was taken at a cut-off b_{max} defined by $P(b_{max})b_{max} < 10^{-10}$.   The contribution from impact parameters beyond this value is completely negligible.   For resonant collisions we found that at $b^* < b < b_{max}$ the contribution to the integral was still considerable, and the trajectory was well approximated by a straight line;   in this case we put our upper cut-off $b_{max} = b^*$ and the cross-section was calculated as

$$\sigma(j_1 j_2 \to j_2 j_1) = 2\pi \int_0^{b^*} P(j_1 j_2 \to j_2 j_1; b; E)\, b\, db \; + \; \sigma_{SLR}^{FO}(j_1 j_2 \to j_2 j_1). \quad (6.28)$$

Some cross-sections have been calculated using the SL limit for the relative motion.   Since in this case there are unphysical small values of R we have introduced in the integral (5.25) a lower limit $b_{min} = r_o \equiv R_m \tilde{r}_o (\tilde{b}=0)$.

Much of the computing time is spent in the four-dimensional integral (6.12), and we feel that any attempt to reduce the computing time should concentrate on this integral.   In evaluating the $V_{\nu_1 \nu_2 \mu_1 \mu_2}$ we have sacrificed generality for speed, and to make the computing program applicable to any transition and system, an integration routine "tailor-made" for rapidly oscillating functions could be more desirable.

The precision of the calculations we present in the next chapters is estimated to be about 3%. The program was run in the University of Manchester CDC 7600 computer through the Stirling University link. The SCCP cross-sections presented in this thesis required about 36 minutes CPU time. An average cross-section required about 55 seconds CPU time.

CHAPTER 7

RESULTS AND DISCUSSION

7.1   Introduction

Probabilities and cross-sections for rotational transitions
in HF-HF and HCl-HCl collisions have been calculated for different
levels of the molecules at different initial relative energies E_i.
Our goal was to investigate the features of the rotationally inelastic
transitions for different collisional parameters.   To allow comparison
with earlier studies, we discuss here some examples of transitions out
of low rotational levels (j_1,j_2), for which there is no formal
justification for using the SCCP; however, quite good accuracy has
in fact been obtained for the $j=0 \rightarrow j'=2$ transition in H_2-He collisions
(Clark 1977), and although the reasons for this are not clear we expect
our predictions to be reasonably accurate.

7.2   The adiabaticity of the collision

It proves convenient to facilitate our discussion by examining
the adiabaticity of the collision.   The adiabaticity parameter is
usually defined as the ratio between the collision time, τ_c, and
the transition time, W^{-1}, for the rotational motion of the system.
As seen in sub-section 6.3.1 for the SL limit this ratio is conveniently
taken as

$$Z = \frac{Wb}{v} ,$$

(7.1)

where $\hbar W$ is the change in rotational energy of the system.   When
$Z \gg 1$ the collision is adiabatic and the molecules rotate a great deal
during the collision; when $Z \ll 1$ the collision is sudden and we may
consider that the molecules do not rotate during the collision.

A numerical estimate of the adiabaticity for the systems studied in this work is obtained by examining the $(1,1) \to (0,2)$ transition. Using ν as given by (4.16) we obtain, in HF-HF collisions, $Z = 0.4 b/a_o$ and $Z = 0.1 b/a_o$ at initial energies $E_i = 500$ and $8000 cm^{-1}$ respectively; for HCl-HCl collisons we have $Z = 0.4 b/a_o$ and $Z = 0.26 b/a_o$ at $E_i = 201.71$ and $500 cm^{-1}$ respectively. These results show that in both cases the collision cannot be considered as sudden, as even for HF-HF at $E_i = 8000 cm^{-1}$ Z is small only for the smaller impact parameters. This large adiabaticity is characteristic of heavy-particle collisions involving hydrides.

At small impact parameters the relative motion is not well represented by a straight line. For the curved trajectories at small b however, there is no comparable ratio to (7.1). Based on the strong dependence of the $V_{\nu_1 \nu_2 \mu_1 \mu_2}$ integrals on the value of the potential at the distance of closest approach, r_o, we define a characteristic adiabaticity parameter $\bar{Z}$ as

$$\bar{Z} = \frac{W r_o}{\bar{V}} \tag{7.2}$$

where $\bar{V}$ is some typical speed. Clearly this would be the adiabaticity parameter if we approximate the curved trajectory by a SL with impact parameter $b = r_o$ and speed $\bar{V}$.

The evaluation of (7.2) involves the choice of a physically convenient $\bar{V}$, which is not unique. Using the simplest cases we have calculated $\bar{Z}$ for the following three choices of $\bar{V}$:

$$(1) \;\; \bar{V} = \nu \;, \quad (2) \;\; \bar{V} = \nu_o = \frac{b \nu}{r_o} \;, \quad (3) \;\; \bar{V} = (\nu + \nu_o)/2 \;, \tag{7.3}$$

where $\mathbf{V}$ is given by (4.16) and $\mathbf{V}_o$ is the actual relative speed of the molecules at the distance of closest approach. For distant collisions, where the curved trajectory converges to a SL, $\bar{Z}=Z$. On physical grounds the third $\bar{V}$ in (7.3) should be the best of these approximations.

We present in table 7.1 our results for $\bar{Z}$ for the $(1,1)\rightarrow(0,2)$ transition at $E_i=8000cm^{-1}$. We notice that for the smaller impact parameters $\bar{Z}>Z$. This is because at these values of b the repulsive part of the potential is dominant, making the relative motion at r_o slower and keeping the molecules apart. No significant difference between $\bar{Z}$ and Z appears at larger b, and they become equal at $b\cong12a_o$ where $b\gtrsim r_o$.

The results discussed above predict, for the systems studied in this work, a breakdown of the time dependent sudden approximation (TDS A). This has been shown by Alexander and DePristo (1979), who have calculated sudden transition probabilities and cross sections for the $(0,0)\rightarrow(1,1),(0,2),(2,2)$ and $(1,1)\rightarrow(0,2)$ transitions in HF-HF collisions at a total energy $E=8000cm^{-1}$. Their results (presented below) show that the main contribution to the cross section comes from distant adiabatic collisions, giving cross sections which can be overestimated greatly in the sudden approximation. This can also be noticed from our discussion in sub-section 6.3.2, as the TDSA in the SCCP framework puts $V_{\nu_1\nu_2\mu_1\mu_2}=V_{oo\mu_1\mu_2}$; from eqs. (6.13) and (6.14) it is clear that at large impact parameters the sudden approximation overestimates a non-resonant transition, while it is exact for a resonant one.

7.3   The correspondence principle transition probability

7.3.1   The function P(b)

We discuss first the behaviour of the transition probability
as a function of the impact parameter b.   To investigate the
importance of curved orbits we have calculated the SCCP probabilities
using both, a straight line (SL) and curved trajectory under the
spherically symmetric potential $\bar{C}_{oo}$ (R) - the latter being termed the
full SCCP result.

We present the function P(b) for the $(0,0) \rightarrow (1,1)$ transition
at energies E_i =1000 and 8000cm^{-1} in figures 7.1 and 7.2 for HF-HF
collisions.   Since the lowest energy E_i is much smaller than the well
of the potential,$\mathcal{E}$, orbiting occurs at b=b$_o$.   When b becomes just
larger than b$_o$ three turning points exist, and b$_o$ marks a jump in the
classical distance of closest approach (from r$_o$<R$_m$ to r$_o$>>R$_m$).   The
trajectory integrals, $V_{\nu_1 \nu_2 \mu_1 \mu_2}$, are not defined at b=b$_o$ but the integral
over b for the cross section exists.

The results in figures 7.1 and 7.2 show that at small impact
parameters in the SL limit the SCCP probability is negligible.   This
is because at these impact parameters the trajectory integrals are
extremely large, being roughly proportional to the value of the
potential $\bar{C}_{11}$(R) at R=b.   Here we expect for the rotor-rotor probability
a behaviour similar to the strong-collision limit of the atom-rotor
probability (Dickinson and Richards 1978), so that a statistical limit
$P(b) \propto 1/|V_{0011}|$ is likely to be valid (Benstein et.al., 1963).   There the
number of strongly coupled levels, N, is proportional to V_{oo11} (Dickinson
and Richards 1976); if $\bar{C}_{11}$(R) increases, N increases and more levels
are classically accessible.   Thus, to conserve probability, the flux
to a particular level must decrease.   When b increases the SL
probability increases, reaches a maximum and decreases to become
negligible again at large b.

For the full SCCP the picture is slightly different. At the low impact parameters the distance of closest approach r_o changes very slowly, and the strength of the collision, as measured by the $V_{\nu_1 \nu_2 \mu_1 \mu_2}$ integrals, is almost constant. As b increases the change in r_o is more noticeable and the probability increases, reaches a maximum and decreases becoming negligible at large impact parameters. This shows the dependence of the probability on the dynamics of the relative motion. The same shape occurs in the calculations of Bhattacharyya et.al. (1977) for rotor-rotor collisions,

While at the lower energy E_i most of the probability arises from impact parameters where the effect of the spherical potential on the trajectory is still noticeable, at the higher energy the contribution to P(b) comes mainly from b's where the trayectory is very well represented by a SL. These represent what we have termed short and long-range transitions respectively. In the short-range transitions we notice that after the maximum is reached the probability falls sharply to a very low value. This is because the collision is very adiabatic, and at these impact parameters the transition probability decreases as square of K Bessel functions (Abramowitz and Stegun 1965, p.374). The physical factors that make a transition short or long-ranged are discussed below.

7.3.2   The FOCP probability

The transitions presented in figures 7.1 and 7.2 are first-order allowed. In all these cases the FOCP transition probability does not satisfy unitarity at small impact parameters, and becomes less than 1 at $b \gtrsim b_m^{(*)}$ for both the short and long-range transitions. Some FOCP probabilities are presented in figures 7.1 and 7.2 for large

(*) $\max P(b) = P(b_m)$.

impact parameters, with the same qualitative picture in both cases: the FOCP overestimates the transition probability, which deviates from the correct value even at impact parameters where the value of the probability is very small (figure 7.1).   Eventually, the SCCP probability converges to the FOCP value, but this convergence usually occurs when the probability is negligible.

The FOCP probability has also been calculated using both curved and SL trayectories.   The comparison between them (not shown) showed that in the region where the repulsive part of the potential $\bar{C}_{oo}$ (R) is dominant (very low impact parameters), the SL limit gives results very much larger than the curved orbit result, while when the attractive part of the potential dominates the SL limit result becomes smaller. This is consistent with the fact that the distance of closest approach is a dominant effect in evaluating the $V_{\nu_1\nu_2\mu_1\mu_2}$ integrals.   The impact parameters for which both probabilities become less than 1 are approximately the same, so in our approach the SL limit of the first-order result is not improved by the curved trayectory version.   This result is a semiclassical confirmation of the prediction of DePristo and Alexander (1977) that the DWBA treatment of the collision would not remedy the failure of the BA.   As seen in sub-section 6.3.2 the failure of the FOCP model is mainly because of the adiabatic nature of the collision.

7.3.3   The change of the probability with E_i

We now study the transition probability as a function of the initial relative energy E_i.   The impact parameter b, and the net change of rotational energy of the system, $\Delta E_j = \Delta E_{j_1} + \Delta E_{j_2}$, are considered constant.   It is important in the following discussion to

separate the transitions into resonant $(\Delta E_j = 0, \Delta E_{j_1} = -\Delta E_{j_2} \neq 0)$ and non-resonant $(\Delta E_j \neq 0)$ cases.

Consider first a non-resonant transition. It is clear from figures 7.1 and 7.2 that when E_i increases the transition probability also increases. This is generally valid for large impact parameters, and so a transition which is short-ranged at low energies can become long-ranged when the energy increases. Another example is presented in figure 7.3 where we show the probabilities for the $(1,1) \rightarrow (0,2)$ transition at $E_i = 1000$ and $8000 cm^{-1}$. Note here that the difference in the range of the transition at the two energies is not as marked as for the $(0,0) \rightarrow (1,1)$ transition (see figures 7.1 and 7.2). This is because, although E_i has been increased by the same amount for the two cases, the $(1,1) \rightarrow (0,2)$ transition is less adiabatic. The fact that at $E_i = 1000 cm^{-1}$ the $(1,1) \rightarrow (0,2)$ transition is longer-ranged than the $(0,0) \rightarrow (1,1)$, indicates that a low E_i is not sufficient for a non-resonant transition being short-ranged; the collision should also be adiabatic.

In the FOCP result at large impact parameters, the non-resonant transition probability increases as E_i increases; this is because at large b the trajectory integrals are increasing functions of the speed. Since the FOCP is invalid at small impact parameters we do not consider it further.

For a resonant transition the dependence of the probability on E_i is different. At large impact parameters, where the trajectory is well represented by a SL, an increase in the energy E_i produces a decrease in the transition probability. This is because here FOCP is valid and the resonant trayectory integrals are decreasing functions of the speed (see eq. 6.17). At small impact parameters there is strong coupling and the probability behaves more like a non-resonant transition

probability; this is illustrated in figure 7.4 where we present the
probability for the resonant transition $(0,1) \to (1,0)$ at $E_i = 1000$ and $8000 cm^{-1}$
in HF-HF collisions.

In contrast to the non-resonant case, a resonant transition is
longer ranged at smaller energies, which is a feature of sudden collisions.
Overall, a resonant transition cross section is mainly determined by
the long-range contribution and we shall see below that the resonant
cross section is a decreasing function of the energy E_i.

7.3.4 The variation of the probability with ΔE_j.

We now consider the transition probability as a function of
the net change in the rotational energy ΔE_j (b and E_i constants), which
is equivalent to studying the probability as a function of the
frequency W.

It proves convenient to consider first the FOCP result, as
it is directly proportional to the squares of the trayectory integrals
$V_{s,s_2\mu_1\mu_2}$.   As shown by Dickinson and Richards (1977) these integrals
decrease rapidly as W increases for curved orbits, and so the first-
order result increases when W decreases.

For the SCCP result the extension of above picture to the
region where the coupling is weak is straightforward, and at large
impact parameters an increase in W produces a decrease in the transition
probability.   This means that at a given energy E_i, the transition is
shorter-ranged as the collision is more adiabatic.   This is clearly
shown in figure 7.5, where we present the probability for the $(0,0) \to (1,1)$
and $(1,1) \to (0,2)$ transitions in HF-HF collisions at $E_i = 8000 cm^{-1}$, and
in figure 7.6, where we present results for the $(0,0) \to (0,2)$, $(2,2) \to (3,3)$
and $(5,1) \to (2,2)$ transitions, for the same system at the same energy.

At large impact parameters the larger probabilities correspond to the smaller ΔE_j's associated with the transitions.

In the strong-coupling region however, the situation is different and complex. While in figure 7.5 the largest probability is associated with the smallest change in rotational energy, in figure 7.6 there is not a clear pattern associated with the variation of ΔE_j. This is because the probability is not a single valued function of the collision strength. In our picture the form of this dependence is non-linear and it does not seem possible to give a simple account of its effects on the probability.

It is interesting to note that in collisions between identical molecules, for the (j_1,j_2) $(j_1\pm s,j_2\mp s)$ transitions there are sets $\left\{(j_1,j_2)\right\}$, of initial rotational quantum numbers for which, for a given s, the value of ΔE_j associated with the transition is the same for any element (j_1,j_2) of a particular set. So for instance, $\Delta E_j=0$ for all (j_1,j_2) such that $j_1=j_2\mp s$, and $\Delta E_j=2Bs^2$ for all (j_1,j_2) such that $j_1=j_2$, B being the rotational constant of the molecules. Clearly for distant collisions the transition probabilities for such a transition are equal for any element (j_1,j_2) of a given set. In the strong-coupling region however, the probabilities are different for different initial quantum numbers, as at a given collision energy E_i, the number of accessible channels changes for different initial (j_1,j_2). As an example we show in figure 7.7 probabilities for the resonant transitions $(2,1)\to(1,2)$ and $(1,0)\to(0,1)$ for HF-HF collisions at $E_i=8000cm^{-1}$. We notice that in this case the probability for the larger initial (j_1,j_2) is the larger, and this is so even at b's where the trayectory is a SL $(r_o=b$ at $b \gtrsim 12a_o)$, showing that the coupling is still strong when the

spherically symmetric potential is negligible.   This dependence of
the rotor-rotor probability on the initial quantum numbers highlights
an important difference with the atom-rotor case, where a large initial
quantum number has associated a large ΔE_j.   In the rotor-rotor case
transitions with very small ΔE_j can occur in collisions between highly
excited molecules.

7.4   Comparison of the SCCP probability with that obtained in other theories

7.4.1   Introduction

In the last section we have discussed different features of
the SCCP transition probability, and how these depend on the different
parameters of the collision.   Since our discussion has not delimited
the validity of our calculations, we aim in this section to investigate
the usefulness of our model.   To do so we compare here with the Close-
Coupling calculations (CC) of DePristo and Alexander (1977), the
Perturbed Rotational States calculations (PRS) of Hashi et.al. (1978),
the Classical Trayectory calculations (CT) of Alper et.al. (1978), and
the Adiabatically-Corrected-Sudden calculations (ACS) of Alexander
and DePristo (1979).

Despite the CC and PRS calculations should, in principle,
provide accurate results we feel that there is not, so far, a
dipole-dipole rotationally inelastic calculation we can consider a yardstick
against which to test our approximation.   Hence, here we discuss not
only the validity of the SCCP results but also the validity of the
results we compare with.   However, after this work was substantially
completed we received a preprint from Alexander (1980) describing a
more extensive close-coupling study which may well be almost converged.
Comparison with these Alexander results are presented in section 7.5.

Inadvertantly the SCCP calculations were performed with a spherically symmetric potential which was $(2\sqrt{\pi})^3$ times too strong. Thus comparisons with other works in regions where curvature of the orbit is important can only be qualitative. We have obtained a numerical estimate of such a region looking into the deflection angle, $\bar{\Theta}$, as given by the first-order momentum approximation (Pauly 1979, p.140). For HF-HF collisions at E_i=500,1000 and 8000cm^{-1} the trajectory is well represented by a SL at impact parameters $b \gtrsim b_{SL}$=9,8 and 5.5a$_o$ respectively.

We include in the comparison SCCP results using a SL trajectory for the relative motion - henceforth termed the straight line correspondence principle (SLCP). At $b \gtrsim b_{SL}$ the effect, on the probability, of using a stronger spherical potential is shown by the difference between SLCP and SCCP. For $b<b_{SL}$ it is difficult to estimate such effect; however, it is likely that for those b where the trayectory is dominated by the repulsive core of the potential, the transition probability is underestimated.

7.4.2 Comparison with Close Coupling calculations

To test the adequacy of our approach we compare here with the close coupling theory (CC) which, in principle, can give exact results for this problem. The application of the CC theory to the collision of two rotors has been presented by Takayanagi (1965), see for example Green (1975) for H_2-H_2 collisions, and DePristo and Alexander (1977) for HF-HF collisions.

The CC theory exploits conservation of the total angular momentum of the system. Consequently, basis functions in the total angular momentum representation $I^{JM}(j_1 j_2 j l ; \Omega, \Omega_l \Omega)$ - formed from the internal wave functions of the separated molecules - are introduced

(Takayanagi 1965, eq. 6).   Here J and M are the total angular
momentum and its projection quantum number respectively, ℓ is the
orbital quantum number, and j is the quantum number corresponding to
the vector sum of $\underline{J_1}$ and $\underline{J_2}$. j_i, Ω_i (i=1,2) and Ω are the same as
used in this work.   The wave function for the rotor-rotor system
$\Upsilon(\Omega_1, \Omega_2, R)$ is expanded in terms of the I^{JM} functions, and, when
substituted in the time independent Schrodinger equation, the usual
CC equations for the coefficients of the expansion for each J,M are
obtained (Takayanagi 1965, eq.9).   A major difficulty with the CC
calculations is the $(2j_i+1)$ degenerate levels which must be included
for each rotational level, j_i of each molecule, making the calculations
prohibitively long when the number of levels increases.

The CC transition probability $P_J^{cc\pm}$ is taken to be

$$P_J^{cc\pm}(j_1 j_2 \rightarrow j_1' j_2' ; E) = \frac{1}{(2j_1+1)(2j_2+1)} \sum_{\ell,\ell'} \left| \delta_{nn'} \delta_{\ell\ell'} - S_{n\ell,n'\ell'}^{J\pm} \right| \qquad (7.4)$$

where n(n') represents the triple index $j_1 j_2 j (j_1' j_2' j')$, and $S_{n\ell,n'\ell'}^{J\pm}$
is the usual S-matrix;   the $\pm$ sign indicates that, since we consider
collisions between identical molecules, properly symmetrized functions,
$I^{JM\pm}$, are used.   We compare with the results of DePristo and Alexander
(1977) who studied HF-HF collisions at total energies E=500,1000 and 8000cm^{-1}.
These CC calculations have been done mostly using a basis B3 containing
the (0,0), (1,1), (0,2), and (2,2) rotational levels and correspond
to both interchange symmetries.

In figures 7.8 and 7.9 we show weighted probabilities for
the (0,0)$\rightarrow$(1,1) transition at E_i=1000 and 8000cm^{-1} respectively.   At
the larger energy we notice that for distant collisions (b>18a$_o$), the
SCCP agrees well (error $\leq$ 15%) with the CC results.   There is also

good agreement between FOCP and BA at both energies.   This is
significant as it shows that the quantization of the internal rotational
states (eq. 4.6) is not producing serious errors, even for this
transition out of the ground rotational level.   It is interesting to
point out that at $E_i = 8000 \text{cm}^{-1}$ the CC probability converges to the
first-order result faster than the SCCP.   This suggests that the
SCCP considers the collision as less adiabatic and converges to the
FOCP slower than expected.   A further discussion on this point is
presented below.

From the results presented above it seems clear that the
SCCP provides a reasonably good description of distant collisions.
At small impact parameters the correspondence principle results
(SCCP and SLCP) are inaccurate, and we cannot estimate the error
because the CC results are unconverged.   It is likely that a basis
containing more rotational levels than B3 is necessary to assure
convergence (DePristo and Alexander 1977, Alexander and DePristo 1979).
Close coupling calculations using an extended basis $B4 = \{ B3, (1,3), (3,3) \}$,
have been performed for the (0,0) (1,1) transition at $E_i = 1000 \text{cm}^{-1}$ at
J=40, 60 and 80 (DePristo and Alexander 1977).   The results, presented
in figure 7.8, show that at J=40 the CC probability using B4 is
smaller than the result using B3, while no change occurs at J=60.
The result at J=80 is unexpected, as the CC probability using B4
becomes so large that it is off the scale of figure 7.8 ($(2J+1) \, P_J^{cc} \cong 18.2$).
Although just a few, these results suggest that to achieve convergence
at small J, the CC calculations need a basis containing more states
than B4.

It is interesting at this point to reexamine CPT. Using (5.15) in (6.7) we obtain for the classical change in the rotor angular momentum

$$\Delta j \equiv \Delta j_1 + \Delta j_2 = -2 R_+ \cos(\gamma_+ + \delta_+) .$$

(7.5)

From (6.8a) and (6.6) we can see that there is at least one (β_1, β_2) for which Δj is given by

$$\Delta j \equiv \Delta j_1 + \Delta j_2 = -\frac{12}{32\pi} \left(\frac{15}{2\pi}\right)^{1/2} V_{1111} \cos(\gamma_+ + \delta_+),$$

(7.6)

It is clear from (7.6) that the maximum Δj allowed classically in CPT is

$$\max(\Delta j) = \frac{12}{32\pi} \left(\frac{15}{2\pi}\right)^{1/2} |V_{1111}| .$$

(7.7)

We show in table 7.2 values of $\max(\Delta j)$ for different b's in HF-HF collisions at $E_i = 500$, 1000 and 8000cm^{-1}, using the parameters for the $(0,0) \rightarrow (1,1)$ transition and assuming a straight line trajectory for the relative motion. We present also the highest level $(j_1, j_2 = j_1)$, satisfying $\max(\Delta j)$ which is classically accessible. Clearly from table 7.2, the SLCP has probability flux in energetically forbidden channels. This is likely to make the SLCP underestimate the transition probability (Clark et.al., 1977).

At small impact parameters the collision is very strong, and the change of the action $A(\bar{\Omega}_1, \bar{\Omega}_2)$, is unlikely to be small compared with the action associated with the isotropic potential. From table 7.2 we see that in these very strong collisions CPT may produce transitions up to $\Delta j = 50$. It is our feeling that CPT cannot cope accurately with these strong-coupling collisions, and $A(\bar{\Omega}_1, \bar{\Omega}_2)$ does not describe precisely the coupling between the two rotors. While this produces errors in the cross sections for short-ranged collisions at the smaller energies, it is almost unnoticed for long-range

collisions.

Overall the SCCP should provide an accurate description of long-range collisions, with errors which, due to averaging, may be smaller than the possible CPT errors in determining the change of the action A($\bar{\Omega}_1$, $\bar{\Omega}_2$).

7.4.3 Comparison with Perturbed Rotational State calculations

We have seen above that both the FOCP and BA are in good agreement and give overestimated transition probabilities. We have also shown in subsection 6.3.2 that this is due to the size of the dipole-dipole coupling potential and the non-sudden nature of the collision. In adiabatic collisions it is likely that the coupling potential will affect strongly the phase of the rotational motion of the molecules, and, to describe this, CC will require a large number of rotational states. To take this perturbation into account it is convenient to use an adiabatic formulation in which $I^{JM}(j_1 j_2 l; \Omega_1, \Omega_2 \Omega)$ functions are replaced by the adiabatic internal states $\chi_j(R; \Omega_1, \Omega_2)$. These are eigenfunctions of the full internal part of the Hamiltonian (Child 1974, pp.87-88):

$$\left[H_{o_1}(j_1) + H_{o_2}(j_2) + V(R, \Omega_1, \Omega_2) \right] \chi_j(R; \Omega_1, \Omega_2) = W_j(R) \, \chi_j(R, \Omega_1, \Omega_2) \tag{7.8}$$

where $H_{oi}(j_i)$ (i=1,2) is the Hamiltonian for a free rotor in the rotational level j_i, and $W_j(R) \underset{R \to \infty}{\cong} E_{j_1} + E_{j_2}$, the rotational energy of the non-interacting rotors.

This method has been used in rotationally inelastic collisions between two diatomic molecules by Hashi et.al. (1978), and been termed Perturbed Rotational States (PRS). Expanding the wave function of the system in terms of the χ_j, they solved the time-dependent Schrodinger equation obtained assuming a SL trajectory with constant

speed, both numerically and using a first-order approach. This latter approximation can be termed the first-order perturbed rotational state (FOPRS). SCCP, SLCP, PRS and FOPRS results are compared in figure 7.10, where we present probabilities for the $(0,0) \to (1,1)$ transition at $E_i = 500 cm^{-1}$ in HF-HF collisions as a function of the reduced impact parameter $\tilde{p} = b/(D^2/B)^{1/3}$ (Hashi et.al., 1978).

The marked difference in the form of the PRS and the correspondence principle probabilities (SCCP and SLCP) indicates that the distortion of the rotational states by the coupling potential during the collision is strong, and affects the dynamics of the transfer of rotational energy. This is very important at small energies since, as shown in figure 7.10, most of the cross section arises from the region where the distortion of the rotational states is noticeable. The good agreement between PRS and FOPRS suggests that the PRS results are converged, and that a major source of error in the usual first-order perturbation calculations (BA,FOTDPT) for adiabatic collisions is the failure to take into account the distortion of the rotational states by the coupling potential.

In principle the PRS treats the coupling between rotational states exactly, and should provide a very convenient description of the dynamics of near-adiabatic rotational energy transfer. As the energy increases the use of the χ_j's offers little advantage. From the above comparison it is clear that the SCCP does not describe accurately adiabatic collisions.

7.4.4   Comparison with Classical Trajectory calculations

Here we compare with results obtained from completely classical calculations. The method is usually termed Classical Trajectory (CT)

calculations as it involves the study of the trajectories followed by the collision partners.

These are determined by solving the classical equations of motion

$$\dot{p}_i = -\partial H/\partial q_i \quad , \quad \dot{q}_i = \partial H/\partial p_i \quad , \tag{7.9}$$

where H is the classical Hamiltonian of the system, q_i a coordinate variable and p_i its conjugate momentum. The detailed methodology of trajectory calculations has been recently reviewed by Pattengill (1979), and some details of the basic concepts of the classical collision theory, as applied to rotationally inelastic collisions, have been given by Clark et.al., (1977), Dicinson (1979b) and Pattengill (1979).

A major problem of the CT calculations is the procedure to be used to quantize the continuous classical variables such as angular momentum. In the context of the problem studied here this produces ambiguities in:

A)   the method to assign a classical rotational energy E_{j_i}, to a given initial quantum level j_i, of the i-th molecule, and

B)   the method to assign a rotational quantum number j_i', to the final rotational energy $E_{j_i'}$, of the i-th molecule, determined by the trajectory calculations.

The most common technique for (A) is to assign a classical rotational energy to a molecule using either the standard quantum-mechanical formula

$$E_j = Bj(j+1) \quad , \tag{7.10a}$$

or to employ the usual semiclassical correction

$$E_j = B\left(j + 1/2\right)^2 \quad . \tag{7.10b}$$

For each set of initial conditions trajectories are computed, and
the final relative translational energy and final rotational energy
of each molecule are determined.   To find j' one uses (7.10) to
determine the classical j_c corresponding to the final rotational
energy, and then associates j' with j_c by (Dickinson 1979a)

$$j' = j_q \quad if \quad j_q - \frac{1}{2} \leq j_c < j_q + \frac{1}{2} \quad . \tag{7.11}$$

So, a trajectory is said to result in the j→j' transition.

We compare here with the CT results of Alper et.al. (1978) on
HF-HF collisions, which have been obtained using both (7.10a) and
(7.10b); we have termed them CT1 and CT2 respectively.   They also
used a third procedure in which a set of rotational energies, chosen
randomly from a given uniform distribution, was taken to correspond
to an initial j.   This technique appeared to be much less accurate
than CT1 and CT2 (Alper et.al. 1978), and we do not compare with it.

In figure 7.11 we present SCP, SLCP and CT weighted probabilities
bP(00→02;b) as function of the impact parameter at $E_i = 8000cm^{-1}$.   We
also include the corresponding CC results (DePristo and Alexander 1977).
At b>$5.5a_o$ (SLCP exact) the agreement between SCCP and CT results is
poor.   Quantitatively the CT probabilities are consistenly smaller
than the SCCP, with CT2 closer.   At close collisions the CT results
show the peak arising in the quantal results, although its value is
 very much smaller than the quantal.   It is interesting to point out
that CT1 and CT2 have differences between them of the order of the
probability.   Also interesting is to notice that the agreement
between SCCP and CC is better than for the (0,0)→(1,1) transition.

In figure 7.12 we show $bP(11 \rightarrow 02;b)$ at $E_i = 1000 cm^{-1}$. In the region where the probability maximum occurs the SCCP results are very much larger than CT, while at very large impact parameters ($b \gtrsim 18a_o$) the CT probabilities are larger than the SCCP results. Since at this large impact parameters the transition is classically forbidden it is clear that CT overestimates greatly the probability.

To draw any conclusions from the above comparison is difficult. The main difficulty is the inherent ambiguity of quantization in CT calculations. Despite the apparently small difference between (7.10a) and (7.10b) the quantitative difference between the predictions of CT1 and CT2 is large, and we shall see below that cross sections differing by more than a factor of two arise; this suggests that any quantization procedure used has inaccuracies of this order, which makes comparison difficult. Another problem is the neglect, by CT, of quantal interference and quantal tunnelling.

7.4.5   Comparison with Adiabatically Corrected Sudden calculations

It was predicted in section 7.2 that the time-dependent sudden approximation (TDSA) would break down and overestimate transition probabilities. This has been confirmed by Alexander and DePristo (1979) who, using a SL for the relative motion, have calculated TDSA probabilities and cross sections for HF-HF collisions at $E_i = 8000 cm^{-1}$; their results are very much larger than CC and CT results. In figure 7.13 we can see that, for the $(0,0) \rightarrow (1,1)$ transition the TDSA probabilities at $b \gtrsim 10 a_o$ are several times larger than those of SCCP. Clearly, from our earlier discussion (section 7.2), the TDSA becomes invalid because most of the contribution to the probability comes from impact parameters giving $Z \gg 1$.

To correct for the adiabatic character of the collision Alexander and DePristo (1979) introduced the "dephasing factor" $\exp(i\bar{w}t)$ into the sudden action, A^S, so that the trajectory integrals, I_{2m}, which determine A^S become

$$I_{2m}(\bar{w}) = \int_{-\infty}^{\infty} \left[R(t)\right]^{-3} \exp(i\bar{w}t)\, Y_{2m}^{*}(\theta,\varphi)\, dt \quad, \tag{7.12}$$

where $\hbar\bar{w}$ is an "effective" energy gap. This adiabatic correction to the TDSA has been termed adiabatically corrected sudden approximation (ACS). It is important to point out that this is inconsistent with the non-sudden classical action (5.14).

Clearly the above adiabatic correction makes the evaluation of the ACS action A^{ACS}, and the derivation of the ACS transition amplitude S^{ACS}, very much more difficult than in TDSA. To avoid this difficulty and as a first test of ACS Alexander and DePristo (1979) introduced an extra approximation neglecting $I_{20}(\bar{w})$ and $I_{2\pm1}(\bar{w})$:

$$I_{20}(\bar{w}) \equiv I_{2\pm1}(\bar{w}) = 0 \quad, \tag{7.13a}$$

$$I_{2\pm2}(\bar{w}) = \left(\frac{5}{6\pi}\right)^{1/2} \frac{1}{v b^2}\, R_2(\bar{w}b/v) \quad, \tag{7.13b}$$

where

$$R_2(x) = \frac{1}{2}\, x^2\, K_2(x) \quad, \tag{7.13c}$$

with $K_\nu(Z)$ the usual modified Bessel function (Abramowitz and Stegun 1964, p.374). Defining the scaled impact parameter (Alexander and DePristo 1979)

$$\bar{b} = b\left[R_2(\bar{w}b/v)\right]^{1/2} \quad, \tag{7.14}$$

and substituting this in (7.13) we have

$$I_{2\pm2}(\bar{w}) = \left(\frac{5}{6\pi}\right)^{1/2} \frac{1}{v\,\bar{b}^2} \qquad , \qquad (7.15)$$

i.e. $I_{2m}(\bar{w})$ depends on $\bar{b}$ in the same form as $I_{2m}(W=0)$ depends on b in TDSA.   Thus the ACS action satisfies

$$A^{ACS}(\bar{w},b) = A^{ACS}(\bar{w}=0,\bar{b}) \quad , \qquad (7.16)$$

so that the ACS degeneracy-averaged transition probability is

$$P^{ACS}(j_1 j_2 \to j_1' j_2' ; \bar{w} ; b) = \frac{[j_1'][j_2']}{4\pi^2}$$

$$\sum_{\ell\ell'}\left\{\begin{pmatrix} j_1 & \ell & j_1' \\ 0 & 0 & 0 \end{pmatrix}\begin{pmatrix} j_2 & \ell' & j_2' \\ 0 & 0 & 0 \end{pmatrix}\sum_m |a_{\ell\ell'm}|^2\right\} , \qquad (7.17)$$

where $a_{\ell\ell'm}$ is formally given by

$$a_{\ell\ell'm} = \int Y_{\ell m}^*(\theta_1,\varphi_1)\, Y_{\ell'm}^*(\theta_2,\varphi_2)\, e^{-iA^{ACS}/\hbar}\, d\theta_1\, d\varphi_1\, d\theta_2\, d\varphi_2 . \qquad (7.18)$$

To complete the above theoretical picture it is necessary to choose a physically realistic $\bar{w}$.   Alexander and DePristo (1979) based their choice on the dipole-dipole first-order selection rule, and consider a multiple quantum transition as occuring through a series of first-order jumps - which is predicted by CPT; see paragraph following eq. (6.2). Thus they define

$$\bar{w} = \frac{1}{\hbar}\left|[\langle\Delta E_{j_1}\rangle + \langle\Delta E_{j_2}\rangle]/2\right| , \qquad (7.19a)$$

where

$$\langle \Delta E_{j_i} \rangle = B_i \left[j_i'(j_i'+1) - j_i(j_i+1) \right] / |j_i' - j_i| , \quad i = 1, 2 . \tag{7.19b}$$

We notice that $\bar{W}$ is related to the W's determining the trajectory

integrals in the SCCP action A, as

$$\bar{W} = W_+ \quad \text{if} \quad \text{sgn}(\Delta j_1) = \text{sgn}(\Delta j_2) , \tag{7.20a}$$

$$\bar{W} = W_- \quad \text{if} \quad \text{sgn}(\Delta j_1) = -\text{sgn}(\Delta j_2) , \tag{7.20b}$$

where

$$W_\pm = W_1 \pm W_2 \tag{7.20c}$$

and W_i (i=1,2) is given by (5.21).

In figure 7.13 we compare TDSA and ACS weighted transition

probabilities (Alexander and DePristo 1979) with the corresponding

SCCP result for the $(0,0) \to (1,1)$ transition at $E_i = 8000 \text{cm}^{-1}$. The

effects of the adiabatic correction are: (1) to reduce the TDSA

transition probability at large impact parameters, where the collision

becomes very adiabatic, and (2) to shift to position of the maximum

of the TDSA probability to smaller impact parameters. These effects

are general for all transitions studied by Alexander and DePristo (1979).

Since ACS has no rigorous theoretical justification and

contains some subsidiary approximations (eqs. 7.13a and 7.19b), we

would not necessarily expect it to agree closely with SCCP.

Qualitatively its behaviour is consistent with our model of the collision

as the position of both probability maxima in figure 7.13 almost

coincide. Quantitatively however, the agreement is not good, and

despite the large correction introduced by ACS to the sudden approximation,

it still gives probabilities much larger than SCCP. This is because of

the large difference between A^{ACS} and A, as the ACS action is a function

only of W_+ or W_-, and it fails to describe the coupling properly.

There are some transitions for which A^{ACS} and A compare well and the

quantitative agreement between ACS and SCCP improves, for example the

single-molecule transition $(j_1,j_2) \to (j_1+S,J_2)$, where $|\overline{W}| = |W_+| = |W_-|$.

For multiple transitions however, good agreement is somewhat fortuitous

and it cannot justify the application of ACS. In general for rotor-

rotor collisions A^{ACS} is not well founded and it is unlikely that ACS

provides an accurate description of such collisions, in particular

those involving hydrides. For heavier molecules the TDSA becomes

less inaccurate and, consequently, the ACS modification could provide

a more accurate description of the collision.

7.5   The cross section

7.5.1   Introduction

In this section we discuss the SCCP results for the integral

dipole-dipole rotationally inelastic cross sections. Our detailed

discussion in sections 7.3 and 7.4 has examined the main physical

features of the transition, and in the first part of this section

(subsection 7.5.2) we show how these features are reflected in the

cross section. In the second part (subsection 7.5.3) we compare our

results with the other theories discussed in section 7.4, and the most

recent results of Alexander 1980.   As with all semi-classical
approximations in the SCCP cross sections, as given by (5.25), the
integration over impact parameters can allow the cancellation of
errors in different impact parameter ranges (Dickinson and Richards
1977), and the SCCP cross section can compare better with other theories
than the SCCP probabilities.

7.5.2   The SCCP cross section

Cross sections for the $(5,1) \to (2,2)$, $(2,2) \to (3,3)$, $(0,0) \to (1,1)$
and $(4,2) \to (3,3)$ transitions at energies $E_i = 4000$, 6000, 8000 and 10000cm^{-1}
in HF-HF collisions are shown in table 7.3   The corresponding $|\Delta E_j|$
for each of the above transitions are 20B, 12B, 4B and 2B respectively,
where B=20.939cm^{-1} (Herzberg 1950,p.536).   The energy $E_i = 4000$cm^{-1}
is greater than the energy E_{orb} above which no orbiting takes place
and thus quantum barrier penetration effects cannot occur.

From our discussion in subsections 7.3.3 and 7.3.4 we expect
that, for a given transition, the cross section increases when the
energy E_i increases; as the collision becomes sudden the cross section
reaches a maximum and then decreases.   Of the results in table 7.3
only for the $(4,2) \to (3,3)$ transition does the cross section show this
form.   For the $(0,0) \to (1,1)$ and $(2,2) \to (3,3)$ transitions the cross
section increases with the energy, although we have shown that the
former starts decreasing at $E_i = 20000$cm^{-1}; since the $(4,2) \to (3,3)$
transition has the smallest $|\Delta E_j|$ the collision becomes sudden at E_i
smaller than for the other two transitions.   The cross section
$\sigma(51 \to 22; E_i)$ on the other hand, shows a different form, as it
decreases at the lower energies, to start increasing at $E_i = 10000$cm^{-1}.
The transition at these energies is very short-ranged and most of
the cross section arises from the strong-coupling region.   It is

likely that for these strong, short-range, collisions the SCCP cross
section decreases as the energy E_i increases because the transition
p robability is statistical: an energy increase allows more transitions
and the probability becomes smaller.   As the energy is further
increased the contribution from distant collisions becomes more
significant, since they are less adiabatic, and the cross section will
recover its usual dependence on E_i.

For a given energy E_i we can see that, as predicted in sub-
section 7.3.4, the cross section is a decreasing function of $|\Delta E_j|$
Note that for the energies and transitions presented in table 7.3, when
$|\Delta E_j|$ decreases from 20B to 2Bthe cross section increases by almost
two orders of magnitude.

In table 7.4 we present cross sections for the $(0,0) \rightarrow (2,2)$,
$(0,0) \rightarrow (1,1)$ and the resonant $(0,1) \rightarrow (1,0)$ transitions at different
energies in HCl-HCl collisions.   We notice that the resonant cross
section is two orders of magnitude larger than the other rotationally
inelastic cross sections, and as predicted at the end of sub-section
7.3.4, is a decreasing function of the energy.   The dependence of
the other cross sections on E_i and $|\Delta E_j|$ is consistent with the
behaviour discussed above.

7.5.3   Comparison with other theories

Figure 7.14 shows SCCP, PRS, CC, CT and ACS rotationally
inelastic cross sections as functions of the initial relative speed
for the $(0,0) \rightarrow (1,1)$ transition in HF-HF collisions.   At the lower
speeds, where PRS is reliable, we notice that the PRS cross sections
are much larger than all the other theories results, except CT2, which
is more than 3.5 times the CT1 result.   At the higher speeds, where

CC is reliable ($v_i \gtrsim 14/10^4$ a.u.), the SCCP consistently underestimates the cross section.   Note that at the highest speed ACS and CT2 overestimate the cross section about as much as SCCP underestimates it.   No PRS results are available at these larger speeds.   Since SLCP and SCCP results differ only slightly for $E_i > 1000cm^{-1}$ ($v_i > 7/10^{-4}$ a.u.) our conclusions could not be significantly altered if the correct spherical potential were employed.

Also in figure 7.14 we compare SCCP and PRS cross sections for the $(0,0) \rightarrow (1,1)$ transition in HCl-HCl collisions, and for the $(1,1) \rightarrow (0,2)$ transition in HF-HF collisions.   While for HCl-HCl the picture is similar to the one shown for the same transition in HF-HF the agreement for the $(1,1) \rightarrow (0,2)$ transition is good.   This suggests that SCCP underestimates particularly the $(0,0) \rightarrow (1,1)$ transition. The underestimation arises from the SCCP description of the coupling, as the dependence of the action A on W_- indicates that SCCP considers a de-excitation in one of the molecules, which is unphysical for this directly coupled $(0,0) \rightarrow (1,1)$ transition.   This is basically a consequence of the use of CPT for such low initial quantum numbers, and it would be expected to be much less important for higher initial j values.

The most recent CC results (Alexander 1980), as shown in figure 7.14, indicates that at large speeds the SCCP and CC results for the $(0,0) \rightarrow (1,1)$ transition have started to converge.   At the highest energy for which CC results are available ($12500cm^{-1}$; not shown here) SCCP results are about 20% below the CC values.   This shows that at this very high energies the dependence of the action A on W_- becomes less important in determining the cross section, i.e. a first-

order description of the collision becomes more accurate. Note that for the lower speeds the CC cross sections obtained using a B3 basis are smaller than those obtained with a basis B5=$\{$B3;(1,3);(3,3);(0,4);(2,4)$\}$, although normally the cross section would be expected to decrease as the basis size is increased.

In table 7.5 we compare the SCCP and SLCP cross sections with CC, CT, ACS and TDSA results for the $(0,0)\rightarrow(2,2)$, $(0,0)\rightarrow(0,2)$, $(0,0)\rightarrow(1,1)$ and $(1,1)\rightarrow(0,2)$ transitions at $E_i=500$, 1000 and 8000cm^{-1}. The CC results at $E_i=8000$cm^{-1} contain two entries, corresponding to the results of Alexander (1980) using a B4 and B5 basis; they will be referred to as CC4 and CC5 respectively. The CC results at $E_i=500$ and 1000cm^{-1} are those of DePristo and Alexander (1977). For the $(1,1)\rightarrow(0,2)$ transition the CC, ACS and TDSA calculations were performed at a total energy of E=1000 and 8000cm^{-1}. To compare with the CC results we need the symmetrized correspondence principle cross section $\sigma^s(j_1 j_2 \rightarrow j_1' j_2')$:

$$\sigma^s(j_1 j_2 \rightarrow j_1' j_2') \cong \xi(j_1' j_2')\left\{\sigma(j_1 j_2 \rightarrow j_1' j_2') + \sigma(j_1 j_2 \rightarrow j_2' j_1')\right\}, \qquad (7.21a)$$

where

$$\xi(j_1' j_2') = \begin{array}{ll} 1/2 & \text{if} \quad j_1' = j_2' \\ 1 & \text{if} \quad j_1' \neq j_2' \end{array}, \qquad (7.21b)$$

and $\sigma(j_1 j_2 \rightarrow j_1' j_2')$ is the unsymmetrized cross section (5.25). The cross section (7.21a) refers to a collision in which two molecules with initial levels (j_1,j_2) are finally in levels (j_1',j_2'), either the transition $j_1 \rightarrow j_1', j_2 \rightarrow j_2'$ or the transition $j_1 \rightarrow j_2'$, $j_2 \rightarrow j_1'$ having occurred. For the special case $j_1 = j_2, j_1' \neq j_2'$ we have

$$\sigma^s(j_1 j_2 \rightarrow j_1' j_2') = 2\sigma(j_1 j_2 \rightarrow j_1' j_2') \quad .$$

(7.22)

Below we discuss each of the transitions in turn.

A) The $(0,0) \rightarrow (2,2)$ transition

At $E_i = 500$ and 1000cm^{-1} the transition is short-ranged and both
the SCCP and SLCP cross sections are unreliable.   On the other hand,
the CC results are far from being converged (DePristo and Alexander
1977) and the CT cross sections are not reliable at these low energies
(Alper et.al., 1978).   So, no definitive conclusion on the accuracy
of the correspondence principle methods is attempted.

At $E_i = 8000 \text{cm}^{-1}$ the agreement between SCCP and SLCP is within
3%.   This suggests that, at this energy, the use of a stronger spherical
potential does not introduce large errors in the SCCP cross section.
The agreement between SCCP and CC4 is within 30%, while the CC5 cross
section is more than twice the SCCP result.   The large increase of
the CC cross section when the basis is enlarged suggests that the CC
results are not converged.   The CT cross sections are also larger
than SCCP's, CT2 being the larger.   As expected the ACS cross section
is larger than the SCCP, CC and CT results, despite it is less than
a half of the TDSA result.   Again the uncertain convergence of the CC
makes it difficult to reach a definitive conclusion, although the
comparison suggests the SCCP cross section may be somewhat underestimated.

B) The $(0,0) \rightarrow (0,2)$ transition

At $E_i = 500$ and 1000cm^{-1} we have a similar situation as for the
$(0,0) \rightarrow (2,2)$ transition and no definitive conclusion is attempted.

At $E_i=8000cm^{-1}$ the SCCP and SLCP give the largest cross sections and agree with CC5 within 40% and 42% respectively. The CT gives small cross sections, and CT2 is more than two times larger than CT1. The ASC and TDSA are smaller than expected, and agree with CC5 within 30% and 12% respectively. We point out that, in contrast to SCCP, the CT, ACS and TDSA cross sections do not appear to be properly symmetrized, and it is likely that their values in table 7.5 should be doubled. So, ACS and SCCP would be in good agreement, which is what we would expect for this single-molecule transition (see sub-section 7.4.5). As for the (0,0)→(2,2) transition the convergence of CC is uncertain and it is difficult to reach a conclusion. However, for this transition, we would expect the error in the rotor-rotor SCCP cross section being similar to the SCCP error for atom-rotor collisions.

C)   The (0,0)→(1,1) transition

From the results shown in figure 7.14 we have already shown that the SCCP cross sections for this transition are likely to be underestimated. The results shown in figure 7.14 also suggest that at $E_i=500$ and $1000cm^{-1}$ only CT2 gives accurate results, and not only SCCP but also CC and CT1 underestimate the cross section.

At $E_i=8000cm^{-1}$ CC4 and CC5 results agree within 1%. As before CC5 gives a cross section larger than CC4, but as the difference is smaller than the error of the calculations the CC cross section can be considered as fully converged. The SCCP agrees with SLCP within 6% and differs from the CC result in a 45%.

D)   The (1,1)→(0,2) transition

This is the less adiabatic and longer-ranged transition studied here and we expect our approach to become more accurate at the lower energies.

At $E_i = 1000 \text{cm}^{-1}$ SCCP and SLCP cross sections agree within 15%, and are several times larger than the CC result. The CT1 and CT2 results agree within 34% and are also larger than the CC cross section. As in the $(0,0) \rightarrow (0,2)$ transition the CT results should be symmetrized, which makes the CT1 and CT2 cross sections become closer to the correspondence principle cross sections. These results suggest that the CC cross section is greatly underestimated. This underestimation was first suggested by DePristo and Alexander (1977), and explicitly pointed out by Hashi et.al. (1978).

At $E_i = 8000 \text{cm}^{-1}$ the SCCP and SLCP cross sections agree within 6%. They are larger than the CC results, and the SCCP cross section agrees with the CC4 and CC5 results within 7% and 11% respectively. The ACS and TDSA cross sections are smaller than the CC results, which suggests that, as in the $(0,0)$ $(0,2)$ transition, these cross sections are not properly symmetrized and should be doubled. In this case TDSA overestimates the cross section, while the agreement between the ACS and CC results is excellent, with a difference of less than 2%.

From the above discussion, we infer that much work is still needed to establish the accuracy of the various methods, especially for adiabatic collisions. It is clear from table 7.5 that the ambiguities inherent in the CT description (see subsection 7.4.4) can introduce errors of the order of magnitude of the cross sections. It is also clear that while TDSA overestimates the cross section, the "ad hoc" character of the corrections introduced by ACS still makes its accuracy uncertain. On the other hand, the inaccuracies of the SCCP depend on the validity of CPT. At the smaller incident energies, the transitions discussed above cannot be considered favourable cases for the application of CPT, and errors should be expected in the SCCP

cross sections.   A better accuracy should be obtained at larger
incident and rotational energies.   Among the SCCP results presented
in table 7.5 we consider the cross section for the $(1,1) \rightarrow (0,2)$
transition at $E_i = 8000 cm^{-1}$ the more accurate, and, despite the use of
a stronger potential, the error is less than 15%.

7.6   Concluding remarks

We have applied the Strong Coupling Correspondence Principle
to rotational excitation in collisions between two diatomic molecules.
Only the dipole-dipole anisotropic potential is considered, and it is
shown that in this case the transition amplitude is obtained in closed
form.   Transition probabilities and cross sections for HF-HF and HCl-HCl
collisions were calculated, and where possible, compared with other
theories.

As in earlier work the SCCP shows that a first-order description
of the collision is inadequate, as it grossly overestimates the
transition probabilities.   It was also shown that this overestimation
is mainly because of the adiabatic nature of the collisions studied
here.   This large adiabaticity is characteristic of collisions involving
hydrides, and for heavier molecules the first-order theories are
expected to become more adequate to describe long distance collisions -
at the same incident energies considered here.

Comparison with quantal results shows that satisfactory
agreement is obtained for some transitions, although it is difficult
to reach a definitive conclusion on the validity and accuracy of the
SCCP results.   However, the comparison is encouraging as for many of
the transitions studied here the application of SCCP is not formally
justified.   For transitions between excited levels CC becomes increasingly

impractical while the other approximations discussed here become no more accurate.[1]   At present, collisions between heavier rotors at higher incident and rotational energies appear beyond the grasp of the current quantal and classical theories.   In this case, the SCCP becomes of great value in the calculation of rotationally inelastic cross sections for such collisions.

More work needs to be done to determine the range of applicability of SCCP.   The latest results of Alexander (1980) provide a first benchmark for assessing the validity of our approach.   Calculations to compare with Alexander's results are currently in progress (Richards, private communication).   A future publication will also contain reviewed calculations of the SCCP cross sections discussed here, using the correct spherical symmetric potential.   As in atom-rotor collisions the use of SCCP for low rotational quantum numbers has not been theoretically justified.   This still remains a challenge.

(1) On the other hand SCCP can be expected to be more accurate.

CAPTIONS TO TABLES 7.1 - 7.5

Table 7.1: Adiabaticity parameter $\bar{Z}$, as defined by (7.2). The parameters correspond to the $(1,1) \rightarrow (0,2)$ transition in HF-HF collisions at $E_i = 8000 cm^{-1}$.
$\bar{Z}_1, \bar{Z}_2$ and $\bar{Z}_3$ correspond to values of $\bar{Z}$ calculated using speeds (1), (2) and (3), respectively, as defined by (7.3).

Table 7.2: Maximum change in the quantum number $j=j_1+j_2$ as defined by (7.7), and highest level $(j_1, j_2=j_1)$ satisfying max (Δj) which is classically accessible. The parameters correspond to the $(0,0) \rightarrow (1,1)$ transition in HF-HF collisions.

Table 7.3: SCCP rotationally inelastic cross sections in $\overset{\circ}{A}{}^2$, for different transitions and energies in HF-HF collisions.

Table 7.4: SCCP rotationally inelastic cross sections in $\overset{\circ}{A}{}^2$, for different transitions and energies in HCl-HCl collisions.

Table 7.5: Rotationally inelastic cross sections in $\overset{\circ}{A}{}^2$.
CC at 500 and 1000cm^{-1} from DePristo and Alexander (1977).
CC at 8000cm^{-1} from Alexander (1980).
CT from Alper et.al. (1978).
ACS and TDSA from Alexander and DePristo (1979).
a: the first and second entry were obtained using a B4 and B5 bases, respectively.
b: the first and second entry correspond to CT1 and CT2 respectively.
c: obtained using B4 basis at J=40,60,80 and B3 at all other J values.
SCCP and SLCP values for $(0,0) \rightarrow (2,2)$ and $(1,1) \rightarrow (0,2)$ correspond to symmetrized cross sections as given by (7.22).

Table 7.1

b	0	2	4	6	8	10	12
$\bar{Z}1$	0.493	0.496	0.506	0.530	0.645	0.947	1.147
$\bar{Z}2$		1.291	0.671	0.489	0.544	0.939	1.147
$\bar{Z}3$	0.987	0.717	0.577	0.509	0.590	0.943	1.147

Table 7.2

b/a_0	$E(cm^{-1})$	max $(\triangle j)$	(j_1, j_2)
6	500	28.1	(14,14)
8		4.8	(2,2)
10		0.87	(0,0)
12		0.086	(0,0)
6	1000	50.8	(25,25)
8		14.2	(7,7)
10		4.1	(2,2)
12		1.2	(0,0)
6	8000	38.4	(19,19)
8		21.0	(10,10)
10		12.2	(6,6)
12		7.4	(3,3)
14		4.5	(2,2)

Table 7.3

$\sigma(j_1 j_2 \to j_1' j_2')$ $(\mathring{A}^2)$	$E_i (cm^{-1})$			
	4000	6000	8000	10000
$(51 \to 22)$	7.9-1	7.5-1	6.1-1	7.9-1
$(22 \to 33)$	7.4-1	7.9-1	1.2	1.8
$(00 \to 11)$	14.3	23.8	31.0	38.5
$(42 \to 33)$	45.1	53.8	53.0	50.7

Table 7.4

$\sigma(j_1 j_2 \to j_1' j_2')$ $(\mathring{A}^2)$	$E_i (cm^{-1})$		
	20.171	500	1000
$(00 \to 22)$	8.5-1	1.3	-
$(00 \to 11)$	9.6-1	2.2	-
$(01 \to 10)$	245.9	156.8	98.6

Table 7.5

Transition	$E_i(cm^{-1})$	SCCP	SLCP	CC	CT	ACS	TDSA
$(0,0) \rightarrow (2,2)$	500	1.3	2.5-2	3.3-7	0.0[b] / 2.2-2	-	-
	1000	1.8	1.5-1	5.7-5	4.9-2 / 1.5-1	-	-
	8000	4.8	4.9	6.6[a] / 11.3	8.4 / 10.0	15.8	35.7
$(0,0) \rightarrow (0,2)$	500	3.4	-11.6	1.1-4	0.0 / 0.0	-	-
	1000	3.0	4.0	6.3-2[c]	0.0 / 0.0	-	-
	8000	15.8	16.5	7.7 / 9.6	1.7 / 3.9	7.1	10.8
$(0,0) \rightarrow (1,1)$	500	1.1	4.2-1	2.9-1	4.2-1 / 1.9	-	-
	1000	1.3	1.6	2.6[c]	1.9 / 7.1	-	-
	8000	31.0	32.9	56.7 / 57.2	130.0 / 72.0	85.3	207.0
$(1,1) \rightarrow (0,2)$	500	13.8	25.3	-	-	-	-
	1000	32.8	38.0	3.5	8.7	-	-
	8000	62.4	65.3	58.5 / 55.6	-	28.2	45.6

CAPTIONS TO FIGURES 7.1 - 7.14

Figure 7.1: Strong Coupling Correspondence Principle (SCCP) transition probabilities as a function of the impact parameter, b, for the $(0,0) \to (1,1)$ transition in HF-HF collisions at $E_i = 1000 cm^{-1}$. Along the top we show the classical distance of closest approach,

A: using curved trajectory determined by $\bar{C}_{oo}(R)$.

B: using a Straight Line (SL) trajectory.

C: First-order Correspondence principle (FOCP).

Figure 7.2: As in 7.1 for HF-HF collisions at $E_i = 8000 cm^{-1}$.

Figure 7.3: SCCP transition probabilities as a function of the impact parameter, b, for the $(1,1) \to (0,2)$ transition in HF-HF collisions,

A: $E_i = 1000 cm^{-1}$.

B: $E_i = 8000 cm^{-1}$.

Figure 7.4: As 7.3 for the resonant $(0,1) \to (1,0)$ transition

A: $E_i = 1000 cm^{-1}$.

B: $E_i = 8000 cm^{-1}$.

Figure 7.5: SCCP transition probabilities as a function of the impact parameter, b, for HF-HF collisions at $E_i = 8000 cm^{-1}$,

A: $(0,0) \to (1,1)$ transition.

B: $(1,1) \to (0,2)$ transition.

Figure 7.6: As 7.5

A: $(0,0) \to (0,2)$ transition.

B: $(2,2) \to (3,3)$ transition.

C: $(5,1) \to (2,2)$ transition.

Figure 7.7: As 7.5

    A: resonant $(0,1) \rightarrow (1,0)$ transition

    B: resonant $(2,1) \rightarrow (1,2)$ transition

Figure 7.8: Weighted correspondnece principle transition probabilities

b P(b) as a function of the impact parameter b, for the

$(0,0) \rightarrow (1,1)$ transition in HF-HF collisions at $E_i = 1000 \text{cm}^{-1}$.

CC and BA from DePristo and Alexander (1977),

•: FOCP,

Along the top we show the rotational quantum number $J \simeq b/k$

where k is the wave number. The values of J indicated

in the graph correspond to the actual values at which the

CC calculations were performed. The right hand scale shows

$(2J+1)P_J^{CC}$. Abbreviations are explained in the text.

Figure 7.9: As 7.8 for $E_i = 8000 \text{cm}^{-1}$.

Figure 7.10: Transition probabilities for the $(0,0) \rightarrow (1,1)$ transition

at $E_i = 500 \text{cm}^{-1}$ for HCl-HCl collisions, as a function of the

reduced impact parameter p.

The broken curve shows the first-order approximation of the

PRS results, and • corresponds to the full PRS results

(Hashi et.al., 1978).

At the top of the graph we show the corresponding impact

parameters in a_o.

Abbreviations are explained in the text.

Figure 7.11: Weighted transition probabilities as a function of the impact

parameter b, for the $(0,0) \rightarrow (0,2)$ transition at $E_i = 8000 \text{cm}^{-1}$

for HF-HF collisions.

Abbreviations are explained in the text.

CT1 and CT2 from Alper et.al. (1978)

CC from DePristo and Alexander (1977).

Figure 7.12: As 7.11 for the $(1,1) \rightarrow (0,2)$ transition at $E_i = 1000 cm^{-1}$.

Figure 7.13: Weighted transition probabilities as a function of the impact
parameter b, for the $(0,0) \rightarrow (1,1)$ transition at $E_i = 8000 cm^{-1}$
for HF-HF collisions.

Abbreviations are explained in the text.

ACS and TDSA from Alexander and DePristo (1979).

Figure 7.14: Rotational inelastic cross sections (a.u) as a function
of the initial relative velocity v.

●   SCCP for HCl-HCl collisions.

o   SCCP for HF-HF collisions.

▲   PRS for HCl-HCl collisions, Hashi et.al. (1978).

△   PRS for HF-HF collisions, Hashi et.al. (1978).

□   CC for HF-HF collisions using basis B3, Alexander (1980),
(Note: values at $v \cong 5$ and $7x10^4$ (a.u) from DePristo
and Alexander 1977).

▨   CC for HF-HF collisions using basis B5, Alexander (1980),
(Note: value at $v = 7x10^4$(a.u) from DePristo and
Alexander (1977) using basis B4).

θ   CT1, Alder et.al. (1978)

Ω   CT2, Alder et.al. (1978).

■   ACS, Alexander and DePristo (1979).

——   correspond to the $(0,0) \rightarrow (1,1)$ transition

---   correspond to the $(1,1) \rightarrow (0,2)$ transition.

| Basis	Rotor levels
B3	$(0,0)$; $(1,1)$; $(0,2)$; $(2,2)$
B4	$(0,0)$; $(1,1)$; $(0,2)$; $(2,2)$; $(1,3)$; $(3,3)$
B5	$(0,0)$; $(1,1)$; $(0,2)$; $(2,2)$; $(1,3)$; $(3,3)$; $(0,4)$; $(2,4)$

Figure 7.1
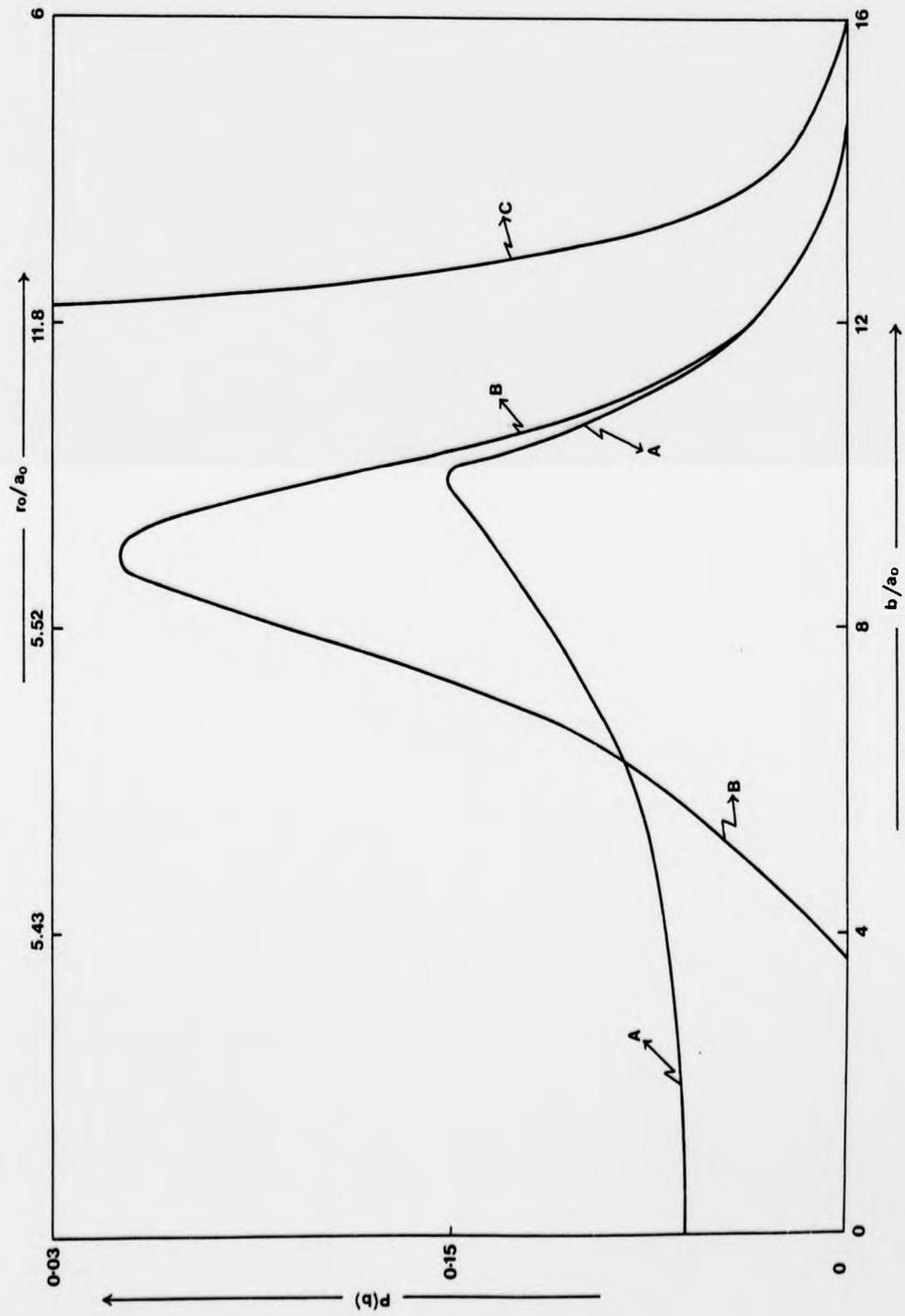
**Figure 7.2**
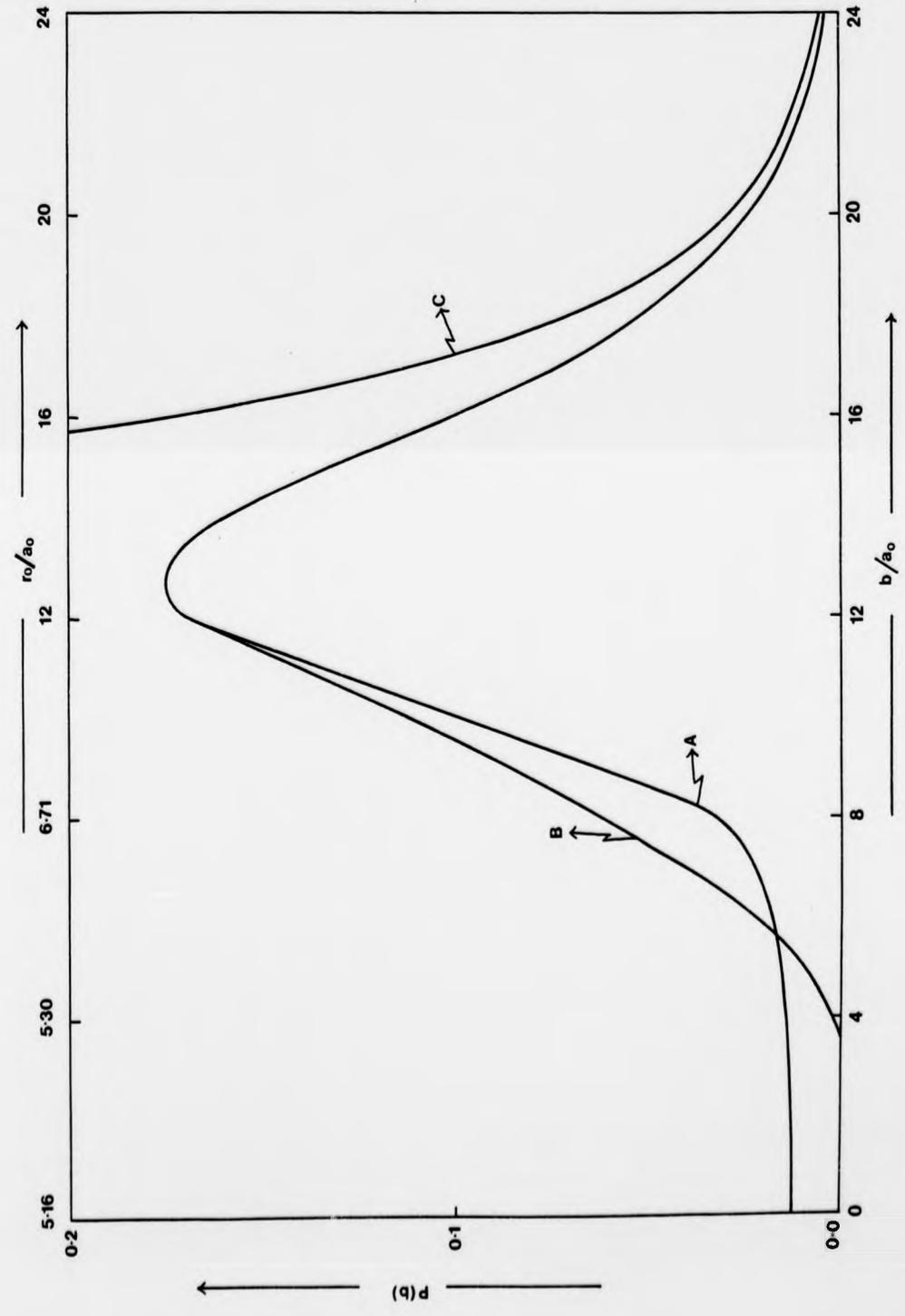
Figure 7.3
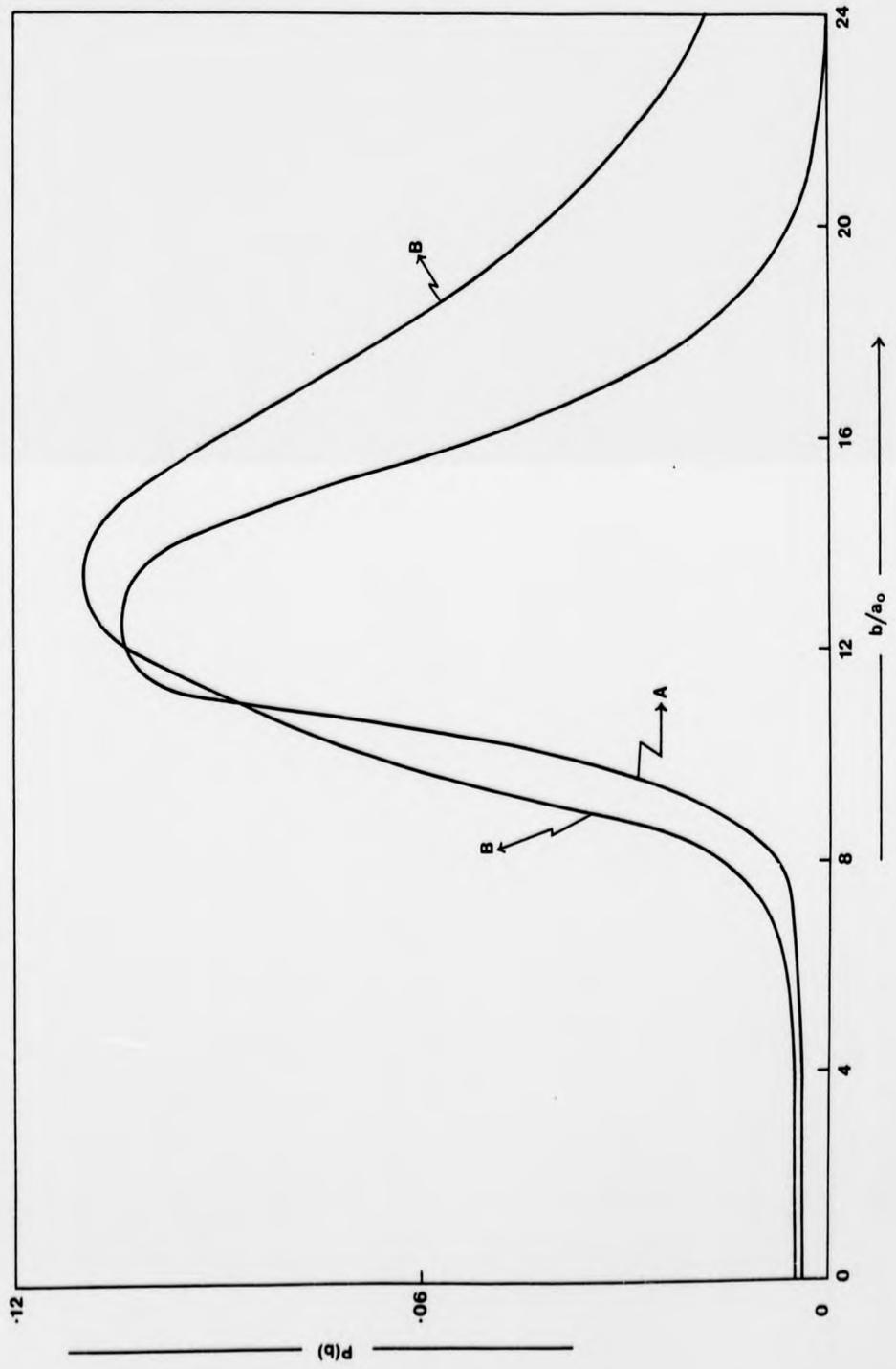
Figure 7.4
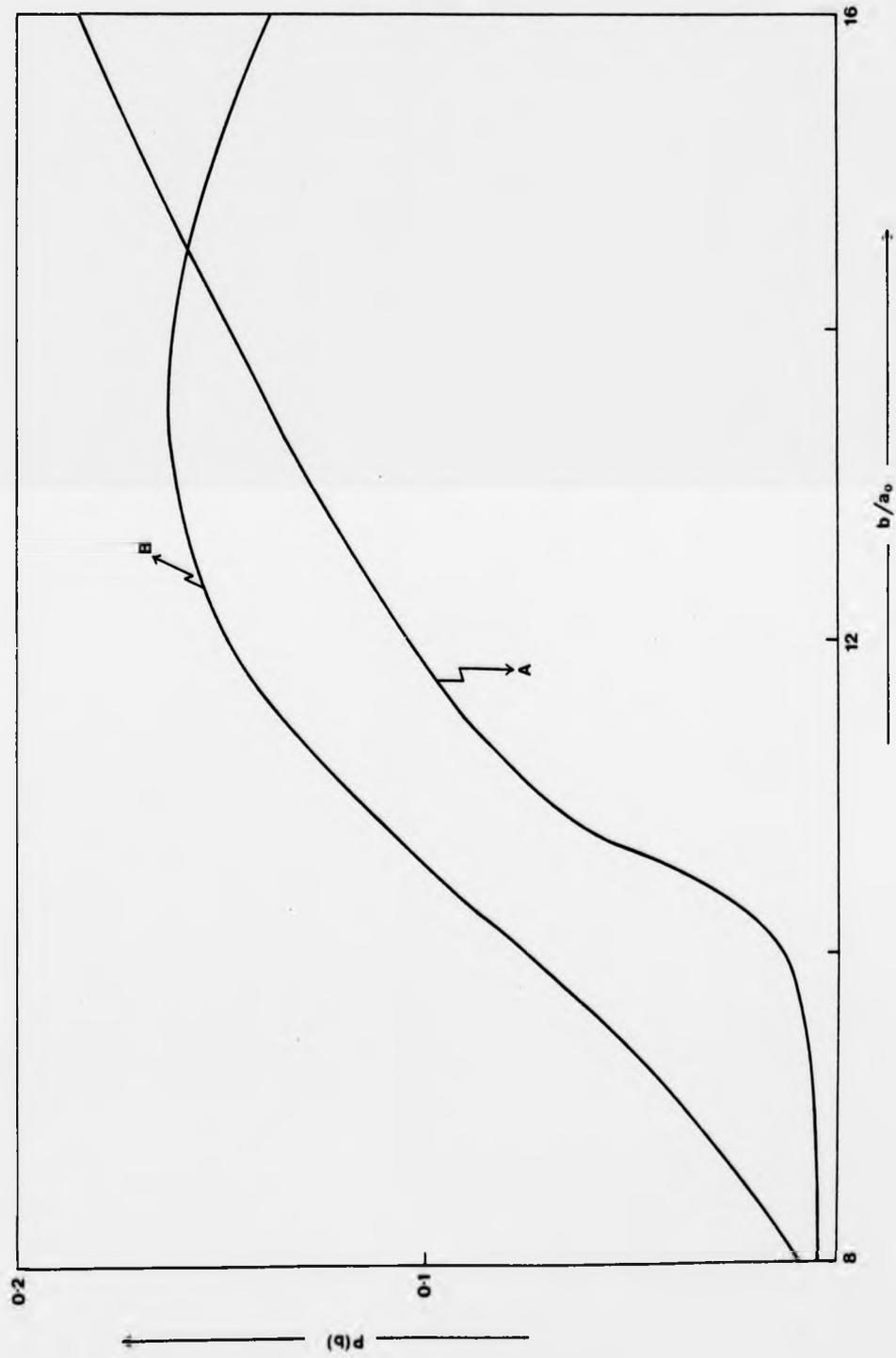
Figure 7.5
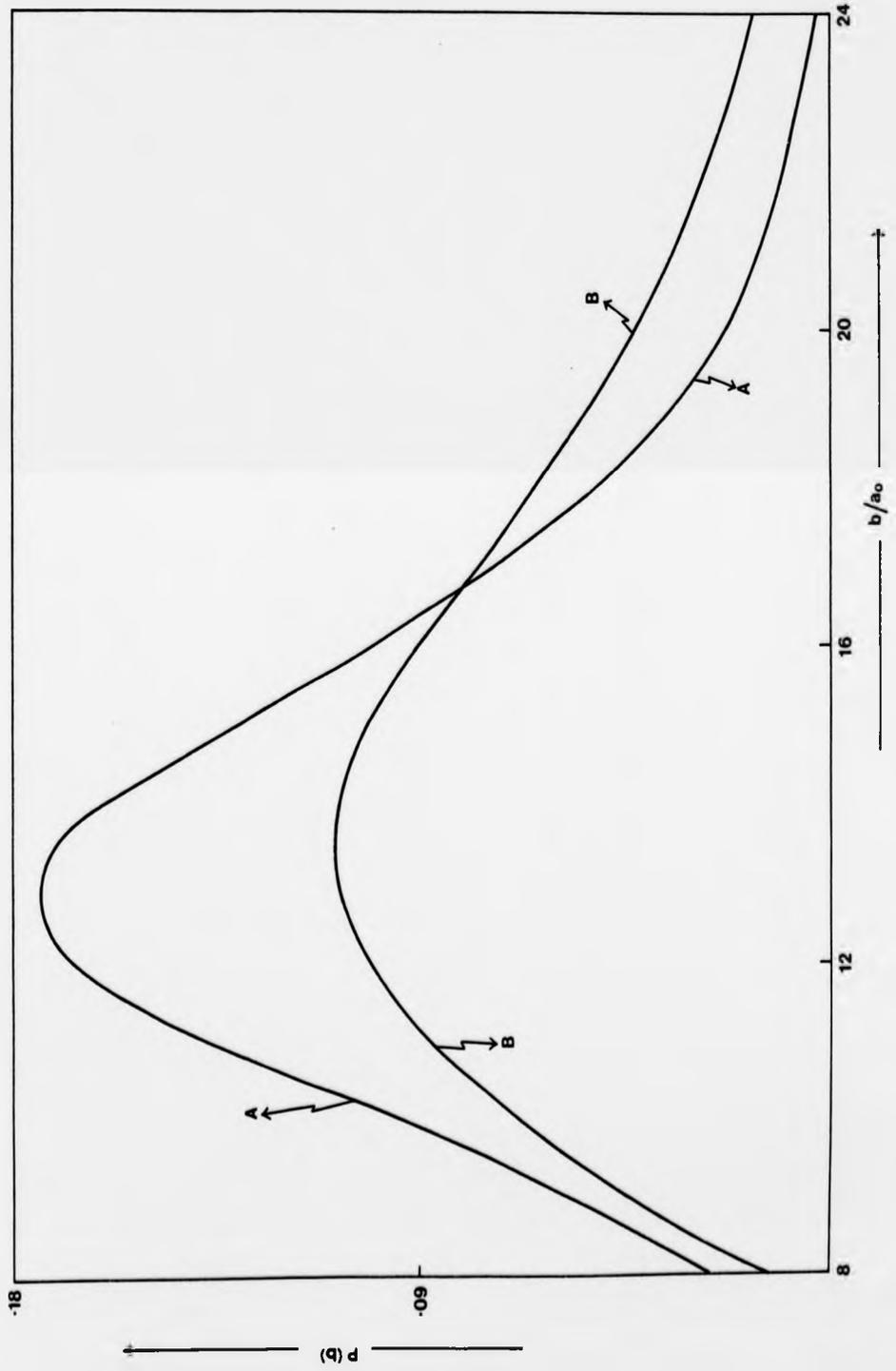
Figure 7.6
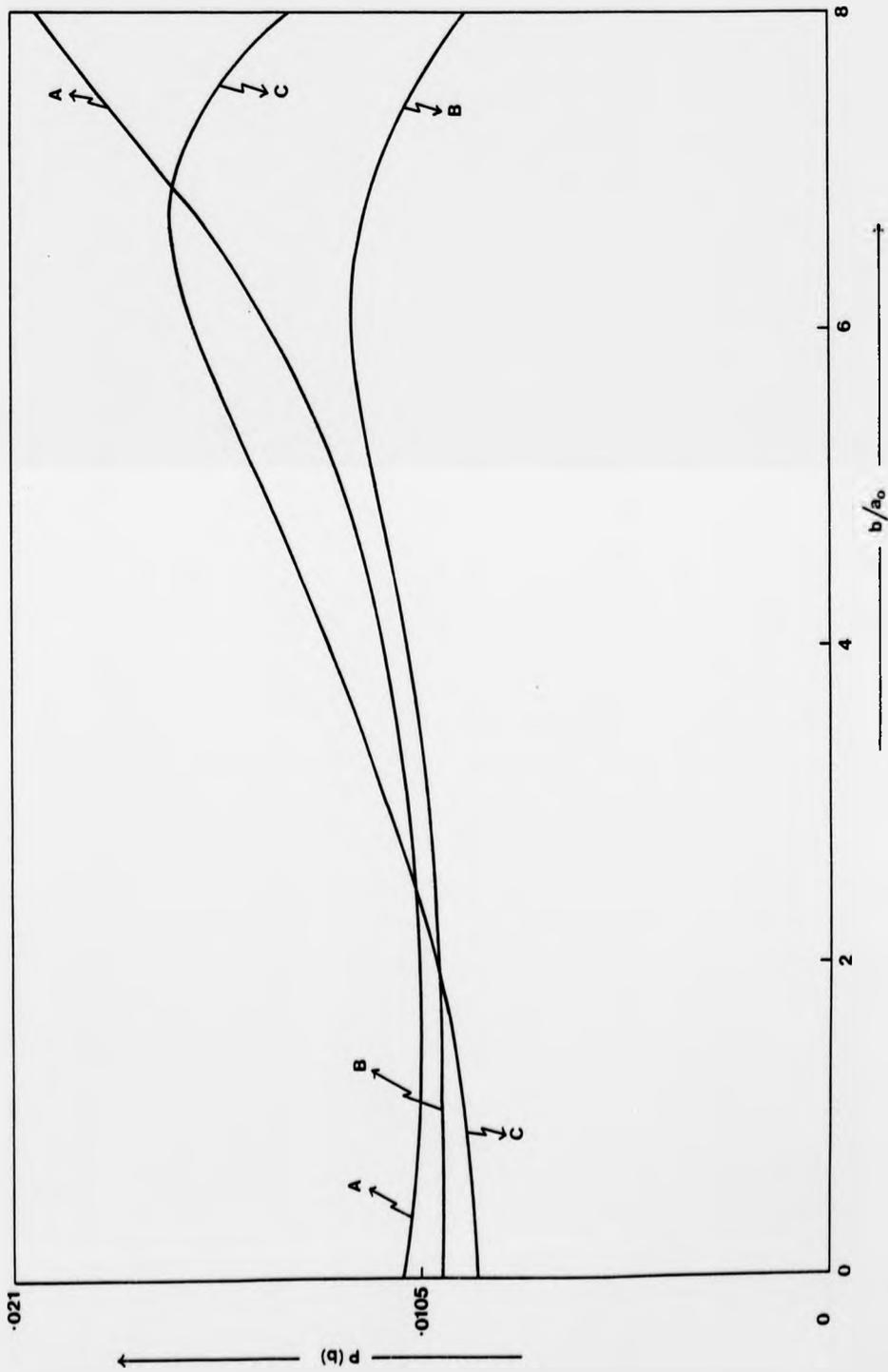
Figure 7.7
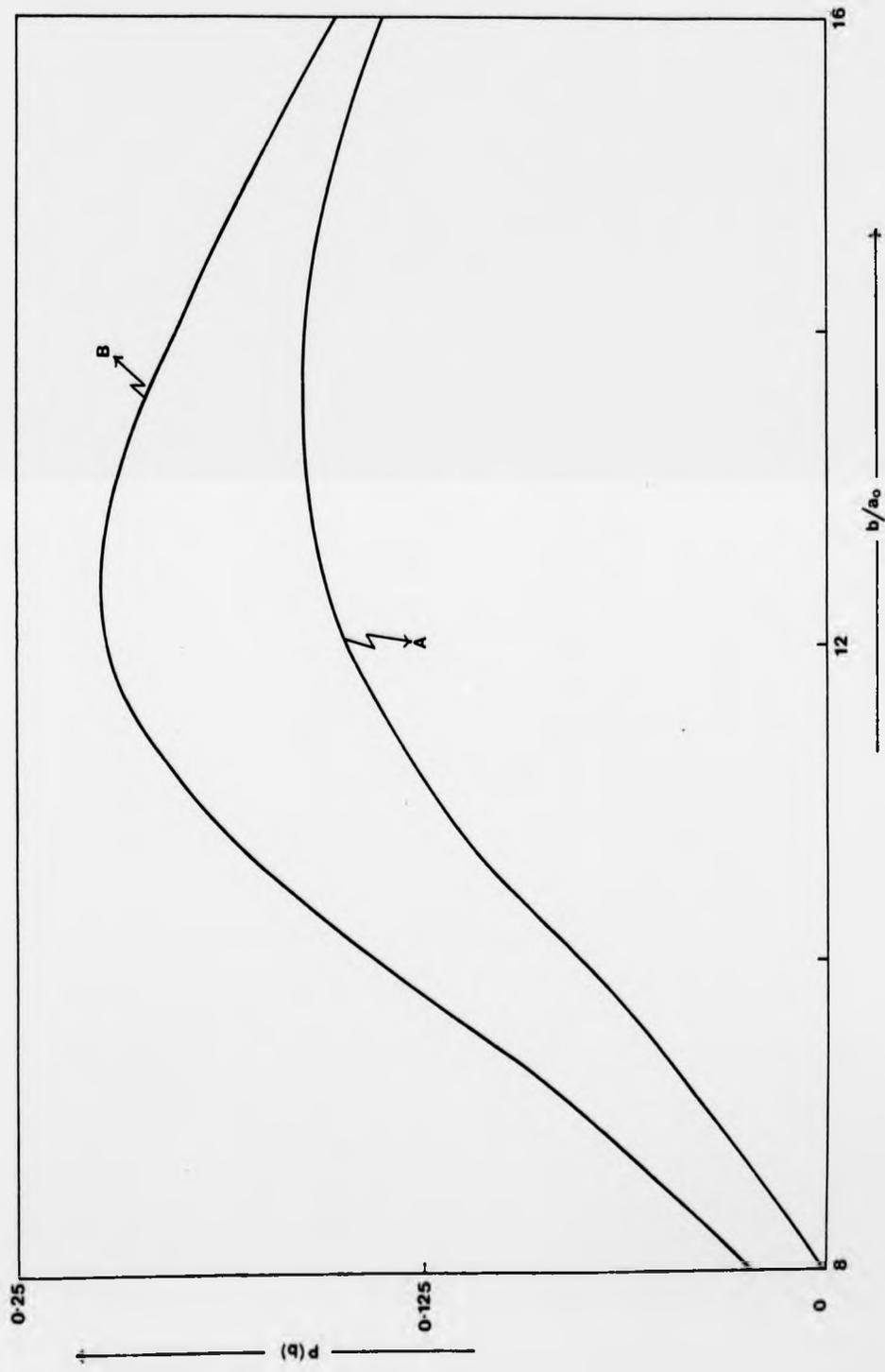
Figure 7.8
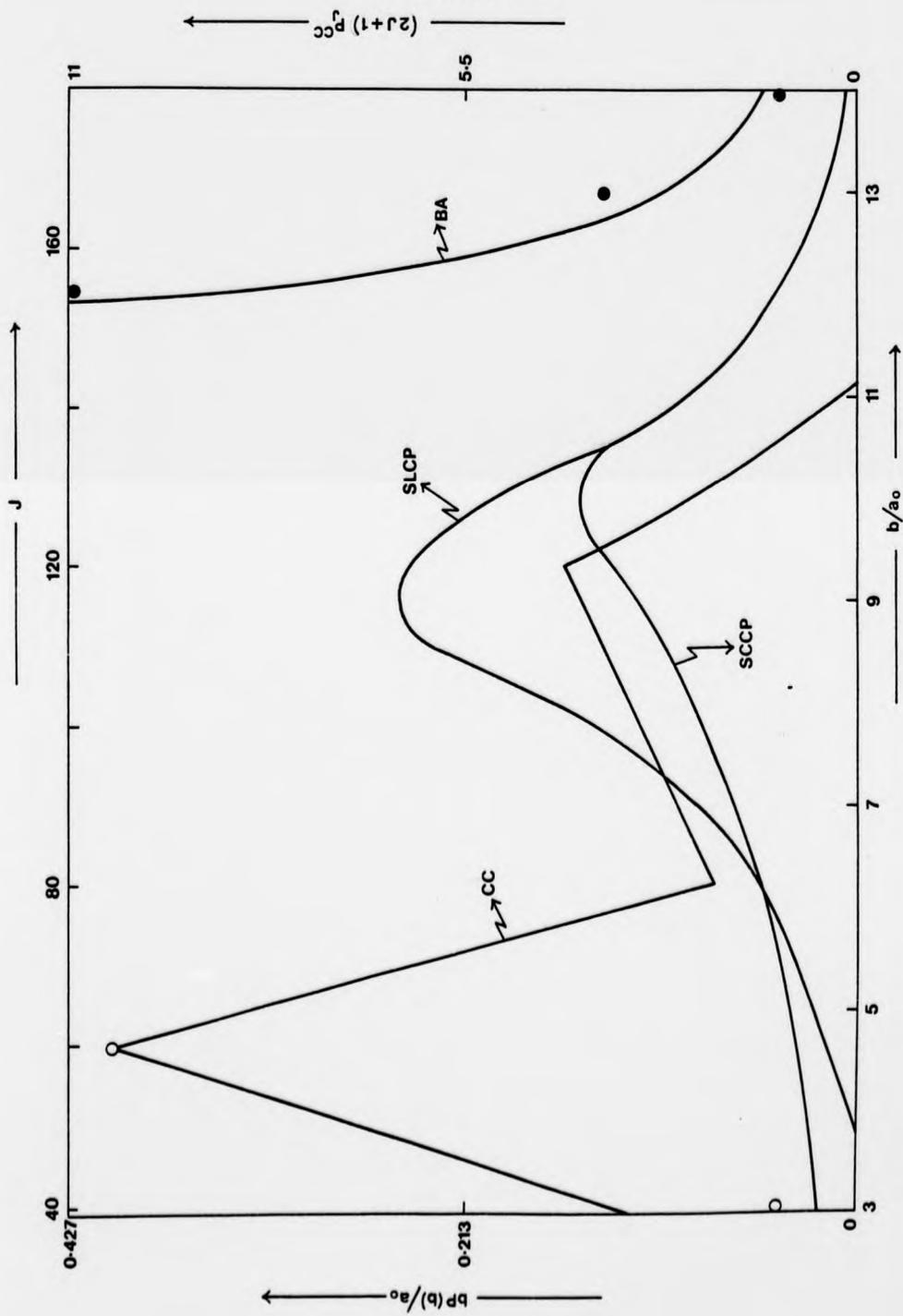
Figure 7.9
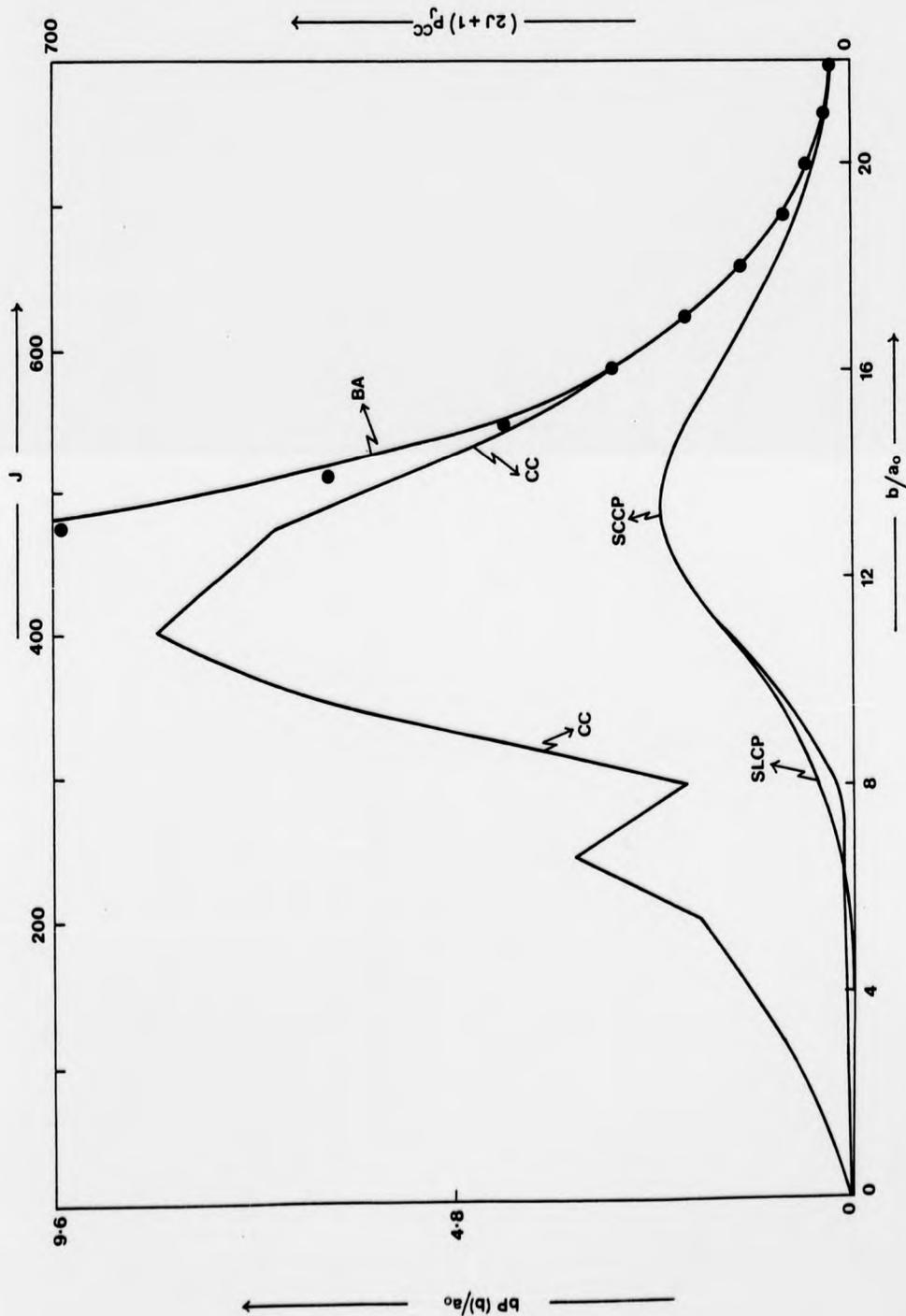
Figure 7.10
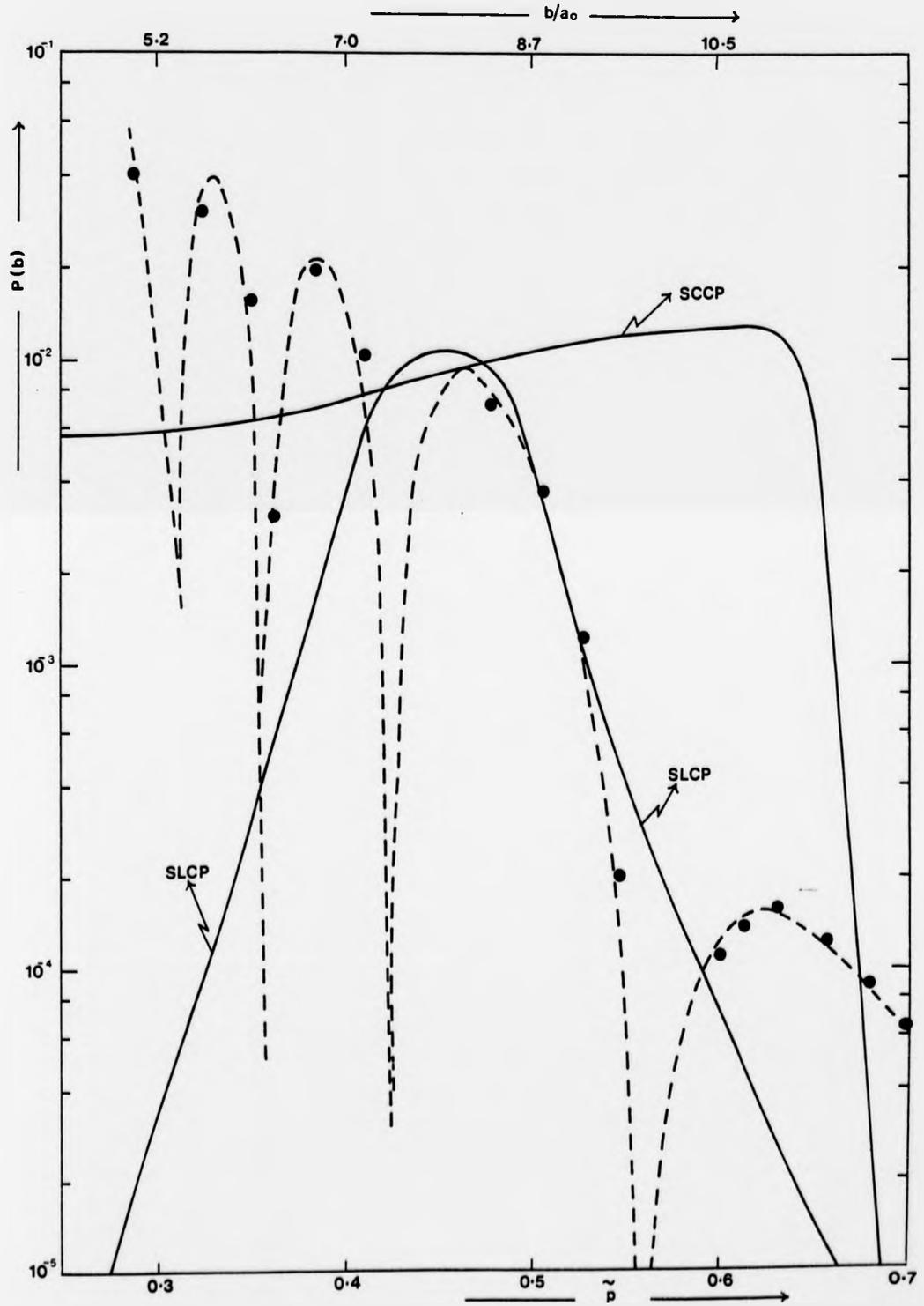
Figure 7.11
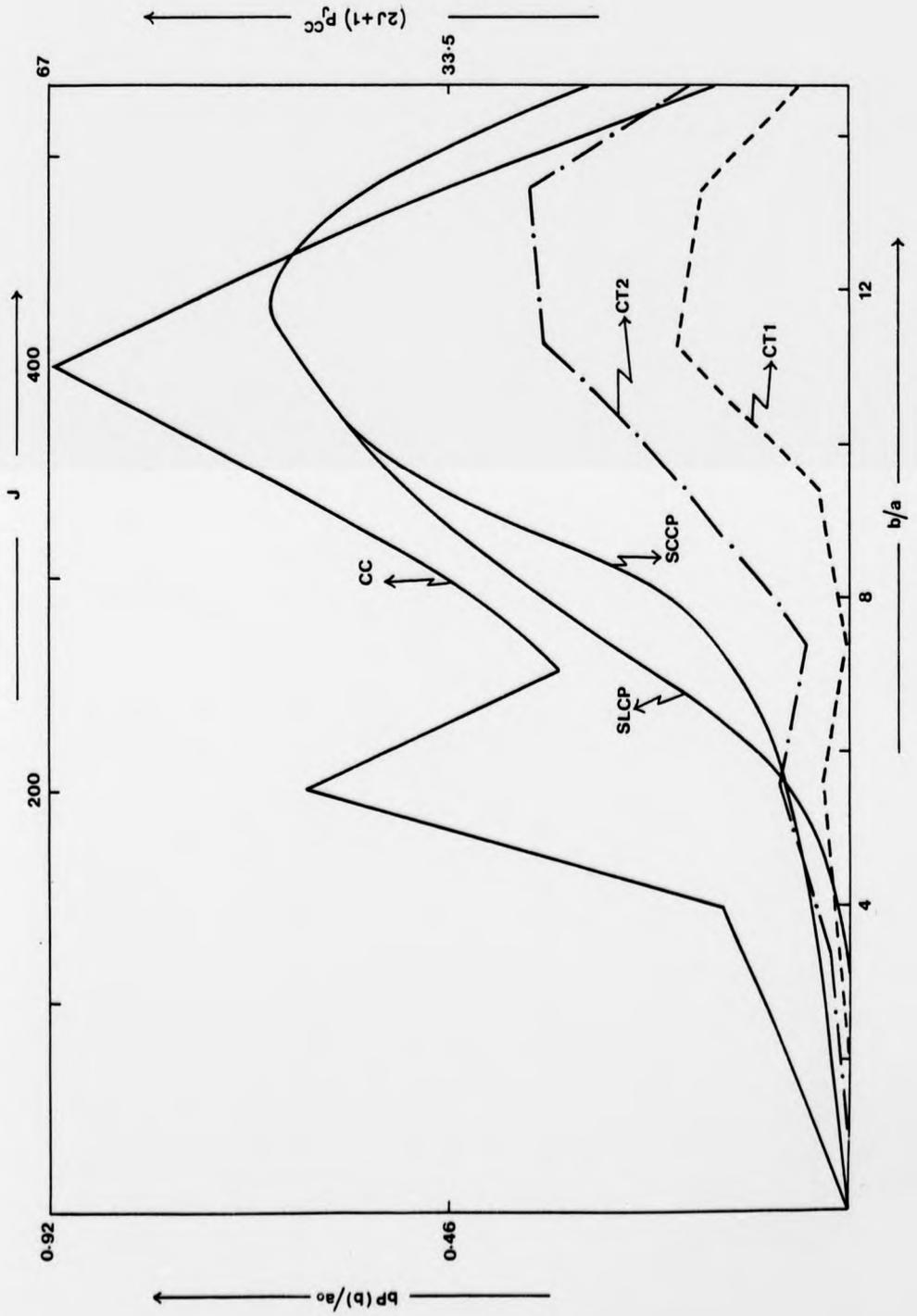
Figure 7.12
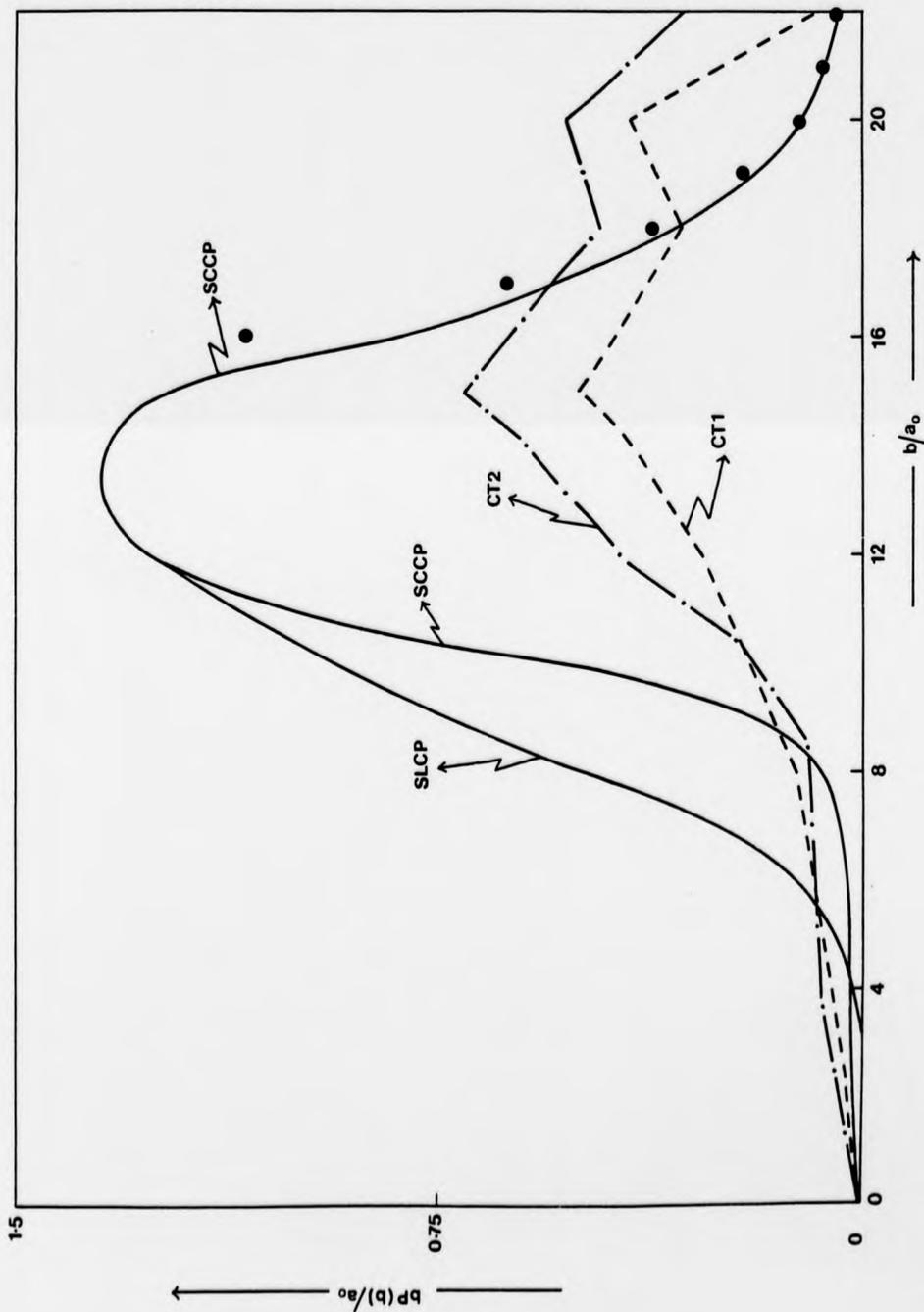
Figure 7.13
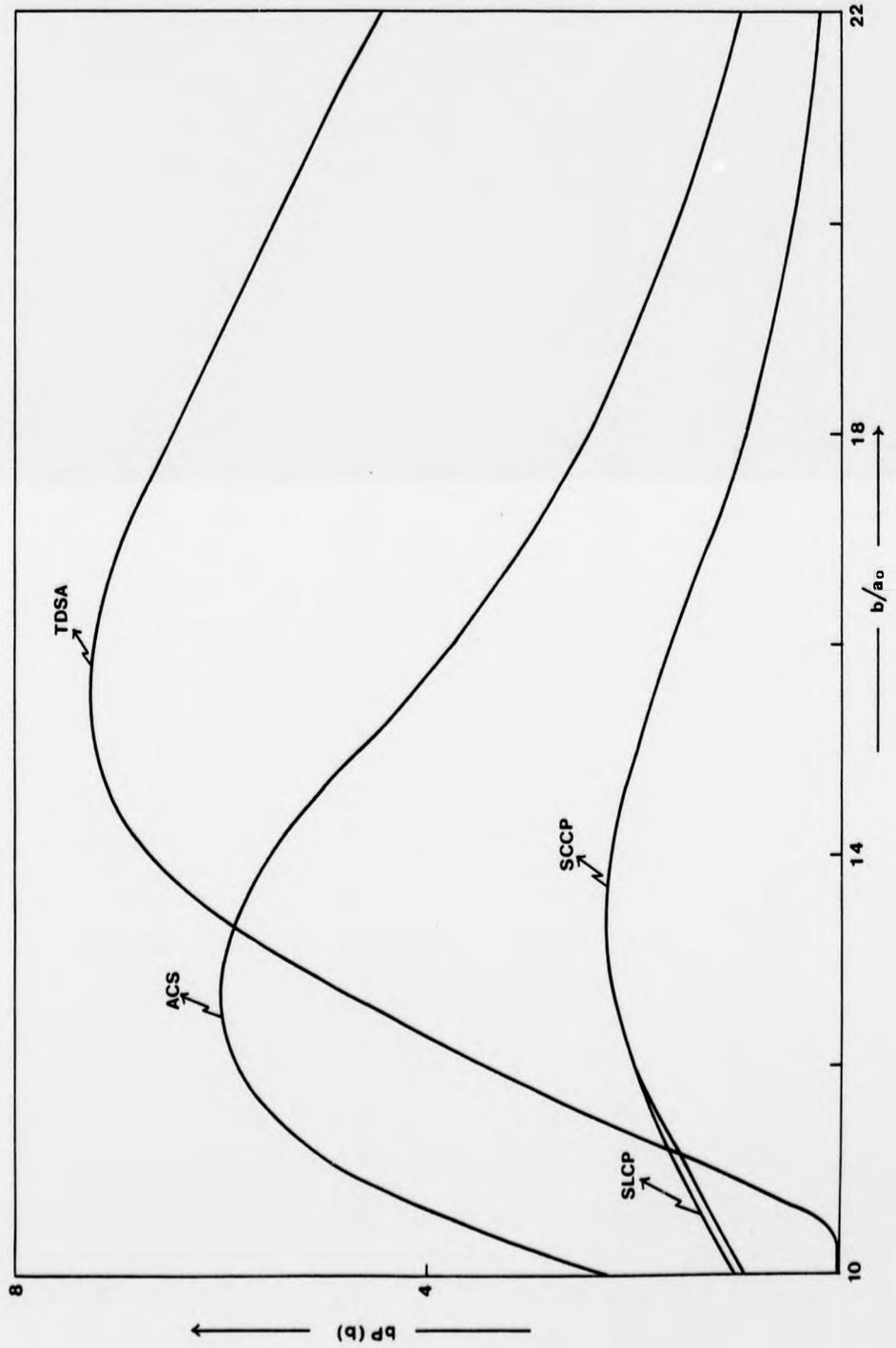
Figure 7.14
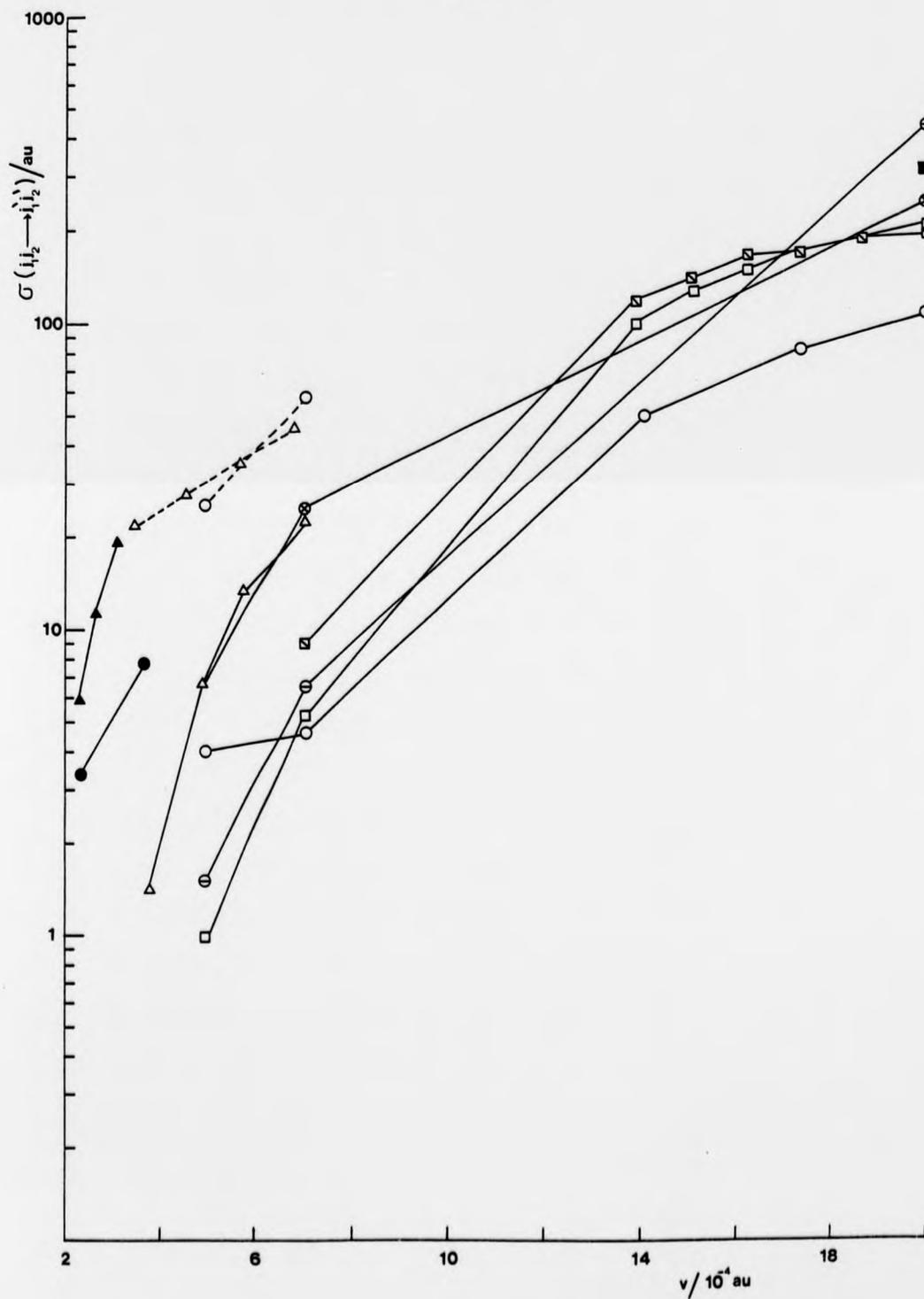
CHAPTER 8

CORRESPONDENCE PRINCIPLE EQUIVALENTS OF SOME

DECOUPLING APPROXIMATIONS

8.1   Introduction

Although in the SCCP the computational effort is largely
independent of the excitation of the rotors, the multidimensional
character of the average in eq. (6.12) can make the calculation of
rotationally inelastic cross sections very expensive.   Consequently,
it is important to look for further approximations, which maintain
the basic SCCP assumptions while easing the computational effort.
This is normally done by making, within the framework of SCCP,
approximations similar to those made in deriving some of the current
decoupling approximations (Dickinson and Richards 1977, 1978).

In this chapter we investigate three different approximations
as applied to the problem studied in this work: the body-fixed
correspondence principle (BFCP) and M-conserving correspondence
principle (MCCP) of Dickinson and Richards (1977 and 1978 respectively),
and the decoupled L-dominant correspondence principle (DLDCP).   The
latter makes approximations similar to the decoupled L-dominant
approximation (DLD) of DePristo and Alexander (1976), and it has been
developed in this work for the first time.

In sections 8.2, 8.3 and 8.4 we present the BFCP, MCCP and
DLDCP approximations respectively.   In section 8.5 we discuss
briefly modifications to the numerical techniques employed for the
full problem.   Our results and discussion are presented in section 8.6.

8.2 The Body-fixed correspondence principle

8.2.1 Theory

To obtain the body-fixed correspondence principle (BFCP) we derive the SCCP equations in a rotating frame of reference OX'Y'Z', with origin O in the centre of mass of molecule 1, and in which the OZ' axis always lies along $\underline{R}$, the vector joining the centre of masses of the colliding molecules (Dickinson and Richards 1977). The orientation of the i-th rotor in the OX'Y'Z' frame is described by the Euler angles α_i', β_i', γ_i' (Edmonds 1960, p.7), which have the same significance as in section 4.2. Since OZ'Y'Z' is rotating, Coriolis and centrifugal terms arise. The BFCP retains only the centrifugal terms for the relative motion. The approximate body-fixed Hamiltonian H^{BF}, is now written as:

$$H^{BF} = H_{o1} + H_{o2} + P_R^2/2\mu + E b^2/R^2 + V(R, \Omega_1', \Omega_2') \, , \qquad (8.1)$$

where H_{oi} is the Hamiltonian for a free rotor, P_R is the momentum of the relative motion, and $\Omega_i' = (\theta_i, \beta_i', \alpha_i')$ with $\theta_i = \gamma_i' + W_i t$. The interaction potential $V(R, \Omega_1', \Omega_2')$ in OX'Y'Z' is expanded as

$$V(R, \Omega_1', \Omega_2') = \sum_{\lambda, \lambda_2} \left[\frac{2\lambda_{12}+1}{4\pi} \right]^{1/2} \bar{C}_{\lambda, \lambda_2}(R) \sum_{\substack{\mu_1, \nu_1 \\ \mu_2, \nu_2}} (\lambda_1 \mu_1 \lambda_2 \mu_2 / \lambda_1 \lambda_2 \lambda_{12} \, 0)$$

$$Y_{\lambda, \nu_1}(\pi/2, \pi/2) \, D_{\nu_1 \mu_1}^{(\lambda_1)}(\Omega_1') \, Y_{\lambda_2 \nu_2}(\pi/2, \pi/2) \, D_{\nu_2 \mu_2}^{(\lambda_2)}(\Omega_2') \, . \quad (8.2)$$

From the properties of the Clebsh-Gordan coefficients (Edmonds 1960, p.38), one sees that $\mu_1 = -\mu_2$, and from the definition of the matrix elements $D_{\nu\mu}^{(\lambda)}$ (Edmonds 1960, p.55), one sees that the potential (8.2) depends only on the difference $\alpha_-' = \alpha_1' - \alpha_2'$.

Proceeding as in section 5.2 we obtain the BFCP change of the action A^{BF}.

$$A^{BF}(\Omega_1', \Omega_2') = \sum_{\lambda_1, \lambda_2} \sum_{\mu_1, \nu_1, \nu_2} \left(\frac{2\lambda_{12}+1}{4\pi}\right)^{1/2} N_{\lambda_1 \nu_1} N_{\lambda_2 \nu_2} (\lambda_1 \mu_1 \lambda_2 - \mu_1 / \lambda_1 \lambda_2 \lambda_{12} 0)$$

$$\mathcal{D}^{(\lambda_1)}_{\nu_1 \mu_1}(\gamma_1', \beta_1', \underline{\alpha}') \; \mathcal{D}^{(\lambda_2)}_{\nu_2 - \mu_1}(\gamma_2', \beta_2', 0) \; V^{(\lambda_{12})}_{\nu_1 \nu_2 0}(E, b) \; , \tag{8.3}$$

where

$$V^{\lambda_{12}}_{\nu_1 \nu_2 0} = \frac{2}{\hbar} \int_0^\infty dt \; \bar{C}_{\lambda_1 \lambda_2}(R) \cos\left[(\nu_1 W_1 + \nu_2 W_2)t\right] \; . \tag{8.4}$$

The action (8.3) yields the BFCP approximation to the transition amplitude from levels (j_1, j_2) to levels (j_1', j_2'):

$$S^{BFCP}_{(j_1 j_2, j_1' j_2')} = \frac{1}{4\pi^2} \int_0^{2\pi} d\gamma_1' d\gamma_2' \; exp\left[i\left(\Delta j_1 \gamma_1' + \Delta j_2 \gamma_2' - A^{BF}\right)\right] \; , \tag{8.5}$$

and the degeneracy-averaged BFCP transition probability is

$$P^{BFCP}_{(j_1 j_2 \to j_1' j_2')} = \left(\frac{E_i}{E_f}\right)^{1/2} \mathcal{C}(j_1 j_2 j_1' j_2') \frac{1}{8\pi} \int_0^{3\pi} d\alpha' \int_{-1}^{1} d(\cos\beta_1') \int_{-1}^{1} d(\cos\beta_2') \left|S^{BFCP}\right|^2 . \tag{8.6}$$

Clearly, the BFCP approximation yields two major simplifications. Firstly, the average over orientation (8.6) is now three-dimensional rather than four-dimensional, and secondly, the number of $V^{(\lambda_{12})}_{\nu_1 \nu_2 \mu_1 \mu_2}$ trajectory integrals is greatly reduced. Each trajectory integral is itself simpler to calculate since only the relative radial motion is required.

8.2.2   The body-fixed correspondence principle error

The BFCP action (8.3) can also be obtained by making the approximation $V^{(\lambda_{12})}_{\nu_1 \nu_2 \mu_1 \mu_2} = V^{(\lambda_{12})}_{\nu_1 \nu_2 00}$ in the space fixed action (5.14), and then making $\mu_1 = -\mu_2$, $\bar{\theta} = 0$. Thus one sees directly that the BFCP is valid when the $V^{(\lambda_{12})}_{\nu_1 \nu_2 \mu_1 \mu_2}$ integrals are independent

of $\mu_{12} = \mu_1 + \mu_2$. Consequently, we define the relative percentage error:

$$E^{BF}_{\nu_1 \nu_2 \mu_{12}}(w,b) = 100\left[1 - V^{(\lambda_{12})}_{\nu_1 \nu_2 \mu_1 \mu_2}(w,b)\Big/V^{(\lambda_{12})}_{\nu_1 \nu_2 0}(w,b)\right] ,\qquad (8.7)$$

where $w = \nu_1 w_1 + \nu_2 w_2$. Equation (8.7) is a measure of the BFCP error. For b=0 the BFCP principle is exact since $\gamma'(t) = 0$ (see eq. (5.11)), but as the impact parameter increases so does the body-fixed error (8.7). Thus the BFCP approximation is expected to be accurate for short range collisions.

8.2.3 The body-fixed correspondence principle equations for the dipole-dipole interaction

Proceeding as in section 6.2 we obtain for A^{BF}

$$A^{BF}(\gamma_1', \beta_1', \gamma_2', \beta_2', \alpha') = R_+ \sin(\gamma_+' + \delta_+') + R_- \sin(\gamma_-' + \delta_-') ,\qquad (8.8a)$$

with

$$R_+ = \frac{6}{32\pi}\left(\frac{15}{2\pi}\right)^{1/2} P \quad , \qquad R_- = \frac{6}{32\pi}\left(\frac{15}{2\pi}\right)^{1/2} P' \quad ,\qquad (8.8b)$$

$$\delta_+' = -\tan^{-1}\left(\frac{\cos\theta}{\sin\theta}\right) \quad , \qquad \delta_-' = \tan^{-1}\left(\frac{\cos\theta'}{\sin\theta'}\right) \quad ,\qquad (8.8c)$$

where P and P' are defined by equation (6.6) and γ_+' , γ_-' are the primed equivalents of (6.3). The BFCP transition amplitude, S^{BFCP}, is

$$S^{BFCP}(j_1 j_2, j_1' j_2') = e^{-i(n_+ \delta_+' + n_- \delta_-')} J_{n_+}(R_+) J_{n_-}(R_-) ,\qquad (8.9)$$

where n_+ and n_- are given by (6.10). From the integer condition for n_+, n_- one sees that BFCP gives the same selection rules (6.11a). The BFCP transition probability (8.6) must be evaluated numerically.

As in the SCCP, the first-order BFCP probability, P^{FOBF}, is obtained in closed form:

$$P^{FOBF}_{(j_1 j_2 \to j_1' j_2' ; b)} = \left(\frac{E_i}{E_f}\right)^{1/2} \mathcal{C}_{(j_1 j_2 j_1' j_2')} \frac{5}{256\, \hbar^3} \left(V_{s_1 s_2 0}\right)^2 ; \quad |s_1| = |s_2| = 1 , \quad (8.10)$$

where $s_i = \Delta j_i$.

For a resonant transition, the straight-line approximation is valid for large impact parameters. In this case we obtain $E^{BF}_{\pm 2}(o,b) = 66.6$, and the relation between the full and body-fixed correspondence principle first-order probabilities is obtained using (6.17) and (6.18):

$$P^{FOBF}_{(j_1 j_2 \to j_2 j_1 ; b)} = 3\, P^{FOCP}_{(j_1 j_2 \to j_2 j_1 ; b)} . \quad (8.11)$$

Thus for a resonant transition in the straight-line limit the BFCP is significantly in error. The relation (8.11) is also valid for sudden collisions at large impact parameters.

8.3   The M-conserving correspondence principle

8.3.1   Theory

Let us consider the collision being described in a space-fixed frame $O\overline{XYZ}$, with origin O in the centre of mass of the molecule 1, the $O\overline{Z}$ axis lying in the plane of the orbit followed by molecule 2 and passing through the point of closest approach. The $\overline{X}$ and $\overline{Y}$ axes are arbitrary. The M-conserving approximation (MC) of Dickinson and Richards (1978) is obtained when the coupling is described in this frame, under the condition that the $\overline{Z}$ component of the rotational angular momentum, M, is conserved. The basis of MC was suggested by Takayanagi (1959), and it has been applied in the TDCC framework to atom-molecule (Saha and Guha 1975), and molecule-molecule (Bhattacharyya and Saha 1978) collisions.

For convenience we express the change of the action in $\overline{OXYZ}$ in terms of the variables $\delta_+, \delta_-, \alpha_+, \alpha_-$ as given by (6.3). Proceeding as in section 5.2 we obtain

$$A(\beta_1, \beta_2, \delta_+, \delta_-, \alpha_+, \alpha_-) = \sum_{\lambda_1, \lambda_2} \sum_{\substack{\mu_1 \ \nu_1 \\ \mu_2 \ \nu_2}} N_{\lambda_1 \nu_1} N_{\lambda_2 \nu_2} \left(\lambda_1 \mu_1 \lambda_2 \mu_2 / \lambda_1 \lambda_2 \lambda_{12} \mu_{12} \right)$$

$$\times \left\{ e^{i \frac{\delta_+}{2} (\nu_1 + \nu_2)} e^{i \frac{\delta_-}{2} (\nu_2 - \nu_1)} d_{\nu_1 \mu_1}^{(\lambda_1)}(\beta_1) d_{\nu_2 \mu_2}^{(\lambda_2)}(\beta_2) e^{i \frac{\alpha_+}{2} (\mu_1 + \mu_2)} e^{i \frac{\alpha_-}{2} (\mu_1 - \mu_2)} \right\} \overline{V}_{\nu_1 \nu_2 \mu_{12}}^{(\lambda_{12})} \quad (8.12)$$

where

$$\overline{V}_{\nu_1 \nu_2 \mu_{12}}^{(\lambda_{12})} = \frac{1}{\hbar} \int_{-\infty}^{\infty} dt \ \overline{C}_{\lambda_1 \lambda_2}(R) \ Y_{\lambda_{12} \mu_{12}}^{*}(\overline{\theta}, \varphi) \ e^{iwt} \quad , \quad (8.13)$$

with $w = \nu_1 w_1 + \nu_2 w_2$ and $\mu_{12} = \mu_1 + \mu_2$. Taking the trajectory in the $\overline{OXZ}$ plane along the $\overline{OX}$ axis the trajectory integral (8.13) is written as

$$\overline{V}_{\nu_1 \nu_2 \mu_{12}}^{(\lambda_{12})} = \frac{1}{\hbar} \int_{-\infty}^{0} dt \ \overline{C}_{\lambda_1 \lambda_2}(R) \ Y_{\lambda_{12} \mu_{12}}^{*}(\theta, \pi) e^{iwt} + \frac{1}{\hbar} \int_{0}^{\infty} dt \ \overline{C}_{\lambda_1 \lambda_2}(R) \ Y_{\lambda_{12} \mu_{12}}(\theta, 0) e^{iw't} . \quad (8.14)$$

If $\hbar m_i$ is the $\overline{Z}$ component of the i-th rotor angular momentum, we can express the M-conserving condition

$$\Delta M = m_1' - m_1 + m_2' - m_2 \equiv \Delta m_1 + \Delta m_2 = 0 \quad . \quad (8.15)$$

Using (5.15) we obtain for the change in the $\overline{Z}$ component of the rotational angular momentum, $\hbar \Delta M$, due to the collision

$$\hbar \Delta M = -2 \frac{\partial A}{\partial \alpha_+} \quad . \quad (8.16)$$

Thus to obtain an approximation in which M is conserved we must approximate the action (8.13) by an action independent of α_+, A^{MC}

$$A^{MC}(\beta_1, \beta_2, \delta_1, \delta_2, \alpha_-) = \sum_{\lambda_1, \lambda_2} \sum_{\mu_1 \nu_1 \nu_2} N_{\lambda_1 \nu_1} N_{\lambda_2 \nu_2} \left(\lambda_1 \mu_1 \lambda_2 -\mu_1 / \lambda_1 \lambda_2 \lambda_{12} 0 \right)$$

$$\left(\frac{2\lambda_{12}+1}{4\pi} \right)^{1/2} \left\{ \mathcal{D}_{\nu_1 \mu_1}^{(\lambda_1)}(\delta_1, \beta_1, \alpha_-) \ \mathcal{D}_{\nu_2 -\mu_1}^{(\lambda_2)}(\delta_2, \beta_2, 0) \right\} \overline{V}_{\nu_1 \nu_2 0}^{(\lambda_{12})} \quad , \quad (8.17)$$

where

$$\bar{\bar{V}}_{\nu_1 \nu_2 0}^{(\lambda_{12})} = \frac{1}{\hbar} \int\limits_{-\infty}^{\infty} dt \; \bar{C}_{\lambda_1 \lambda_2}(R) \, P_{\lambda_{12}}(\cos\bar{\theta}) \, e^{iWt} \; . \tag{8.18}$$

Here $P_{\lambda_{12}}$ is a Legendre polynomial (Edmonds 1960, p.22). The action (8.18), when used in (5.5), yields the M-conserving correspondence principle approximation (MCCP) to the transition amplitude, S^{MCCP}. The MCCP transition probability, P^{MCCP}, is now obtained averaging over β_1, β_2 and α_-:

$$P^{MCCP}(j_1 j_2 \to j_1' j_2') = \left(\frac{E_i}{E_f}\right)^{1/2} C(j_1 j_2 j_1' j_2') \frac{1}{8\pi} \int\limits_0^{2\pi} d\alpha_- \int\limits_{-1}^1 d(\cos\beta_1) \int\limits_{-1}^1 d(\cos\beta_2) \left| S^{MCCP} \right|^2 . \tag{8.19}$$

As the BFCP approximation, the MCCP reduces the dimension of the average over orientation by one degree of freedom , and requires many fewer trajectory integrals $\bar{V}$. This approximation is exact only if $\bar{V}_{\nu_1 \nu_2 \mu_{12}}^{(\lambda_{12})} = 0$, $\mu_{12} \neq 0$.

A subsidiary approximation in the same idea of the MCCP has been studied by Bhattacharyya et.al., (1977). They imposed the condition that $\hbar m_i$, $i = 1, 2$, is individually conserved, i.e. $\Delta m_1 = \Delta m_2 = 0$. Since the change in $\hbar m_i$ due to the collision is $-\partial A / \partial \alpha_i$ (see eq. 5.15), to obtain an approximation in which m_i is conserved we must approximate the action (8.13) by an action independent of α_i , A^{MCI},

$$A^{MCI}(\beta_1, \beta_2, \gamma_1, \gamma_2) = \sum_{\lambda_1, \lambda_2} \sum_{\nu_1, \nu_2} N_{\lambda_1 \nu_1} N_{\lambda_2 \nu_2} (\lambda_1 0 \lambda_2 0 / \lambda_1 \lambda_2 \lambda_{12} 0) \left(\frac{2\lambda_{12}+1}{4\pi}\right)^{1/2}$$

$$(-1)^{\nu_1 + \nu_2} \frac{4\pi}{[(2\nu_1+1)(2\nu_2+1)]^{1/2}} Y_{\lambda_1 \nu_1}(\beta_1, \gamma_1) \, Y_{\lambda_2 \nu_2}(\beta_2, \gamma_2) \, \bar{\bar{V}}_{\nu_1 \nu_2 0}^{(\lambda_{12})} . \tag{8.20}$$

The action (8.2) yields what we have termed the subsidiary M-conserving correspondence principle (SMCCP) to the transition amplitude, S^{SMCCP}. The SMCCP transition probability, P^{SMCCP}, is now

$$P^{SMCCP}_{(j_1 j_2 \to j_1' j_2')} = \left(\frac{E_i}{E_f}\right)^{1/2} \mathcal{C}(j_1 j_2 j_1' j_2') \frac{1}{4} \int_{-1}^{1} d(\cos\beta_1) \int_{-1}^{1} d(\cos\beta_2) \left| S^{SMCCP} \right|^2 \tag{8.21}$$

Thus the SMCCP introduces a further reduction in the dimension of the average over orientation (8.19). This approximation is exact only if $\overline{V}^{(\lambda_{12})}_{\nu_1 \nu_2 \mu_1 \mu_2} = 0$, μ_1 or $\mu_2 \neq 0$.

8.3.2 The M-conserving correspondence principle error

From the discussion above one sees that the action (8.17) is obtained directly from (8.12) by making

Thus we define $E^{MC}_{\nu_1 \nu_2 \mu_{12}}$ as a measure of the MCCP error:

$$E^{MC}_{\nu_1 \nu_2 \mu_{12}}(w, b) = 100 \; \overline{V}^{\lambda_{12}}_{\nu_1 \nu_2 \mu_1 \mu_2}(w, b) \Big/ \overline{V}^{(\lambda_{12})}_{\nu_1 \nu_2 0}(w, b), \tag{8.22}$$

where

$$\overline{V}^{(\lambda_{12})}_{\nu_1 \nu_2 0} = \left[(2\lambda_{12}+1)/4\pi\right]^{1/2} \overline{\overline{V}}^{(\lambda_{12})}_{\nu_1 \nu_2 0}. \tag{8.23}$$

For b=0 we have $\overline{\theta} = 0$ and $\overline{V}^{(\lambda_{12})}_{\nu_1 \nu_2 \mu_{12}} = 0, \mu_{12} \neq 0$; the MCCP approximation is then expected to be good for small impact parameters. In general by setting $\overline{\theta} = 0$ one sees that MCCP reduces to the BFCP approximation. Thus we expect the domain of validity of the M-conserving approximation to include that of the BFCP approximation. However, when $\overline{\theta} \neq 0$, the M-conserving approximation to the action is different, as it takes some account of the curvature of the orbit, through $\overline{V}^{(\lambda_{12})}_{\nu_1 \nu_2 0}$

An error similar to (8.22) can be defined for the SMCCP approximation by imposing the condition μ_1 or $\mu_2 \neq 0$. In general

we do not expect the accuracy of this approximation to be good because the terms of the action (8.17) which are eliminated to obtain (8.20) are of the same order as those retained.

8.3.3 The M-conserving correspondence principle equations for the dipole-dipole interaction

Proceeding as in sections (6.1) and (6.2), the application of MCCP to the dipole-dipole interaction leads to the equations:

$$\bar{P}\cos\bar{\gamma} = \frac{\bar{V}_{110}}{\sqrt{6}}\left[\cos\alpha_-\left\{\sin^2(\beta_1/2)\cos^2(\beta_2/2) + \cos^2(\beta_1/2)\sin^2(\beta_2/2)\right\} + \sin\beta_1\sin\beta_2\right],$$

$$\bar{P}\sin\bar{\gamma} = \frac{\bar{V}_{110}}{\sqrt{6}}\sin\alpha_-\left\{-\sin^2(\beta_1/2)\cos^2(\beta_2/2) + \cos^2(\beta_1/2)\sin^2(\beta_2/2)\right\},$$

$$\bar{P}'\cos\bar{\gamma}' = \bar{V}_{1-10}\left[\cos\alpha_-\left\{\cos^2(\beta_1/2)\cos^2(\beta_2/2) + \sin^2(\beta_1/2)\sin^2(\beta_2/2)\right\} - \sin\beta_1\sin\beta_2\right],$$

$$\bar{P}'\sin\bar{\gamma}' = \frac{\bar{V}_{1-10}}{\sqrt{6}}\sin\alpha_-\left\{-\cos^2(\beta_1/2)\cos^2(\beta_2/2) + \sin^2(\beta_1/2)\sin^2(\beta_2/2)\right\}. \quad (8.24)$$

The change of the action is

$$A^{MCCP} = \frac{3}{4\pi}\bar{P}\sin(\gamma_+ + \bar{\gamma}) + \frac{3}{4\pi}\bar{P}'\sin(\gamma_- + \bar{\gamma}'), \quad (8.25)$$

which yields the MCCP transition amplitude

$$S^{MCCP}(j_1 j_2, j_1' j_2') = e^{-i(n_+\bar{\gamma} + n_-\bar{\gamma}')}J_{n_+}\left(\frac{3}{4\pi}\bar{P}\right)J_{n_-}\left(\frac{3}{4\pi}\bar{P}'\right). \quad (8.26)$$

As the BFCP approximation, the MCCP satisfies the selection rules (6.11a). The transition probability P^{MCCP}, must be evaluated numerically.

For the SMCCP the action (8.25) reduces to

$$A^{SMCCP} = \bar{R} \cos \gamma_{+} + \bar{R}' \cos \gamma_{-} ,$$

(8.27a)

where

$$\bar{R} = \frac{3}{4\pi} \frac{\bar{V}_{110}}{\sqrt{6}} \sin \beta_1 \sin \beta_2 \quad , \quad \bar{R}' = \frac{3}{4\pi} \frac{\bar{V}_{1-10}}{\sqrt{6}} \sin \beta_1 \sin \beta_2 .$$

(8.27b)

The SMCCP transition probability is now

$$S^{SMCCP}(j_1 j_2 , j_1' j_2') = J_{n_+}(\bar{R}) J_{h_-}(\bar{R}') .$$

(8.28)

The first-order MCCP transition probability, P^{FOMC}, is

$$P^{FOMC}(j_1 j_2 \to j_1' j_2') = \left(\frac{E_i}{E_f}\right)^{1/2} \mathcal{C}(j_1 j_2 j_1' j_2') \frac{1}{64\pi^2} \left(\bar{V}_{s_1 s_2 0}\right)^2 , \quad |s_1| = |s_2| = 1$$

(8.29)

where $\bar{V}_{s_1 s_2 0}$ is given by (8.23). It is convenient, to compare
with the full first-order correspondence principle, to express the
trajectory integrals (8.13) in terms of the $V_{\nu_1 \nu_2 \mu_1 \mu_2}$ given by
(5.13). From (8.13) we obtain:

$$\bar{V}_{\nu_1 \nu_2 0} = \frac{3}{16} \left(\frac{5}{\pi}\right)^{1/2} \left[V_{\nu_1 \nu_2 -1-1} + V_{\nu_1 \nu_2 11} + \frac{2}{3} V_{\nu_1 \nu_2 00} \right] ,$$

(8.30a)

$$\bar{V}_{\nu_1 \nu_2 \pm 2} = \frac{1}{16} \left(\frac{15}{2\pi}\right)^{1/2} \left[2 V_{\nu_1 \nu_2 00} - V_{\nu_1 \nu_2 11} - V_{\nu_1 \nu_2 -11} \right] ,$$

(8.30b)

$$\bar{V}_{\nu_1 \nu_2 \pm 1} = \frac{i}{8} \left(\frac{15}{2\pi}\right)^{1/2} \left[V_{\nu_1 \nu_2 -1-1} - V_{\nu_1 \nu_2 11} \right] .$$

(8.30c)

It is interesting to notice that when the BFCP approximation is
valid $\bar{V}_{\nu_1 \nu_2 \pm 2} = \bar{V}_{\nu_1 \nu_2 \pm 1} = 0$, and MCCP is exact.

For a resonant transition in the straight-line limit we obtain $E_{1-1 \pm 2}^{MC}(0,b) \approx 4|$, and the relation between the full and M-conserving correspondence principle first-order probabilities is obtained using (6.17), (6.18) and (8.30a):

$$P^{FOMC}(j_1 j_2 \to j_2 i_1 \; ; b) = \frac{3}{4} P^{FOCP}(j_1 j_2 \to j_2 j_1 \; ; b) .$$ (8.31)

Thus for a resonant transition in the straight-line limit the first-order M-conserving transition probability has an error of 25%, which is much better than the BFCP approximation.

Since the MCCP is also good for small impact parameters the above result suggests that this approximation is reasonably good for all impact parameters. The relation (8.31) is also valid for distant sudden collisions.

The first-order SMCCP transition probability, P^{FOSMC}, is given in terms of P^{FOMC} as

$$P^{FOSMC}(j_1 j_2 \to j_1' j_2') = \frac{2}{3} P^{FOMC}(j_1 j_2 \to j_1' j_2') .$$ (8.32)

For a resonant transition in the straigh-line limit the relation between FOSMC and FOCP result is

$$P^{FOSMC}(j_1 j_2 \to j_1' j_2') = \frac{1}{2} P^{FOCP}(j_1 j_2 \to j_1' j_2') .$$ (8.33)

Thus for a resonant transition in the straight limit the FOSMC transition probability is a half the full first-order result. For small impact parameters this approximation should not be better, and it is not expected to give accurate cross sections.

8.4   The decoupled-L-dominant correspondence principle

8.4.1   Theory

In this section we derive modified SCCP equations using approximations similar to those made in the quantal dominant-L-decoupling approximation (DLD) (DePristo and Alexander 1976).   Consequently, the frame of reference is the usual space-fixed frame as described in section 4.2

The DLD approximation of DePristo and Alexander (1976) is based on the observation that at large J, the quantum number of the total angular momentum, the matrix elements, $V_\lambda(j\ell, j'\ell'; J)$, of standard close coupling are dominated by terms with $\ell, \ell' < J$.   Here $\lambda(j)$ represents the triple index $\lambda_1 \lambda_2 \lambda_{12}(j_1 j_2 j_{12})$.   For the molecule-molecule case the index $\Lambda = \ell - J + j_{12}$ is introduced, with $0 \leqslant \Lambda \leqslant 2 j_{12}$.   From the asymptotic behaviour of the product of a 3-j and 6-j symbols (Edmonds 1960, p.46 and p.92 respectively), a decoupling in Λ is found.   Thus DLD makes $\Lambda = \Lambda'$, which yields

$$\Delta j_{12} \equiv \Delta j_1 + \Delta j_2 = -\Delta \ell . \tag{8.34}$$

Using (5.16) in (8.34) we have that the DLD condition in our approach can be written as

$$\Delta m_1 + \Delta m_2 = \Delta j_1 + \Delta j_2 . \tag{8.35}$$

To see the impact of (8.23) in the SCCP equations we write the transition amplitude (5.1) as

$$S = \left(\frac{1}{2\pi}\right)^4 \int_0^{2\pi} d\gamma_+ \, d\gamma_- \, d\alpha_+ \, d\alpha_- \, \exp\left[i \left\{ \Delta j_+ \, \gamma_+/2 + \Delta j_- \, \gamma_-/2 + \Delta m_+ \, \alpha_+/2 \right.\right.$$
$$\left.\left. + \Delta m_- \, \alpha_-/2 - A(\gamma_+, \gamma_-, \beta_1, \beta_2, \alpha_+, \alpha_-) \right\} \right] , \tag{8.36a}$$

where $\Delta j_\pm = \Delta j_2 \pm \Delta j_1$, $\quad \Delta m_\pm = \Delta m_1 \pm \Delta m_2$. $\hfill (8.36b)$

From (8.36a) one sees that to satisfy (8.35) we must have

$$A(\gamma_+, \gamma_-, \beta_1, \beta_2, \alpha_+, \alpha_-) = A(\gamma_+ + \alpha_+, \gamma_-, \beta_1, \beta_2, \alpha_-) \qquad . \quad \text{Thus we define}$$

$$A^{DLD}(\gamma_+, \gamma_-, \beta_1, \beta_2, \alpha_+, \alpha_-) = \sum_{\lambda_1 \lambda_2} \sum_{\substack{\mu_1, \nu_1 \\ \mu_2, \nu_2}} N_{\lambda_{12}\nu_{12}} N_{\nu_1\mu_1} N_{\nu_2\mu_2} (\lambda_1\mu_1, \lambda_2\mu_2/\lambda_1\lambda_2\lambda_{12}\nu_{12})$$

$$\times \left\{ e^{i\frac{\nu_{12}}{2}(\gamma_+ + \alpha_+)} e^{i\frac{\gamma_-}{2}(\nu_2-\nu_1)} d^{(\lambda_1)}_{\nu_1\mu_1}(\beta_1) d^{(\lambda_2)}_{\nu_2\mu_2}(\beta_2) e^{i\frac{\alpha_-}{2}(\mu_1-\mu_2)} \right\} V^{(\lambda_{12})}_{\nu_1\nu_2\nu_{12}} , \hfill (8.37)$$

where $\nu_{12} = \nu_1 + \nu_2$ and

$$V^{(\lambda_{12})}_{\nu_1\nu_2\nu_{12}} = \frac{2}{\hbar} \int_0^\infty dt \, \bar{C}_{\lambda_1\lambda_2}(R) \cos\left[(\nu_1 W_1 + \nu_2 W_2) t - \nu_{12}\varphi' \right] . \hfill (8.38)$$

The action (8.37) yields the decoupled-L-dominant correspondence principle approximation (DLDCP) to the transition amplitude, S^{DLDCP}. Using (8.37) in (8.36a) one notices that the α_+ dependence of $S(j_1 j_2, j_1' j_2')$ is simply an overall phase, so it can be ignored. Then we define

$$\bar{A} = A^{DLD}(\gamma_+, \gamma_-, \beta_1, \beta_2, 0, \alpha_-) . \hfill (8.39)$$

The DLDCP transition probability, P^{DLDCP}, is now obtained averaging in α_-, β_1 and β_2 :

$$P^{DLDCP}_{(j_1 j_2 \to j_1' j_2')} = \left(\frac{E_i}{E_f}\right)^{1/2} C_{(j_1 j_2, j_1' j_2')} \frac{1}{8\pi} \int_0^{2\pi} d\alpha_- \int_{-1}^1 d(\cos\beta_1) \int_{-1}^1 d(\cos\beta_2) \left| S^{DLDCP} \right|^2 , \hfill (8.40a)$$

where

$$S^{DLDCP} = \frac{1}{4\pi^2} \int_0^{2\pi} d\gamma_+ \, d\gamma_- \, \exp\left[i \left\{ \Delta j_+ \gamma_+/2 + \Delta j_- \gamma_-/2 - \bar{A} \right\} \right] . \hfill (8.40b)$$

Thus the DLDCP reduces the average over orientation by one degree of freedom and requires fewer $V^{(\lambda_{12})}_{\nu_1 \nu_2 \mu_1 \mu_2}$ integrals. This approximation is exact only if $V^{(\lambda_{12})}_{\nu_1 \nu_2 \mu_1 \mu_2} = 0$, $\mu_{12} \equiv \mu_1 + \mu_2 \neq \nu_2$. Here $V^{(\lambda_{12})}_{\nu_1 \nu_2 \mu_1 \mu_2}$ is defined by (5.13).

8.4.2 The decoupled-L-dominant correspondence principle error

The action (8.37) can also be obtained by making, in the action (5.14), $V^{(\lambda_{12})}_{\nu_1 \nu_2 \mu_1 \mu_2} = 0$, $\mu_{12} \neq \nu_{12}$. Thus the quantity

$$E^{DLD}_{\nu_1 \nu_2 \mu_{12}}(w, b) = 100 \, V^{(\lambda_{12})}_{\nu_1 \nu_2 \mu_{12}}(w, b) \Big/ V^{(\lambda_{12})}_{\nu_1 \nu_2 \nu_{12}}(w, b) \tag{8.41}$$

is a measure of the DLDCP error. Here we put $V^{(\lambda_{12})}_{\nu_1 \nu_2 \mu_{12}} = V^{(\lambda_{12})}_{\nu_1 \nu_2 \mu_1 \mu_2}$. For b=0 we have $V^{(\lambda_{12})}_{\nu_1 \nu_2 \mu_{12}} = V^{(\lambda_{12})}_{\nu_1 \nu_2 0}$; since in this limit DLDCP retains only $V^{(\lambda_{12})}_{\nu_1 \nu_2 \nu_{12}}$ we expect this approximation to be largely in error. In general the DLDCP approximation is not good for small impact parameters. As b increases DLDCP should improve. However, this improvement is not general, and we show below that it depends on the nature of the transition.

8.4.3 The decoupled-L-dominant correspondence principle equations
for the dipole-dipole interaction

Proceeding as in sections (6.1) and (6.2) we obtain the equations

$$R \sin \epsilon = V_{112} \, \cos^2(\beta_1/2) \, \cos^2(\beta_2/2) \quad ,$$

$$P \cos \zeta = \frac{V_{1-10}}{3} \left[\cos \alpha_- \left\{ \cos^2(\beta_1/2) \cos^2(\beta_2/2) + \sin^2(\beta_1/2) \sin^2(\beta_2/2) \right\} - \sin \beta_1 \sin \beta_2 \right] ,$$

$$P \sin \zeta = \frac{V_{1-10}}{3} \sin \alpha_- \left\{ \cos^2(\beta_1/2) \cos^2(\beta_2/2) - \sin^2(\beta_1/2) \sin^2(\beta_2/2) \right\} \tag{8.42}$$

which yield the action:

$$\bar{A}(\gamma_+, \gamma_-, \beta_1, \beta_2, \alpha_-) = \frac{6}{32\pi} \left(\frac{15}{2\pi}\right)^{1/2} \left[R\cos\gamma_+ + P\cos(\gamma_- - \gamma) \right] . \quad (8.43)$$

The DLDCP transition amplitude is now

$$S^{DLDCP}(j_1 j_2, j_1' j_2') = e^{i n_- \gamma} J_{n_+}(R_+) J_{n_-}(R_-) , \quad (8.44a)$$

where

$$R_+ = \frac{6}{32\pi} \left(\frac{15}{2\pi}\right)^{1/2} R \quad , \quad R_- = \frac{6}{32\pi} \left(\frac{15}{2\pi}\right)^{1/2} P . \quad (8.44b)$$

As the other approximations presented above, the DLDCP approximation
satisfies the selection rules (6.11a). The DLDCP transition
probability must be evaluated numerically.

The first-order DLDCP transition probability, P^{FODLD}, is

$$P^{FODLD}(j_1 j_2 \to j_1' j_2') = \left(\frac{E_i}{E_f}\right)^{1/2} \mathcal{C}(j_1 j_2 j_1' j_2') \frac{5}{1024\pi^3} S(s_1, s_2) \left(V_{s_1 s_2 s_{12}}\right)^2 , \quad (8.45a)$$
$$|s_1| = |s_2| = 1 ,$$

where $s_{12} = s_1 + s_2$, and

$$S(s_1, s_2) = 1 \quad , \quad \text{if} \quad \text{sgn}(s_1) \ne \text{sgn}(s_2)$$
$$\frac{3}{2} \quad , \quad \text{if} \quad \text{sgn}(s_1) = \text{sgn}(s_2) .$$
$$(8.45b)$$

For a resonant transition in the straight-line limit we obtain
$E^{DLD}_{1-1\pm2} = 33.3$, and the relation between the FODLD and FOCP is

$$P^{FODLD}(j_1 j_2 \to j_2 j_1) = \frac{3}{4} P^{FOCP}(j_1 j_2 \to j_2 j_1) . \quad (8.46)$$

Thus for a resonant transition in the straight-line limit DLDCP
gives the same first-order result as the MCCP approximation. This
can be obtained directly by just applying the MCCP and DLDCP conditions
to the trajectory integrals in the FOCP probability (6.14).

In contrast to the MCCP approximation the relation (8.46) is valid for distant sudden collisions only when $\text{sgn}(s_1) \neq \text{sgn}(s_2)$. For transitions where $\text{sgn}(s_1) = \text{sgn}(s_2)$ the FODLD approximation retains only $V_{\pm 1 \pm 1 \pm 2}$, and the relation between FOCP and FODLD for sudden collisions in the straight-line limit is

$$P^{FODLD}_{(j_1 j_2 \rightarrow j_1' j_2')} = \frac{1}{8} \, P^{FOCP}_{(j_1 j_2 \rightarrow j_1' j_2')} \, , \qquad (8.47)$$

which shows that the FODLD is largely in error.

For adiabatic collisions we must also consider two types of transition:

A)   when $\text{sgn}(s_1) \neq \text{sgn}(s_2)$ FODLD retains only $V_{\pm 1 \mp 1 \, 0}$, and the error (8.41), in the straight-line limit is,

$$E^{DLD}_{\pm 1 \mp 1 \, 2} (w,b) = 133.3 \, Z \quad , \quad E^{DLD}_{\pm 1 \mp 1 -2}(w,b) = \frac{25}{Z} \, , \qquad (8.48)$$

where Z is the adiabaticity parameter.   Clearly the elimination of $V_{\pm 1 \mp 1 \, 2}$ produces large errors, and FODLD is not good.

B)   when $\text{sgn}(s_1) = \text{sgn}(s_2)$ FODLD retains only $V_{\pm 1 \pm 1 \pm 2}$,

and the error (8.41), in the straight-line limit, is now

$$E^{DLD}_{\pm 1 \pm 1 \, 0} (w,b) \approx \frac{3}{4Z} \quad , \quad E^{DLD}_{\pm 1 \pm 1 \mp 2} \approx \frac{3}{2Z} \, . \qquad (8.49)$$

Since for adiabatic collisions $Z \gg 1$ the errors are small.   Thus for adiabatic collisions in the straight-line limit FODLD should be accurate.

From our discussion above we infer that for distant collisions DLDCP is reasonable accurate to describe: 1) a first-order allowed resonant transition, and 2) a first-order allowed transition with $\Delta j_1 = \Delta j_2$.   However, DLDCP is largely in error to describe:

3) a first-order allowed transition with $\Delta j_1 = - \Delta j_2$, $w \neq 0$.

The larger error in 3) is because DLDCP retains only the trajectory integral $V_{\Delta j_1 \, -\Delta j_2 \, 0}$, i.e. it considers the collision with $\Delta m_1 + \Delta m_2 = 0$.

8.5 Numerical techniques

The main computational feature of all the approximations presented above, is that they reduce the dimension of the average to obtain the transition probability. To make full use of this feature it is then necessary to modify the computer program used to evaluate SCCP probabilities and cross sections. In this section we discuss the main changes to the numerical techniques described in section 6.4. First, we describe the numerical techniques used to make MCCP and SMCCP calculations.

8.5.1 Evaluation of the $\overline{V}_{v_1 v_2 \mu_{12}}$

No attempt was made to evaluate directly the $\overline{V}_{v_1 v_2 \mu_{12}}$ integrals. Thus the usual integrals (5.13) are evaluated, and the $\overline{V}_{v_1 v_2 \mu_{12}}$ are obtained using equations (8.30).

8.5.2 Evaluation of the transition amplitude

Given the $\overline{V}_{v_1 v_2 \mu_{12}}$ the calculation of $\overline{P}$ and $\overline{P}'$ for specified values of α_- and β_i (i=1,2) is straightforward. The J_ν Bessel functions are evaluated as described in subsection 6.4.2.

8.5.3 Evaluation of the transition probability

Since the transition amplitude is now evaluated in terms of α_- and β_i , the integrations over α_1 and α_2 was replaced by an integral over α_- . As before Clenshaw-Curtis quadratures were used. The accuracy of the integration was checked by using the

approximation $V_{\nu_1 \nu_2 \mu_1 \mu_2} = V_{\nu_1 \nu_2 00}$, for which MCCP reduces to the
BFCP approximation; then we compare with BFCP results performed
with the SCCP program described in section 6.4.   The differences
were less than 0.5%.   Since during tests the program described here
run much faster than the SCCP program, it was also used to perform
the BFCP calculations.   When performing SMCCP calculations a
flag was set to save the integration over α_+ .

8.5.4   Evaluation of the cross section

To evaluate the cross sections we use the same techniques
described in subsection 6.4.4.

The program implemented using the techniques described above
was used to evaluate MCCP, SMCCP and BFCP rotationally inelastic
cross sections.   The savings in CPU time were dramatic, and the
program proved to be up to four times faster - for MCCP calculations -
and up to five times faster - for SMCCP and BFCP calculations - than
equivalent SCCP calculations.

No special program was implemented to evaluate DLDCP cross
sections.   The calculations were performed with the SCCP program,
where we made $V_{\nu_1 \nu_2 \mu_{12}} = 0$, $\mu_{12} \neq \nu_{12}$.   Since the DLDCP transition
amplitude is independent of α_+ , the integrand in (6.12) is smoother
and there is some savings of CPU time.   For some DLDCP calculations
the program run up to 1.5 times faster than for the equivalent SCCP
calculations.

8.6   Numerical results and discussion

In this section we present numerical results obtained using
the BFCP, MCCP, SMCCP and DLDCP approximations.   Our aim is to study
the accuracy of above approximations and consequently we compare with

the SCCP. Since our results were obtained using a spherical
potential which was too strong, we do not compare with the quantal
coupled states (CS) and DLD results for HF-HF collisions presented by
DePristo and Alexander [1977] As before only the dipole-dipole interaction
is considered.

8.6.1 The error terms

Before we discuss the transition probabilities,it is convenient
to compare some numerical values of the errors $E^{BF}_{\nu_1 \nu_2 \mu_{12}}$, $E^{MC}_{\nu_1 \nu_2 \mu_{12}}$
and $E^{DLD}_{\nu_1 \nu_2 \mu_{12}}$. In table 8.1 we show the behaviour of E^{BF} and E^{DLD}
for various impact parameters; the transition is $(0,0) \rightarrow (1,1)$ in
HF-HF collisions.

The results confirm our earlier predictions. For b=0 the
BFCP approximation is exact, but as the impact parameter increases
so does E^{BF}.   On the other hand DLDCP has the largest error at b=0,
and decreases as b increases. We notice that E^{BF}_{112} and E^{BF}_{11-2} have
opposite signs. As pointed out by Clark et.al. (1977), this suggests
that some cancellation of the errors due to the BFCP approximation is
likely in calculating orientation-averaged transition probabilities.

In table 8.1 we also show the effects of varying the energy.
We notice that as the energy increases E^{BF} increases, while E^{DLD}
decreases. The decrease of E^{DLD} is valid for adiabatic collisions
only; if the energy increase makes the collision to become sudden,
at large impact parameters $E^{DLD}_{11-2} \rightarrow 100$ and $E^{DLD}_{110} \rightarrow 300$. For the same
limit we have that $E^{BF}_{11\pm2} \rightarrow 66.6$ (see section 8.2.3).

In table 8.2 we show E^{BF}, E^{MC} and E^{DLD} for various impact
parameters; the transition is $(1,1) \rightarrow (0,2)$. As expected E^{DLD} is
large showing that for this transition DLDCP is largely in error.

We notice that E_{111}^{MC} and E_{112}^{MC} have opposite signs, suggesting as before cancellation of errors. The situation is similar for E_{112}^{BF} and E_{1-1-2}^{BF}. The comparison in table 8.2 suggests that almost everywhere the MCCP is better than the BFCP.

8.6.2. The transition probability

In table 8.3 we show SCCP, BFCP, and MCCP transition probabilities for various impact parameters; the transitions are $(0,0) \rightarrow (1,1)$ at $E_i = 500 cm^{-1}$ and $(0,0)$ $(0,2)$ at $E_i = 8000 cm^{-1}$ in HF-HF collisions. For b=0 both BFCP and MCCP are exact, but as the impact parameter increases they deviate from the exact result. Overall the MCCP approximation is better than BFCP, and maintains a better agreement with SCCP in the whole range of impact parameters.

In table 8.4 we show SCCP, MCCP and DLDCP transition probabilities for the $(1,1) \rightarrow (0,2)$ and $(0,0) \rightarrow (1,1)$ transitions at $E_i = 8000 cm^{-1}$. For the $(1,1) \rightarrow (0,2)$ transition the MCCP approximation is much better than DLDCP. For the smaller impact parameters DLDCP overestimates the transition probability by one order of magnitude; as the impact parameter increases the agreement between SCCP and DLDCP becomes better but still DLDCP is largely in error. For the $(0,0) \rightarrow (1,1)$ transition at small impact parameters MCCP is better than DLDCP, which gives probabilities largely overestimated. As the impact parameter increases DLDCP improves dramatically and at the larger impact parameters becomes more accurate than MCCP, with errors smaller than 7%. These results confirm our earlier predictions that DLDCP fails to describe properly a collision where an excitation-deexcitation occurs, while is good for collisions in which the two molecules are excited or deexcited.

An interesting comparison is presented in figure 8.1. There we show SCCP, MCCP, SMCCP and the classical path results of Bhattacharyya et.al., (1977), for the $(0,1) \rightarrow (1,0)$ resonant transition in HCl-HCl collisions at $E_i = 201.71 cm^{-1}$. The results of Bhattacharyya et.al., correspond to a subsidiary M-conserving calculation in the time-dependent close coupling framework (TDCC). The comparison shows that at large impact parameters the shape of their probability is similar to the shape of the correspondence principle probability, although it decreases faster than the SCCP, MCCP and SMCCP probabilities. The comparison for small impact parameters is not valid as the potential used by Bhattacharyya et.al. (1977) included the quadrupolar interaction.

We also show in figure 8.1 the results, at large impact parameters, of Bhattacharyya and Saha (1978). These results correspond to a M-conserving calculation in the TDCC framework. Although for most of the impact parameters these M-conserving probabilities are larger than the correspondence principle results, they decrease to become smaller than MCCP.

8.6.3 The cross section

In table 8.5 we show SCCP, BFCP, MCCP, SMCCP and DLDCP rotationally inelastic cross sections for the $(2,2) \rightarrow (3,3)$, $(0,0) \rightarrow (1,1)$ and $(4,2) \rightarrow (3,3)$ transitions, at initial energies $E_i = 4000 - 10000 cm^{-1}$, in HF-HF collisions. For the more adiabatic collisions we notice that the BFCP approximation agrees with SCCP within 10%. As the energy increases, or W decreases, BFCP becomes less accurate and consistently underestimates the cross section. These results are consistent with our earlier predictions on BFCP being accurate for short-range collisions since the more adiabatic collisions are the shorter-ranged.

The SMCCP approximation overestimates the cross sections for the $(2,2) \rightarrow (3,3)$ transition at $E_i = 4000 - 8000 cm^{-1}$. As the collisions become less adiabatic SMCCP consistently underestimates the cross sections. In general, for the transitions presented in table 8.5, the SMCCP is better than the BFCP approximation.

The DLDCP approximation underestimates the cross section for the $(2,2) \rightarrow (3,3)$ transition at $E_i = 4000 cm^{-1}$ by more than a factor of 2. For the other energies DLDCP agrees well with SCCP, giving errors of less than 10%. For the $(0,0) \rightarrow (1,1)$ transition the errors of DLDCP, for all the energies considered here, are less than 6%. For the $(4,2) \rightarrow (3,3)$ transition however, the DLDCP approximation consistently underestimates the cross section, and give errors of more than 50%.

The more consistent approximation presented in table 8.5 is the MCCP approximation. For the $(2,2) \rightarrow (3,3)$ and $(0,0) \rightarrow (1,1)$ transitions MCCP consistently gives errors smaller than 6%. while for the $(4,2) \rightarrow (3,3)$ transition agrees with SCCP within 15%.

In table 8.6 we show cross sections for HCl-HCl collisions at $E_i = 201.71$ and $500 cm^{-1}$; the transitions are $(0,0) \rightarrow (2,2)$ and $(0,0) \rightarrow (1,1)$ For the $(0,0) \rightarrow (2,2)$ transition the BFCP approximation is the better of all the approximations, while SMCCP is the worst. The MCCP approximation overestimates the cross section and gives errors between 25% and 30%. The DLDCP approximation is better than MCCP at the larger energy, but MCCP is better for the smaller E_i.

For the $(0,0) \rightarrow (1,1)$ transition the body-fixed approximation is good at $201.71 cm^{-1}$, but underestimates by more than a factor of two the cross section at $E_i = 500 cm^{-1}$. In general MCCP and DLDCP give errors smaller than 30%, and SMCCP has errors of 36% and 12% for $E_i = 201.71$ and 500 respectively.

In table 8.6 we also show the cross sections for the resonant transition $(0,1) \rightarrow (1,0)$ at E_i = 201.71,500 and 1000 cm^{-1}. For this sudden like transition the BFCP overestimates the cross section, and this overestimation increases as the energy increases. As we showed in subsection 8.2.3 in the sudden limit for distant collisions the FOBF probability is three times the FOCP probability. The MCCP and DLD, at E_i = 201.71 and 500 cm^{-1}, agree between them within 1%. At E_i = 1000 cm^{-1} the MCCP has the better agreement with SCCP. The SMCCP approximation underestimates the cross sections and gives errors up to 34%.

8.6.4   Conclusions

In earlier sections we have derived the body-fixed, the M-conserving and the decoupled-L-dominant versions of the strong coupling correspondence principle. We have termed them BFCP, MCCP and DLDCP respectively. A subsidiary approximation in the spirit of the MCCP has also been derived; we termed it SMCCP. These correspondence principle decoupling approximations have been applied to the rotational excitation of two linear molecules. The equations for the dipole-dipole interaction were obtained for each of above approximations and some interesting limits were studied. In particular we showed the relation between the BFCP and MCCP approximations, and the first-order result for each approximation was studied. Finally we presented, earlier in this section, some numerical results for rotationally inelastic transition probabilities and cross sections in rotor-rotor collisions.

The goal of this work was not to make a detailed study on the validity of the above approximations, but to show how they can be extended to the rotor-rotor collision problem, and make preliminary findings on the deviation of these approximations from the full SCCP

result. Another of our aims was also to look for feasible ways of easing the computational effort of the SCCP approximation.

Our findings were both encouraging and rewarding. We found that the BFCP approximation is accurate within 10% to describe short-range adiabatic collisions. This suggests that, as in the atom-rotor case (Dickinson and Richards 1977), the BFCP is adequate to describe rotor-rotor collisions dominated by a strong short-range inisotropy. We have also found that in general the MCCP approximation is valid wherever the BFCP is valid, but that MCCP is significantly better for distant adiabatic, as well as sudden collisions. Our results show that the MCCP produces significant savings in computations of probabilities and cross sections with little loss of accuracy. Some MCCP cross sections, with deviations from the exact SCCP result of less than 10%, were obtained in up to a fourth the CPU time spent to calculate the corresponding SCCP cross section.

The DLDCP results show that for close collisions (small b) this approximation is largely in error. This suggests that, in contrast to the BFCP, the DLDCP approximation is not adequate for collisions dominated by a strong short-range anisotropy. For distant collisions the situation tends to improve, and reasonably good agreement with the exact SCCP result was obtained for a resonant transition, and for transitions satisfying $\text{sgn}(\Delta j_1) = \text{sgn}(\Delta j_2)$. There is however, one non-resonant transition for which the DLD approximation has proved to be grossly in error: $(j_1, j_2) \longrightarrow (j_1 + \Delta j_1, j_2 + \Delta j_2)$, $\Delta j_1 = -\Delta j_2$. The large error arises from the DLD condition (8.35), which, for this transition, makes $\Delta m_1 + \Delta m_2 = 0$. Consequently, for long distance collisions DLD retains only trajectory integrals associated with $\Delta m_1 + \Delta m_2 = 0$ transitions. Since these integrals are exact for head-on collisions, the DLDCP at large b is largely in error.

Clearly, much more work needs to be done on assessing the validity of the semiclassical approximations presented here in rotor-rotor collisions. Since the domain of validity of the SCCP should include those of the BFCP, MCCP, SMCCP and DLDCP approximations, it seems necessary, as a first stage, to determine such a domain. Then a study of rotor-rotor collisions using the SCCP and these correspondence principle decoupling approximations (CPD) can prove convenient to assess the ranges of validity and computational convenience of the CPD approximations. The different ranges of validity and computational conveniences suggest that a combination of some of the CPD approximations can provide a useful tool to calculate rotationally inelastic cross sections and rates. Surely, such a tool may be appreciated by some theoretitians and experimentalists. There is much to be done...

CAPTIONS TO TABLES 8.1 - 8.6

TABLE 8.1

Percentage error as defined in the text. The parameters
correspond to the $(0,0) \rightarrow (1,1)$ transition in HF - HF
collisions.

TABLE 8.2

As table 8.1 for the $(1,1) \rightarrow (0,2)$ transition at
$E_i = 8000 \text{ cm}^{-1}$.

TABLE 8.3

SCCP, BFCP and MCCP transition probabilities for
HF - HF collisions.

TABLE 8.4

SCCP, MCCP and DLDCP transition probabilities in
HF - HF collisions at $E_i = 8000 \text{ cm}^{-1}$.

TABLE 8.5

SCCP, BFCP, MCCP, SMCCP and DLDCP cross sections for
HF - HF collisions.

TABLE 8.6

As table 8.5 for HCl - HCl collisions.

Table 8.1

$b(a_0)$	E_{112}^{BF}	E_{11-2}^{BF}	E_{1-12}^{BF}	E_{1-1-2}^{BF}	E_{11-2}^{DLD}	E_{110}^{DLD}	E_{1-12}^{DLD}	E_{1-1-2}^{DLD}	$E_i(cm^{-1})$
0	0	0	0	0	100	100	100	100	8000
2	-15.7	17.9	4.7	4.7	70.9	86.4	95.3	95.3	
4	-29.6	38.9	19.5	19.5	47.1	77.2	80.5	80.5	
6	-44.3	64.8	47.0	47.0	24.4	69.3	52.9	52.9	
0	0	0	0	0	100	100	100	100	500
2	-9.6	8.7	2.4	2.4	83.3	91.2	97.6	97.6	
4	-20.2	16.9	9.7	9.7	69.0	83.1	90.3	90.3	
6	-32.1	23.9	22.3	22.3	57.5	75.6	77.6	77.6	

Table 8.2

$b(a_o)$	E_{112}^{BF}	E_{11-2}^{BF}	E_{1-12}^{BF}	E_{1-1-2}^{BF}	E_{111}^{MC}	E_{112}^{MC}	E_{1-11}^{MC}	E_{1-12}^{MC}	E_{11-2}^{DLD}	E_{110}^{DLD}	E_{1-12}^{DLD}	E_{1-1-2}^{DLD}
0	0	0	0	0	0	0	0	0	100	100	100	100
2	-19.4	-19.5	14.7	9.24	-11.9	0.35	7.5	0.85	67.4	83.7	85.3	109.2
4	-40.9	40.6	34.8	-11.5	-24.9	0.47	15.6	3.9	42.2	70.9	65.1	111.5
6	74.9	64.7	61.9	-2.7	-41.16	1.5	25.4	11.6	20.2	57.2	38.1	102.7

Table 8.3

$b(a_o)$	$E(cm^{-1})$	$(j_1,j_2) \rightarrow (j_1',j_2')$	P^{SCCP}	P^{BFCP}	P^{MCCP}
0	500	$(0,0) \rightarrow (1,1)$	4.9-3	4.9-3	4.9-3
2			5.1-3	4.9-3	4.8-3
4			5.3-3	4.9-3	5.2-3
6			6.1-3	5.0-3	5.7-3
8			9.1-3	7.2-3	1.0-2
10			1.2-2	9.3-3	1.5-2
11			1.3-2	9.5-3	1.6-2
0	8000	$(0,0) \rightarrow (0,2)$	1.1-2	1.1-2	1.1-2
2			1.05-2	1.08-2	1.09-2
4			1.1-2	9.8-3	1.1-2
6			1.4-2	9.3-3	1.3-2
8			2.0-2	9.6-3	1.97-2
10			5.5-2	9.1-2	9.2-2
12			5.6-2	3.5-2	5.8-2
14			3.1-2	6.7-3	1.7-2
16			1.0-2	1.1-3	4.1-3

Table 8.4

$b(a_o)$	$P^{SCCP}(1,1 \to 0,2)$	$P^{MCCP}(1,1 \to 0,2)$	$P^{DLDCP}(1,1 \to 0,2)$	$P^{SCCP}(0,0 \to 1,1)$	$P^{MCCP}(0,0 \to 1,1)$	$P^{DLDCP}(0,0 \to 1,1)$
0	4.4 – 3	4.4 – 3	4.3 – 2	1.2 – 2	1.2 – 2	4.1 – 2
2	4.6 – 3	4.6 – 3	3.3 – 2	1.3 – 2	1.2 – 2	4.0 – 2
4	4.9 – 3	4.5 – 3	3.3 – 2	1.4 – 2	1.3 – 2	3.8 – 2
6	6.3 – 3	5.1 – 3	2.9 – 2	1.8 – 2	1.5 – 2	3.4 – 2
8	1.3 – 2	9.1 – 3	2.1 – 2	2.6 – 2	3.8 – 2	2.6 – 2
10	6.9 – 2	7.2 – 2	8.9 – 2	9.4 – 2	2.0 – 1	9.6 – 2
12	1.0 – 1	1.5 – 1	7.2 – 2	1.7 – 1	2.6 – 1	1.6 – 1
14	1.1 – 1	1.2 – 1	3.9 – 2	1.6 – 1	1.5 – 1	1.5 – 1
16	9.0 – 2	7.8 – 2	1.9 – 2	1.0 – 1	6.9 – 2	9.9 – 2

Table 8.5

$E(cm^{-1})$	$(j_1 j_2) \rightarrow (j_1' j_2')$	SCCP	BFCP	MCCP	SMCCP	DLDCP
4000	(2,2)→(3,3)	7.4-1	6.9-1	7.8-1	1.0	3.0-1
6000		7.9-1	7.8-1	7.7-1	9.7-1	9.3-1
8000		1.2	7.9-1	1.3	1.4	1.3
10000		1.8	8.1-1	1.7	1.2	1.9
4000	(0,0)→(1,1)	14.3	4.0	16.3	5.76	15.3
6000		23.8	7.4	26.2	15.0	23.9
8000		31.0	10.2	32.9	19.4	31.6
10000		38.5	13.8	39.5	25.6	37.3
4000	(4,2)→(3,3)	45.1	32.3	43.0	40.9	22.1
6000		53.8	35.4	46.6	38.4	25.3
8000		53.0	38.0	45.2	42.7	22.4
10000		50.7	38.4	46.1	41.3	26.2

Table 8.6

$E_t(cm^{-1})$	$(j_1j_2 \rightarrow j_1'j_2')$	SCCP	BFCP	MCCP	SMCCP	DLDCP
201.71	$(0,0) \rightarrow (2,2)$	8.5-1	6.6-1	1.1	3.1-1	5.9-1
500		1.3	1.1	1.8	7.0-1	1.1
201.71	$(0,0) \rightarrow (1,1)$	9.6-1	9.2-1	1.0	1.5	1.3
500		2.2	8.7-1	2.8	2.5	3.0
201.71	$(0,1) \rightarrow (1,0)$	245.9	399.8	210.7	182.4	209.6
500		156.8	267.0	135.2	103.0	136.3
1000		98.6	189.8	90.4	78.3	84.3

CAPTION TO FIGURE 8.1

Correspondence principle transition probabilities as functions
of the impact parameter b, for the resonant $(0,1) \rightarrow (1,0)$ transition
in HCl-HCl collisions at $E_i = 201.71 \text{ cm}^{-1}$.

_____ : SCCP

------------ : MCCP

–·–·–·–·–·– : SMCCP

············ : Subsidiary M-conserving approximation in the TDDC

framework, Battacharayya et.al. (1977).

oooooooooooo: M-conserving approximation in the TDCC framework,

Bhattacharayya and Saha (1978).

Figure 8.1
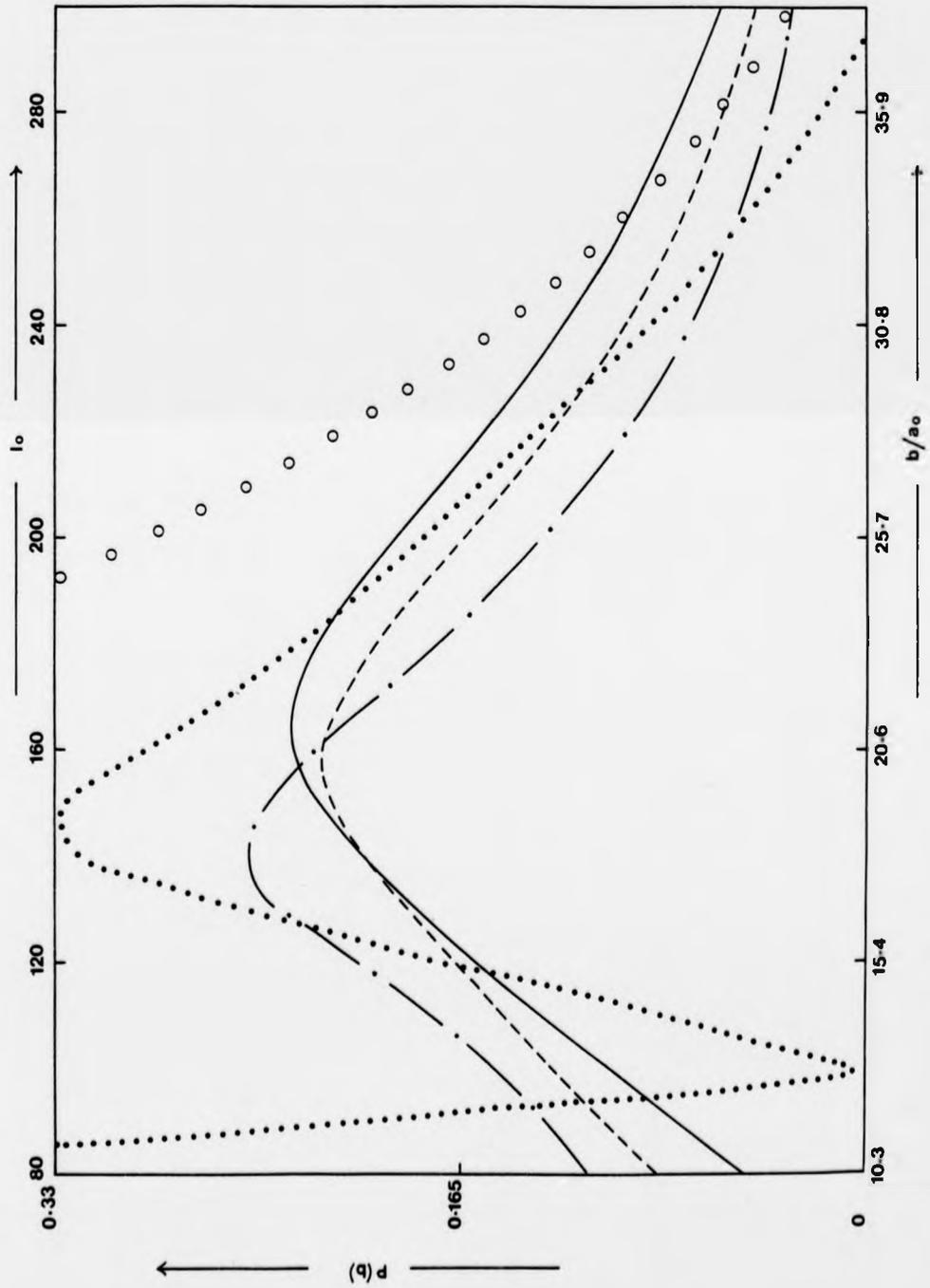
REFERENCES (*)

Abramowitz M and Stegun I A , 1965 "Handbook of Mathematical
Functions" (New York : Dover).

Alder K , Bohr A, Huus T, Mottelson B and Winter A,
1956 Rev. Mod. Phys, <u>28</u>, 432 (reprinted 1966,
"Coulomb Excitation" ed. K Alder and A Winther (New
York : Academic Press).

(*)
Alexander M H and DePristo A E, 1979, J. Phys. Chem., <u>83</u>, 1499.

Alexander M H, 1980, submitted to J. Chem. Phys.

Alper J S, Carroll M A and Gelb A, 1978, Chem. Phys., <u>32</u>, 471.

(*)
Bhattacharayya S S, Saha S and Basua A K, 1977, J. Phys. B.,
<u>10</u>, 1557.

Bhattacharayya S S and Saha S, 1978, J. Chem. Phys., <u>68</u>, 4292.

Biedenharn L C, Brussaard P J, Sheth C V, Swamy N V V S and
Cooper J, Physical Review D, <u>5</u>, 1288.

Birnbaum G, 1967, Advan. Chem. Phys., <u>12</u>, 487.

Boikova R F and Ob'edkov V D, 1968, Sov. Phys. - JETP <u>27</u>, 772-4.

Child M S, 1974, "Molecular Collision Theory", (Academic Press,
London).

Chu S I and Dalgarno A, 1974, Phys. Rev. A, <u>10</u>, 788-92.

Chu S I, 1975, Phys. Rev. A, <u>12</u>, 396-405.

(*)
Clark A P, Dickinson A S and Richards D, 1977, Adv. Chem. Phys.,
<u>36</u>, 63.

Cohen A O and Marcus R A, 1970, J. Chem. Phys., <u>52</u>, 3140.

Cottrell T L and McCoubrey J C, 1961, "Molecular Energy Transfer
in Gasses", Butterworth, London.

Crane R L and Klopfenstein R W, 1965, J. Assoc. Comp. Math,
<u>12</u>, 227-241.

Cross, Jr. R J and Gordon R G, 1966, J. Chem. Phys., <u>45</u>, 3571.

(*) indicates that reference has been added at the end

Davison W D, 1962, Disc. Faraday Soc., $\underline{33}$, 71.

DePristo A E and Alexander, 1976, J. Chem. Phys., $\underline{63}$, 3552.

DePristo A E and Alexander M H, 1977, Chem. Phys. $\underline{19}$, 18.
(*)

Dickinson A S and Richards D, 1974, J. Phys. B., $\underline{7}$, 1916.

$\qquad$ 1975, J. Phys. B., $\underline{8}$, 2846.

$\qquad$ 1976, J. Phys. B., $\underline{9}$, 515.

$\qquad$ 1977, J. Phys. B., $\underline{10}$, 323.

$\qquad$ 1978, J. Phys. B., $\underline{11}$, 1085.

Dickinson A S, 1979a, Computer Physics Communications, $\underline{17}$, 51-80.

$\qquad$ 1979b, "Semiclassical Methods in Molecular Scattering
and Spectroscopy". Edited by Child M S,
1980, 263-96.

Edmonds A R, 1960, "Angular Momentum in Quantum Mechanics"
(Princeton, N J; Princeton University Press).

Faisal F H M, 1971, Phys. Rev. A, $\underline{4}$, 596-601.

Fano U, 1970, Phys. Rev. A, $\underline{4}$, 596-601.

Goldstein M and Thaler R M, 1959, Mathematical Tables and Other
Aids to Computation, $\underline{13}$, 1-7.

Gray C G, 1968, Can. J. Phys., $\underline{46}$, 135.

Green S, Bagus P, Liu B, McLean A D and Goshimine M, 1972, Phys.
Rev. A, $\underline{5}$, 1614-8.

Green S, 1973, unpublished work quoted by Chu.

$\qquad$ 1975, J. Chem. Phys., $\underline{62}$, 2271.

Hamming R W, 1962, "Numerical Methods for Scientists and Engineers",
(McGraw-Hill, New York).

Hashi M, Tsuchiya S and Takayanagi K, 1978, Atomic Collision
Research in Japan, Prog. Rep. No 4, 48.

Herzberg G, 1950, "Molecular Spectra and Molecular Structure I,
Spectra of Diatomic Molecules" (Van Nostrand Reinhold).

$\qquad$ 1970, J Molec. Spectrox., $\underline{33}$, 147-68.

Herzfeld K F and Litovititz T A, 1959, "Absorption and Dispersion

of Ultrasonic Waves", Academic Press, New York.

Hirschfelder J O, Curtiss C F and Bird R B, 1966, "Molecular

Theory of Gases and Liquids" (John Wiley : New York).

Itakawa Y, 1971, J. Phys. Soc. Japan, $\underline{30}$, 835-42.

Landau L D and Lifshitz E M, 1960, "Mechanics - Course in

Theoretical Physics", Vol. 1, Pergamon, Oxford.

1965, "Quantum Mechanics - Course in Theoretical

Physics", Vol. 3, Pergamon, Oxford.

1971, "Classical Theory of Fields, Course in

Theoretical Physics", Vol. 2, Pergamon, Oxford.

Levine R D, Bernstein R B, 1974, "Molecular Reaction Dynamics",

Oxford University Press, New York.

Marcus R A, 1970, Chem. Phys. Lett., $\underline{7}$, 525.

Mehrotra S C and Boggs A K, 1975, J. Chem. Phys., $\underline{62}$,1453.

Miller W H, 1970, J. Chem. Phys., $\underline{53}$, 1949.

1974, Advan. Chem. Phys. $\underline{25}$, 69.

1975, Advan. Chem. Phys. $\underline{30}$, 77.

Miller W H and Smith F F, 1978, Phys. Rev. A., $\underline{17}$, 939.

Moskowitz J W and Harrison M C, 1965, J. Chem. Phys., $\underline{43}$, 3550-5.

O'Hara H and Smith F J, 1968, Comp. J. $\underline{11}$, 213-9.
(*)
Patengill M D , 1979, "Atom-Molecule collision Theory, a guide

for the experimentalist", ed. Bernstein R B, chap. 10.

(Plenum, New York).
(*)
Percival I C and Richards D, 1970, J. Phys. B., $\underline{3}$, 1035.

Rabitz H and Gordon R G, 1970a, J. Chem. Phys., $\underline{53}$, 1815.
(*)
Rabitz H, 1974, Ann. Rev. Phys. Chem. $\underline{19}$, 215.

Ray S and Barua A K, 1975, J. Phys. B. Atom. Molec. Phys., $\underline{8}$, 2283.

Saha S and Guha E, 1975, J. Phys. B., $\underline{8}$, 2293.

Schiff L I, 1955, "Quantum Mechanics" Kogakusha, Tokyo.

Somerville W B, 1977, Adv. At. Mol. Phys. $\underline{13}$, 383.

Takayanagi K, 1959, Sci. Rep. Saitama Univ. Ser., $\underline{A3}$, 65.

Temkin A, 1976, Comm. Atom. Molec. Phys., $\underline{6}$, 27-33.

Ter - Martirosyan K A, 1952, Zh. Eksp. Teor. Fiz., $\underline{22}$, 284

        (reprinted, 1966, "Coulomb Excitation" ed. K Alder

        and A Withers (New York : Academic Press) pp 15).

Takayanagi K, 1954, Prog. Theor. Phys., $\underline{11}$, 557.

        1965, Adv. Atom. Mol. Phys., $\underline{1}$, 149.

Wolf A A, 1969, American Journal of Physics, $\underline{37}$, No 5, 531.

Yarkony D R, O'Neil S V, Schaefer H F, III, Baskin C P and

        Bendor C F, J. Chem. Phys., $\underline{60}$, 855.

(*)

Clark A P, 1977, J. Phys. B : Atom Molec. Phys., $\underline{10}$, L389.

Dickinson A S and Munoz J M, 1977, J. Phys. B : Atom Molec. Phys.,

        $\underline{10,}$ 3151.

Oka T, 1973, Adv. Atom. Mol. Phys., $\underline{9}$, 127.

Alexander M H and De Pristo A E, 1976, J. Chem. Phys., $\underline{65}$, 5009.

Pauly H, 1979, "Atom-Molecule Collision Theory, a guide for the experimentalist", ed. Bernstein R.B., chap. 4, (Plenum, New York).

Rabitz H A and Gordon R G, 1970b, J. Chem. Phys., $\underline{53}$, 1831.

Bernstein R B, Dalgarno A, Massey H S W and Percival I C, 1963, Proc. R. Soc. A, $\underline{274}$, 427.

Rotational excitation of polar molecular ions by slow electrons

A S Dickinson† and J M Muñoz‡

† Department of Atomic Physics, School of Physics. The University, Newcastle upon Tyne NE1 7RU, England
‡ Department of Physics, University of Stirling, Stirling FK9 4LA, Scotland

Abstract. An impact-parameter method using hyperbolic paths and perturbation theory has been used to calculate rotational-excitation cross sections for polar-ion electron collisions. Good agreement with corresponding Coulomb Born calculations is obtained even close to threshold. The focusing effect of the Coulomb field is shown to be important for close collisions. Previous calculations including the dipole potential only are shown to underestimate substantially the $\Delta J = \pm 1$ rotational cross section, particularly for weak dipoles. Calculations using the quadrupole interaction only are shown to be unreliable. Cross sections including an empirical estimate of short-range effects have been performed for HD^+, CH^+ and H_3O^+ at electron energies up to a few electron volts.

1. Introduction

Despite a recent increase in theoretical work on the rotational excitation of molecular ions by slow electrons, this process has attracted relatively little attention compared to the analogous process in neutral molecules. The measurement of excitation cross sections for molecular ions is difficult, but such cross sections are of interest for studies of low-temperature partially-ionised gases.

We concentrate here on the excitation of polar molecular ions. Previous work on linear ions (Boikova and Ob'edkov 1968, Chu and Dalgarno 1974) has considered the transition as due solely to the dipole potential, which has been treated in the Coulomb–Born approximation. Following Faisal (1971) and Ray and Barua (1975), we use a time-dependent method based on a classical trajectory for the incident particle. Employing first-order perturbation theory (FOTDPT), we show that, in this approach, unphysically low values are used for the transition probability for close collisions. The existence of strong rotational coupling in the interaction of slow electrons with H_2^+ is shown by the mixing observed by Herzberg (1970) between two Rydberg series of H_2 terminating on the $J = 0$ and $J = 2$ levels of the ground vibrational state of H_2^+, J being the rotor quantum number. Fano (1970) has argued that this situation should be general in electron molecular-ion collisions.

In the absence of a detailed description of the short-range electronic interactions, we assume a conservative value of the transition probability in the strong-coupling region. This shows that the Coulomb Born approximation almost certainly underestimates significantly the total $\Delta J = \pm 1$ cross section.

For symmetric-top ions, we examine the contributions from the quadrupolar inter-action and we find that the regions for which perturbation theory and the quadrupo-lar interaction are valid are very limited. We compare also with the work of Ray and Barua (1975) on the rotational excitation of HD^+ by electrons and positrons. They used at short range a truncated form of the long-range anisotropic interaction. Since this modification takes little account of the strong coupling occurring for elec-trons in close encounters their results differ little from the Coulomb-Born values.

In §2, we examine time-dependent perturbation theory for the dipole and quadru-pole potentials using a hyperbolic classical path for the incident electron. Limiting forms for low and high velocities are derived and comparison with the Coulomb–Born results confirms the validity of the time-dependent approach. Our simple modification to the short-range contribution is made in §3 and compared with other results. Our conclusions are presented in §4.

The values of the various molecular parameters needed are collected in table 1. We use a_0, e and m for the Bohr radius, electron charge and mass respectively and we use Ry for $me^4/2h^2 \equiv 13.6$ eV.

Table 1. Table of the molecular data used in this work. A and B are rotational constants. (All values in atomic units.)

Ion	D	Q	A	B
CH^+	0.67[a]	—	—	6.46×10^{-5} [c]
HD^+	0.34[b]	1.578[b]	—	1.02×10^{-4} [c]
H_3O^+	0.22[d]	-2.214[e]	2.85×10^{-5} [f]	5.55×10^{-5} [f]

[a] Green (1973), unpublished work (quoted by Chu and Dalgarno 1974) based on the wavefunction given by Green *et al* (1972).
[b] Ray and Barua (1975).
[c] Herzberg (1950).
[d] Moskowitz and Harrison (1965).
[e] Chu (1975).
[f] Derived by Chu (1975) from OH distance and HOH angle calculated by Moskowitz and Harrison (1965).

2. Theory

2.1. First-order time-dependent perturbation theory

The rotational state of a symmetric-top molecular ion is characterised by the three quantum numbers J, M and K, which have their usual significance (Herzberg 1950). The corresponding rotational eigenfunctions are given by Edmonds (1960):

$$\Psi_{JKM} = [(2J + 1)/8\pi^2]^{1/2} \mathscr{D}_{MK}^{(J)}(\Omega) \tag{2.1}$$

where $\mathscr{D}_{MK}^{(J)}$ is the matrix element of the operator of finite rotations and $\Omega \equiv (\alpha, \beta, \gamma)$ are the Euler angles specifying the orientation of the ion with respect to a space-fixed frame.

The asymptotic interaction potential between the molecular ion and the electron can be expanded in the form (Chu 1975)

$$V(r, \chi, \psi) = -e^2/r + \sum_{l,k} v_{lk}(r) Y_{lk}(\chi, \psi) \tag{2.2}$$

where r is the electron distance from the centre of mass of the molecular ion, (χ, ψ) specify the direction of the incident electron with respect to the symmetry axis of the molecular ion and Y_{lk} is the spherical harmonic (Edmonds 1960). In symmetric-top molecular ions with symmetry C_{3v} the term v_{lk} vanishes unless $|k| = 3n$ ($n = 0, 1, 2, \ldots$). In this work, we are particularly interested in the first two non-vanishing terms. These are (Itiwaka 1971)

$$v_{10}(r) = -(4\pi/3)^{1/2}\frac{eD}{r^2} \qquad v_{20}(r) = -(4\pi/5)^{1/2}\frac{eQ}{r^3} \qquad (2.3)$$

where D and Q are the dipole and quadrupole moments respectively. Transforming (2.2) into the space-fixed frame, we obtain (Edmonds 1960)

$$V(r, \theta, \phi, \Omega) = -e^2/r + \sum_{lkv} v_{lk}(r)\mathscr{D}^{(l)}_{-v-k}(\Omega)Y_{lv}(\theta, \phi) \qquad (2.4)$$

where (θ, ϕ) specify the direction of the incident electron in the space-fixed frame.

We assume the incident electron moves on a classical trajectory determined by the spherical part of the potential (2.2). The energy E, on the trajectory, is taken to be

$$E = \tfrac{1}{2}mv^2 \qquad v = (v_i v_f)^{1/2} \qquad (2.5)$$

where v_i and v_f are the initial and final speeds respectively of the electron. Thus, the first-order transition amplitude $S(i \to f; b)$, for a transition between two states $|i\rangle \equiv |JKM\rangle$ and $|f\rangle \equiv |J'K'M'\rangle$ at impact parameter b is given by

$$S(i \to f; b) = -\frac{i}{\hbar}\int_{-\infty}^{\infty} dt \exp(i\omega_{if}t)\langle f|V[r(t), \Omega]|i\rangle \qquad (2.6)$$

where $\omega_{if} = (E_i - E_f)/\hbar \equiv \Delta E/\hbar$, the electron coordinates have been written explicitly as functions of the time and E_i (E_f) is the initial (final) translational energy of the electron. For notational simplicity, we derive transition probabilities for upward transitions only; probabilities for downward transitions are derived using the detailed-balance relation.

The calculation of the degeneracy-averaged probability $\mathscr{P}$, for a transition from the level JK to $J'K'$ is straightforward:

$$\mathscr{P}(JK \to J'K'; b; E) = (2J' + 1)\sum_{lv}\frac{1}{2i + 1}\left|\sum_k \begin{pmatrix} J & J' & l \\ K & -K' & -k \end{pmatrix} V_{lv}\right|^2 \qquad (2.7)$$

where the 3-j symbol is defined by Edmonds (1960) and V_{lv} is given by

$$V_{lv} = \frac{1}{\hbar}\int_{-\infty}^{\infty} dt \exp(i\omega_{if}t)v_{lk}[r(t)]Y_{lv}[\theta(t), \phi(t)] \qquad (2.8)$$

The terms in the potential contributing in first order to the transition $JK \to J'K$ are those v_{lk} with (l, k) satisfying

$$|J - J'| \leqslant l \leqslant J + J' \qquad K - K' = k. \qquad (2.9)$$

If $K = K' = 0$, as occurs for a linear molecular ion, there is the additional condition

$$J + J' + l = \text{even}. \tag{2.10}$$

Since we treat the target quantum-mechanically and the projectile classically, the probability (2.7) does not satisfy the detailed-balance relation. To enforce detailed balance, we redefine our first-order probability for initial translational energy E_i as

$$P^{FO}(JK \rightarrow J'K'; b; E_i) = (v_f/v_i)\mathscr{P}(JK \rightarrow J'K'; b; E) \tag{2.11}$$

where E is obtained from (2.5).

The first-order cross section σ^{FO} is

$$\sigma^{FO}(JK \rightarrow J'K'; E_i) = 2\pi \int_0^\infty P^{FO}(JK \rightarrow J'K'; b; E_i) b \, db. \tag{2.12}$$

2.2. The $V_{l\nu}$ integral

Since we consider the electron moving classically in a Coulomb potential its trajectory is a hyperbola and we choose $\theta = \pi/2$. We take $v_{lk} = C_l/r^{l+1}$ where C_l is a constant, see (2.3). Proceeding as for Coulomb excitation of nuclei (Alder *et al* 1956) we find

$$V_{l\nu} = [C_l Y_{l\nu}(\pi/2, 0)/h v a^l] I_{l\nu}(\epsilon, \beta) \tag{2.13}$$

where a is given by

$$a = e^2/2E \equiv a_0(Ry/E) \tag{2.14}$$

and

$$I_{l\nu}(\epsilon, \beta) = \int_{-\infty}^\infty \exp[i\beta(\epsilon \sinh \xi - \xi)] \frac{[\epsilon - \cosh \xi + i(\epsilon^2 - 1)^{1/2} \sinh \xi]^\nu}{(\epsilon \cosh \xi - 1)^{l+\nu}} \, d\xi \tag{2.15}$$

with β defined by

$$\beta = a\omega_{if}/v \tag{2.16}$$

and ϵ, the eccentricity of the hyperbola, can be written as

$$\epsilon = (1 + b^2/a^2)^{1/2}. \tag{2.17}$$

The corresponding $I_{l\nu}(\epsilon, \beta)$ integral for a repulsive Coulomb potential has been examined by Alder *et al* (1956).

2.3. The dipolar contribution

2.3.1. The transition probability. From the condition (2.9), the dipole term $v_{10}(r)$ of the potential can produce only the transition $|\Delta J| = 1$. Because of the slow decrease of $v_{10}(r)$ with r it is the dominant term for distant collisions.

Following Ter-Martirosyan (1952), we obtain for P_{10}^{FO}, the probability due to the dipole potential

$$P_{10}^{FO}(JK \rightarrow J'K; b; E_i)$$

$$= \tfrac{1}{3}(\pi\beta a_0/a)^2 (D/ea_0)^2 G(J, J', K)(Ry/E_i)$$

$$\times \left(-\frac{(\epsilon^2 - 1)}{\epsilon^2}[H_{i\beta}^{(1)}(i\beta\epsilon)]^2 + [H_{i\beta}^{(1)'}(i\beta\epsilon)]^2 \right) \qquad (2.18)$$

where $H_\nu^{(1)}(z)$ and $H_\nu^{(1)'}(z)$ are the Hankel function of the first kind and its derivative respectively (Abramowitz and Stegun 1965, p 358) and $G(J, J', K)$ is given by

$$G(J, J', K) = (2J' + 1)\begin{pmatrix} J & J' & 1 \\ K & -K & 0 \end{pmatrix}^2. \qquad (2.19)$$

For ν and z imaginary the Hankel function $H_\nu^{(1)}(z)$ is purely imaginary, while its derivative is real.

We consider the probability (2.18) for $b = 0$ ($\epsilon = 1$), where the probability takes its maximum value. Then

$$P_{10}^{FO}(JK \rightarrow J'K; 0; E_i) = \tfrac{1}{3}(\pi\beta a_0/a)^2 (D/ea_0)^2 G(J, J', K)(Ry/E_i)[H_{i\beta}^{(1)'}(i\beta)]^2. \qquad (2.20)$$

There are two natural energy regions: $\beta \gg 1$ and $\beta \ll 1$. The transition between these two regions occurs at energy $\bar{E}$ where $\beta = 1$, i.e.

$$\bar{E}/Ry = (\Delta E/2Ry)^{2/3}.$$

For high energies ($\beta \ll 1$), we have (Landau and Lifshitz 1971, p 185)

$$H_{i\beta}^{(1)'}(i\beta) \cong H_0^{(1)'}(i\beta) \cong 2/\pi\beta \qquad (2.21)$$

which, when substituted in (2.20), yields

$$P_{10}^{FO}(JK \rightarrow J'K; 0; E_i) \cong \tfrac{1}{3}(2D/ea_0)^2 G(J, J', K)E_i/Ry \qquad E_i \gg \bar{E} \qquad (2.22)$$

using $E_i \cong E$ at high energies.

The energy E_c at which the sum of the upward and downward transition probabilities at impact parameter $b = 0$ is equal to one, in the high-energy limit (2.22) of first-order perturbation theory, is

$$E_c/Ry = 3(ea_0/2D)^2/g(J,K) \qquad (2.23)$$

where

$$g(J,K) = 1 - K^2/J(J + 1). \qquad (2.24)$$

Clearly for systems with $D \leqslant 1ea_0 = 2.54$ Debye and $\Delta E \leqslant 0.1$ eV, $E_c \gg \bar{E}$. As will be shown below, for head-on collisions the breakdown of the assumption of a dipole potential is more significant than the non-conservation of flux.

For small energies ($\beta \gg 1$), we have (Landau and Lifshitz 1971, p 185)

$$H_{i\beta}^{(1)'}(i\beta) \cong (1/\pi\sqrt{3})(6/\beta)^{2/3}\Gamma(\tfrac{2}{3}) \qquad (2.25)$$

and the probability in this limit is

$$P_{10}^{FO}(JK \rightarrow J'K; 0; E_i) \cong C(v_i/v_i)(D/ea_0)^2 G(J, J', K)(\Delta E/2Ry)^{2/3} \qquad E_i \ll \bar{E} \qquad (2.26a)$$

where

$$C = (\tfrac{4}{3})^{2/3}[\Gamma(\tfrac{2}{3})]^2 = 2\cdot221. \qquad (2.26b)$$

For all realistic systems the probability in this limit is much less than 1.

We note that in the time-dependent perturbation theory approximation used in this work, departures from unitarity become increasingly important as the energy increases—the reverse of the situation for neutrals (Dickinson and Richards 1975). The difference is caused by the strong acceleration of the electron by the attractive Coulomb field.

2.3.2. Cross section. Using (2.18) in (2.12), we obtain for the cross section (Landau and Lifshitz 1971, p 184)

$$\sigma_{10}^{FO}(JK \to J'K;E_i) = (2\pi^3\beta a_0^2/3)(D/ea_0)^2 G(J,J',K)(Ry/E_i)[iH_{i\beta}^{(1)}(i\beta)H_{i\beta}^{(1)\prime}(i\beta)]. \qquad (2.27)$$

The low-energy behaviour ($E \ll \bar{E}$; $\beta \gg 1$) is obtained from (2.27) using (2.25) and the relation (Landau and Lifshitz 1971, p 185)

$$H_{i\beta}^{(1)}(i\beta) \cong -(i/\pi\sqrt{3})(6/\beta)^{1/3}\Gamma(\tfrac{1}{3}) \qquad (2.28)$$

yielding

$$\sigma_{10}^{th}(JK \to J'K;E_i) \cong (8\pi^2 a_0^2/3\sqrt{3})(D/ea_0)^2 G(J,J',K)(Ry/E_i) \qquad E_i \ll \bar{E}. \qquad (2.29)$$

This is identical with the threshold dipolar cross section in the Coulomb–Born approximation (Chu 1975).

For high energies ($E \gg \bar{E}$; $\beta \ll 1$) we have (Landau and Lifshitz 1971, p 185)

$$iH_{i\beta}^{(1)}(i\beta) \cong iH_0^{(1)}(i\beta) \cong (2/\pi)\ln(1\cdot1229/\beta). \qquad (2.30)$$

Using (2.21) and (2.30) in (2.27) we obtain for the high-energy cross section

$$\sigma^{H}(JK \to J'K;E_i) = \tfrac{1}{3}\pi a_0^2(2D/ea_0)^2 G(J,J',K)(Ry/E_i)\ln[5\cdot04E^3/\Delta E^2 Ry] \qquad E_i \gg \bar{E} \qquad (2.31)$$

recovering the usual Bethe limit for an optically allowed transition. This high-energy limit of the cross section does not appear to have been derived previously. All the above equations hold for linear polar ions when $K = 0$.

To evaluate the Hankel functions used in (2.18) and (2.27) we use the method of Goldstein and Thaler (1959) to compute the Bessel functions $J_\nu(z)$ and $Y_\nu(z)$. The calculation of the Hankel function is then straightforward (Abramowitz and Stegun 1965, pp 385 and 361).

In table 2 we compare our results for CH^+ with the Coulomb–Born results of Chu and Dalgarno (1974) for the $0 \to 1$ transition. In the energy range [0·007, 2·04] eV, the agreement is within 4%. For energies less than 0·007 eV Bessel functions of large imaginary argument and order ($\beta \gtrsim 45$) are required and the routine employed suffered from rounding errors. The low-energy limit (2.29) agrees within 10% with the full result (2.27) for $E_i \leqslant \bar{E}/2$, while the high-energy limit (2.31) agrees within 15% for $E_i \geqslant 6\bar{E}$. For this transition $\bar{E} = 0·0348$ eV. Thus the low-energy approximation (2.29) gives acceptable accuracy in the region where our direct method of evaluating the Bessel functions suffered numerical difficulties. Overall, the

Table 2. Comparison of the $0 \rightarrow 1$ rotational-excitation cross sections of CH$^+$ by electron impact.

E_i (eV)	$\sigma(0 \rightarrow 1)$(Å^2)		E_i (eV)	$\sigma(0 \rightarrow 1)$(Å^2)	
	Equation (2.27)	Coulomb–Born[b]		Equation (2.27)	Coulomb–Born[b]
0·00351	7403[a]	7409	0·20	235	229
0·005	—	4809	0·31	174	173
0·007	3826	3835	0·40	145	142
0·010	2728	2619	0·50	124	121
0·017	1669	1675	0·61	108	105
0·028	1072	1071	0·75	93	91
0·045	719	709	1·01	75	73
0·072	496	491	2·04	44	43
0·10	381	370			

[a] From (2.29).
[b] Chu and Dalgarno (1974).

agreement between the time-dependent and the time-independent approximations is very satisfactory.

2.4. The quadrupolar contribution

To calculate the quadrupolar contribution ($|\Delta J| = 1$ and $|\Delta J| = 2$) it is necessary to evaluate the I_{2v} integral (2.15) numerically. For small velocities (large β) and large ϵ, it is difficult to obtain accurate values because of the fast oscillation of the integrand. We have used a modified Simpson's rule and tested our methods by comparing our results with: the tabulated values of Alder *et al* (1956) for the corresponding I_{2v} integral for a repulsive potential; the analytical result for I_{1v}; and finally the analytical expressions for I_{2v}, in the case of a sudden collision ($\beta = 0$). In that limit

$$I_{20}(\epsilon, 0) = \frac{2}{(\epsilon^2 - 1)}\{1 + [\pi - \tan^{-1}(\epsilon^2 - 1)^{1/2}]/(\epsilon^2 - 1)^{1/2}\}$$

$$I_{2\pm 2}(\epsilon, 0) = 2/3\epsilon^2. \tag{2.32}$$

In figure 1, we show the quadrupolar first-order probability P_{20}^{FO} as a function of the impact parameter for collisions with H_3O^+ and HD$^+$. The probabilities do not satisfy unitarity for small impact parameters. Since P_{20}^{FO} diverges strongly as b tends to zero, the quadrupole contribution to the cross section will be discussed below after we have considered a short-range cut-off. No such cut-off was necessary for the dipole potential since P_{10}^{FO} was finite for head-on collisions.

3. The short-range contribution

The theory presented above may become invalid at small impact parameters for the following reasons:

(i) the incident electron must have an orbital angular momentum of at least $s\hbar$ to excite the molecular ion by an amount $\Delta J = s$;
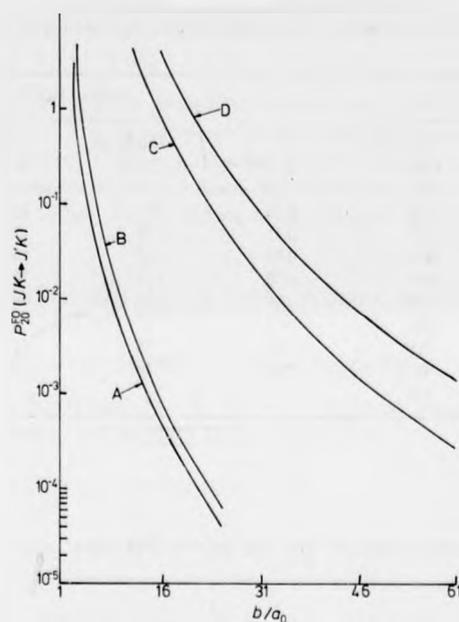
Figure 1. First-order quadrupolar probabilities P_{20}^{10} as a function of the impact parameter A: $P_{10}^{10}(6.6 \to 7.6; E_i = 1 \text{ eV})$ for H_3O^+; B: $P_{20}^{10}(0 \to 2; E_i = 1 \text{ eV})$ for HD^+; C: as B except $E_i = 0.1 \text{ eV}$; D: as B except $E_i = 0.06 \text{ eV}$.

(ii) the interaction potential (2.2) is not valid for small r;

(iii) the transition probability for an anisotropic term with $l \geqslant 2$ is greater than unity for small impact parameters.

To allow for (i) we define

$$b_1 = sh/mv \tag{3.1}$$

and we assume a probability (Dickinson and Richards 1975)

$$P(JK \to J + s \, K; b; E_i) = 0 \qquad b < b_1. \tag{3.2}$$

To correct for (ii) it is necessary to estimate the region where the potential (2.2) is reliable. We suppose that this is for electron–molecular-ion separations larger than the charge-cloud size, r_c, of the molecular ion. Thus, we define b_2 as the impact parameter at which the Coulomb field focuses the incident electron to the edge of the charge cloud r_c

$$b_2 = (r_c^2 + e^2 r_c/E)^{1/2}. \tag{3.3}$$

When the incident electron penetrates the core region, $r < r_c$, it has considerable kinetic energy from the Coulomb field and can easily excite the high rotational levels of the ion, so becoming captured temporarily. Subsequent collisions will then occur. While our knowledge of the details of this process is limited, we consider it likely and it certainly should not be excluded until detailed calculations with a realistic

short-range potential have been made. To give a plausible estimate of the likely contribution from this mechanism, we assume a short-range probability

$$P(JK \to J'K; b; E_i) = \begin{cases} \dfrac{v_f}{v_i} \eta \dfrac{b}{b_M} & b_1 \leqslant b \leqslant b_M \\[2ex] \dfrac{v_f}{v_i} \eta \dfrac{b_2 - b}{b_2 - b_M} & b_M \leqslant b \leqslant b_2 \end{cases} \tag{3.4}$$

where η is a parameter. Strictly, $P(b_2) = P^{FO}(b_2)$ would preserve continuity but $P^{FO}(b_2)$ is generally small so such a modification makes negligible difference to the cross sections. This form has been adopted so that the probability first increases due to the stronger collisions occurring as h decreases to b_M. There we assume that the unitarity requirement causes P to decrease in the strong-coupling region $b_M \geqslant b \geqslant b_1$. A similar model for the strong-coupling probability in electron–polar-molecule collisions (Dickinson and Richards 1975) yielded cross sections in good agreement with those obtained using close-coupling calculations. Thus we can write the cross section σ^T as

$$\sigma^T(JK \to J'K; E_i) = \sigma^{sh}(JK \to J'K; E_i) + \sigma^L(JK \to J'K; E_i) \tag{3.5a}$$

where

$$\sigma^{sh}(JK \to J'K; E_i) = 2\pi \int_0^{b_2} b \, db \, P(JK \to J'K; b; E_i) \tag{3.5b}$$

and

$$\sigma^L(JK \to J'K; E_i) = 2\pi \int_{b_2}^{\infty} b \, db \, P^{FO}(JK \to J'K; b; E_i). \tag{3.5c}$$

For simplicity we take

$$b_M = (b_1 + b_2)/2 \tag{3.6}$$

obtaining for σ^{sh}

$$\sigma^{sh}(JK \to J'K; E_i) = (v_f/6v_i)\eta\pi[b_2(3b_2 + b_1) - 8b_1^3/(b_1 + b_2)]. \tag{3.7}$$

For the dipole case σ^L can be obtained by a minor modification to (2.27):

$$\sigma^L_{10}(JK \to J'K; E_i) = (2\pi^3 \beta a_0^2/3)(D/ea_0)^2 G(J,J',K)(Ry/E_i)[i\epsilon_2 H_{i\beta}^{(1)}{}'(i\beta\epsilon_2)H_{i\beta}^{(1)}{}''(i\beta\epsilon_2)] \tag{3.8}$$

where ϵ_2 is obtained from b_2 using (2.17).

We have estimated the charge-cloud size, r_c, as twice the equilibrium internuclear distance, R_c, in diatomic ions, and twice the OH distance in the H_3O^+ ion. We have taken $\eta = 0.2$, which should give a conservative estimate of the short-range contribution.

3.1. Results and discussion for dipole interactions

The effect of the short-range modification is shown for CH^+ in figure 2. The increase in the cross section falls smoothly from about 30% at threshold to 10% at 2 eV.
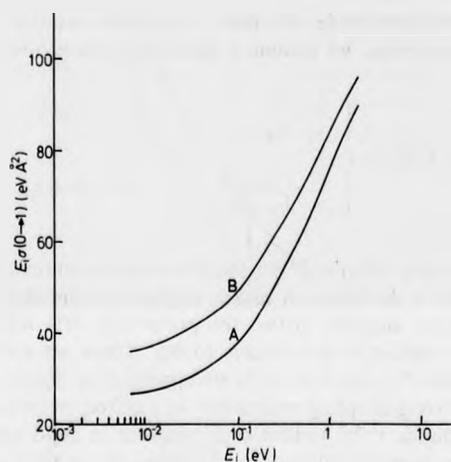
Figure 2. Graph of $E_i\sigma(0 \to 1)$ for CH^+ plotted against energy. Curve A shows the pure dipole potential result, equation (2.27) and curve B shows the modified results (3.5a).

An interesting comparison may be made with the results of Ray and Barua (1975) for electron excitation of HD^+. They have used time-dependent perturbation theory with the long-range potential given by (2.2) and (2.3) with an additional polarisability term. Their short-range potential is given by

$$V(r,\chi) = -(e^2/r_0) - (eD/r_0^2)P_1(\cos\chi) - (eQ/r_0^3 + \alpha'e^2/r_0^4)P_2(\cos\chi) \qquad r < r_0 \qquad (3.9)$$

where α' is the non-spherical part of the polarisability and r_0 is a cut-off parameter. They assume $r_0 = 2a_0$.
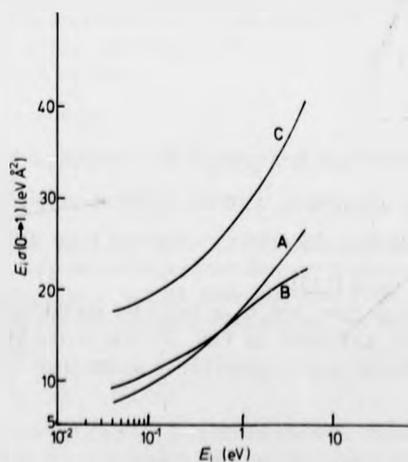

Figure 3. Graph of $E_i\sigma(0 \to 1)$ for HD^+ plotted against energy. Curve A shows the pure dipole potential results, equation (2.27), curve B shows the results of Ray and Barua (1975) and curve C shows the modified results (3.5a).

In figure 3, we present a comparison for the $0 \rightarrow 1$ transition between our results from (2.27), their results, and our modified result (3.5a) for the dipolar contribution. The agreement between their results and FOTDPT at low energies shows that the modified potential (3.9) yields small probabilities for close collisions. Since they use a straight-line trajectory inside the core, comparison with the case of neutral molecules suggests that this straight-line part will lead to higher probabilities, thus enhancing the cross section, as shown in figure 3. At higher energies, the effect of the straight-line trajectory is less marked and their use of a weaker short-range interaction (3.9) leads to smaller cross sections. Again, the effect of the modified probability (3.4) is to increase the cross section above the pure dipole value, in this case more than doubling the cross section at threshold.

Since $\sigma_{10}^{L}(JK \rightarrow J'K; E_{i})$ depends mainly on the value of the dipole moment, for small dipole moments, such as HD^{+}, the short-range cross section σ^{sh} becomes relatively more important. This is illustrated in table 3, where we compare the dipolar σ^{sh} and σ_{10}^{L} for $H_{3}O^{+}$ ($D = 0.22\ ea_{0}$).

Table 3. Rotational-excitation cross sections of H_3O^+ by electron impact for the $(5,0 \rightarrow 6,0)$ transition.

	$\sigma(5,0 \rightarrow 6,0)(\text{Å}^2)$	
E_i (eV)	Equation (3.7)	Equation (3.8)
0·1	89	19
0·2	45	10·4
0·4	23	6
0·6	16	4·4
0·8	12	3·6
1·0	10	3
1·2	8·4	2·6
1·4	7·4	2·3
1·6	6·6	2·1
1·8	6	1·9

3.2. Results and discussion for quadrupolar interactions

As discussed in §2.4, there is a singularity at $b = 0$ in the quadrupolar transition probability. To avoid this, we have obtained cross sections for the quadrupole interaction using (3.1) and (3.2) for close encounters and FOTDPT otherwise. The integration over impact parameter has been done using Simpson's rule. Almost all the contribution comes from small impact parameters and the effective upper limit of the integral is always less than $130\ a_0$, while for the dipole case this limit was about $10^3\ a_0$.

Comparison with the quadrupolar Coulomb-Born results of Chu (1975) for the $(5,2 \rightarrow 6,2)$ transition in H_3O^+ (an example with an intermediate K value) shows differences of less than 5% for $0.1\ \text{eV} \leqslant E_i \leqslant 1.4\ \text{eV}$. This suggests that our cut-off procedure is reasonable. Since the transition probabilities at the cut-off increased from 1·45 to 1·61 as the energy increased, it appears unlikely that the Coulomb-Born approximation satisfies unitarity for close collisions even at electron energies of several electron volts.

The arguments presented above for the effect of Coulomb focusing for close collisions should be equally valid for the quadrupolar interaction. Thus the use of the quadrupole interaction for these collisions is unreliable. Since any cross section derived using approximations similar to (3.3) and (3.4) would be dominated by the assumed short-range contribution, we have not thought it worthwhile to make such a calculation. However, any cross section derived using a first-order perturbation theory and the quadrupole interaction is likely to exceed the true cross section considerably.

4. Conclusions

For electron–polar-molecular-ion collisions, we have used an impact-parameter method to investigate the reliability of the usual approximation of combining the Coulomb–Born approximation with the dipole and quadrupole anisotropic potentials. We find that for a dipole potential, this method underestimates the cross section, particularly for weak dipoles. A modified expression for the cross section has been presented. By contrast, for collisions of electrons with neutral polar molecules, the use of the Born approximation and the dipole potential is more reliable, overestimating the cross section for large dipole moments (Dickinson and Richards 1975). In collisions where the long-range interaction is the quadrupole, the full short-range interaction must be included to obtain reliable results.

Clearly there is a need for an accurate calculation including the detailed electronic structure of the target, similar to those already performed for electron scattering by H_2, N_2 and CO (Temkin 1976).

Acknowledgments

References

Abramowitz M and Stegun I A 1965 *Handbook of Mathematical Functions* (New York: Dover)
Alder K, Bohr A, Huus T, Mottelson B and Winther A 1956 *Rev. Mod. Phys.* **28** 432–542 (reprinted 1966 *Coulomb Excitation* ed K Alder and A Winther (New York: Academic Press) pp 77–187)
Boikova R F and Ob'edkov V D 1968 *Sov. Phys.-JETP* **27** 772–4
Chu S I 1975 *Phys. Rev.* A **12** 396–405
Chu S I and Dalgarno A 1974 *Phys. Rev.* A **10** 788–92
Dickinson A S and Richards D 1975 *J. Phys. B: Atom. Molec. Phys.* **8** 2846–57
Edmonds A R 1960 *Angular Momentum in Quantum Mechanics* (Princeton, NJ: Princeton University Press)
Faisal F H M 1971 *Phys. Rev.* A **4** 596–601
Fano U 1970 *Phys. Rev.* A **2** 353–65
Goldstein M and Thaler R M 1959 *Mathematical Tables and Other Aids to Computation* **13** 1–7
Green S, Bagus P, Liu B, McLean A D and Yoshimine M 1972 *Phys. Rev.* A **5** 1614–8
Herzberg G 1950 *Molecular Spectra and Molecular Structure I. Spectra of Diatomic Molecules* (New York: Van Nostrand Reinhold)
—— 1970 *J. Molec. Spectrosc.* **33** 147–68

Itikawa Y 1971 *J. Phys. Soc. Japan* **30** 835-42

Landau L D and Lifshitz E M 1971 *The Classical Theory of Fields* 3rd revised edn (Oxford: Pergamon)

Moskowitz J W and Harrison M C 1965 *J. Chem. Phys.* **43** 3550-5

Ray S and Barua A K 1975 *J. Phys. B: Atom. Molec. Phys.* **8** 2283-92

Temkin A 1976 *Comm. Atom. Molec. Phys.* **6** 27-33

Ter-Martirosyan K A 1952 *Zh. Eksp. Teor. Fiz.* **22** 284-96' (reprinted 1966 *Coulomb Excitation* ed K Alder and A Winther (New York: Academic Press) pp 15-29)

926'82

END